2-1-2016

SIGNIFICANCE OF U-WRAP FRP SHEAR STRENGTHENING ON FLEXURAL BEHAVIOR OF RC BEAMS STRENGTHENED USING NEAR SURFACE MOUNTED FRP BARS

RahulReddy ChennaReddy

RahulReddy ChennaReddy

Candidate

Civil Engineering

Department

This thesis is approved, and it is acceptable in quality and form for publication:

Approved by the Thesis Committee:

Mahmoud Reda Taha , Chairperson

Arup Maji

Yu-Lin Shen

SIGNIFICANCE OF U-WRAP FRP SHEAR STRENGTHENING ON FLEXURAL BEHAVIOR OF RC BEAMS STRENGTHENED USING NEAR SURFACE MOUNTED FRP BARS

By

RAHULREDDY CHENNAREDDY
B.E., CIVIL ENGINEERING, OSMANIA UNIVERSITY INDIA, 2012
M.S., CIVIL ENGINEERING, UNIVERSITY OF NEW MEXICO, 2015.

THESIS

Submitted in Partial Fulfillment of the
Requirement for the Degree of

Masters of Science
Civil Engineering

The University of New Mexico
Albuquerque, New Mexico

December, 2015

DEDICATION

I would like to dedicate this thesis to my parents, ManoharReddy ChennaReddy and UshaaReddy ChennaReddy, my mentor and advisor Dr. Mahmoud Reda Taha who has given me support and strength that was needed to succeed.

ACKNOWLEDGEMENTS

I would like to thank my advisor and committee chair, Dr. Mahmoud Reda Taha for his help, guidance, motivation and support through this program. Without Dr.Taha's guidance this would not have been possible. I am honored to work under his supervision. I would also like to thank my committee members, Dr. Arup Maji and Dr. Yu-Lin-Shen, for their support.

I would further like to acknowledge Mr. Ken Martiez for his help with conduct experiments for this study. I would also like to specially thank Shreya Vemuganti and Moneeb Genedy for being my mentors and extending their support by help me in conducting my experiments. I would like to extend a special thanks to my colleagues, Alauddin Douba, Amy Garner, Elisa Borwsky, Nicole Trujilo, Venkatesh Jatla, Jagadeesh Krishna Chaitanya Sima, Krishna Poddar and Sherif Aboubakr for their help and assistance with concrete casting and experimental testing required for this project. I would also like to thank my friends from home Suraj Goverdhanam, Sri Bhargav Marreddy, Sunil Vadla, Abhishek Reddy Kuchikula and Satish for their motivation and support.

SIGNIFICANCE OF U-WRAP FRP SHEAR STRENGTHENING ON FLEXURAL BEHAVIOR OF RC BEAMS STRENGTHENED USING NEAR SURFACE MOUNTED FRP BARS

By

RahulReddy ChennaReddy

B.E., CIVIL ENGINEERING, Osmania University, India, 2012

M.S., CIVIL ENGINEERING, University of New Mexico, 2015

Abstract:

The aim of this study is to investigate the significance of U-wrap shear strengthening on the flexural behavior of Near Surface Mounted (NSM) Fiber Reinforced Polymers (FRP) strengthened Reinforced Concrete (RC) beams. It is well-known that the performance of NSM-FRP technique is strongly dependent on bond performance between adhesive-concrete and adhesive-FRP interface. Although a full development length is provided for the NSM FRP bar, rupture of the FRP bar is highly unlikely. This is attributed to the fact that the NSM FRP bar typically observes a stress level lower than 60% of its ultimate capacity at RC beam failure by debonding of NSM-FRP from the surrounding adhesive. Here, a typical three-side FRP U-wrap using wet layup was employed to improve the shear strength of the RC beam. A test matrix of 25 beams was tested under static load to failure. Four sets were considered including conventional RC beams, RC-beams with U-wrap only, RC-beams with NSM-FRP strengthening only without U-wrap FRP

shear strengthening, RC beams with NSM-FRP flexural strengthening and U-wrap FRP shear strengthening, RC beams with NSM-FRP flexural strengthening and U-wrap FRP shear strengthening in shear zone only. The experimental results showed that incorporating FRP U-wrap has a significant effect of the performance of NSM-FRP strengthened RC beams. While a limited improvement of flexural strength of 20% was observed, NSM-FRP strengthened beams with FRP U-wrap experienced a significant reduction in ductility causing sudden failure. The change in the NSM-FRP strengthening system behavior might be attributed to the confinement provided by the U-wrap FRP which resulted in improving the bond strength of the NSM-FRP to the adhesive. This in its turn lead to NSM-FRP bar picking significantly high load level up to rupture with abrupt RC beam failure. The experimental results shed light on the need to consider design limitations when NSM-FRP flexural strengthening is combined with U-wrap FRP shear strengthening in RC beams.

Contents

List of Figures:

List of Tables

Chapter 1 Introduction

1.1. Motivation and problem statement

Federal highway administration (FHWA) statistics in 1989 stated that 40% of the highway bridges in the US are structurally deficient. These bridges were designed to take lower traffic loads than what they observe today. Rebuilding all deficient bridges would not be cost efficient. This made a pathway for extensive research in the fields of rehabilitation and retrofitting of existing concrete structures in early 1990's. Traditional methods for strengthening of reinforced concrete beams is by increasing the cross sectional area and adding additional tension steel reinforcement which is time consuming and expensive. At the inception, external post-tensioning and additional externally bonded steel plates using epoxy were used to increase the load carrying capacity of reinforced concrete (RC) members because for the ease of installation and economic feasibility of these techniques (Charif, 1983; Dussek, 1980; F. W. Klaiber, Dunker, Wipf, & Sanders Jr, 1988; W. F. Klaiber, Dunker, & Sanders, 1982; Saadatmanesh, Albrecht, & Ayyub, 1989; Swamy, Jones, & Bloxham, 1987). However, these techniques showed durability limitations because of potential corrosion, heavy weight and practical difficulties with respect to external post-tensioning. Hence, the need for a corrosion free material for retrofitting techniques arose.

The advancements in the area of fiber reinforced polymer (FRP) composites in aerospace applications brought the attention to their potential in civil engineering applications. FRP are resistant to corrosion and thus help in improving strength and durability. (Saadatmanesh & Ehsani, 1990) first suggested that FRP plates can be used to strengthen beams, by externally bonding (EB) the FRP plate on the tension flange of flexural members.

(Nanni et al., 1999) suggested the idea of Near-Surface Mounting (NSM) reinforcement using FRP. It was then implemented on a bridge located in Central America, constructed in first half of the 19th century. This bridge was structurally deficient for the existing traffic condition. The strengthening procedure was carried out while in service. Two main procedures, EB-FRP and NSM-FRP were implemented to strengthen both flexural and compression members of the beam. In EB-FRP, FRP plate is bonded externally to the tension surface/face of RC flexural members. For NSM-FRP, a pre-cut groove using saw is made on the tension surface/face of the beam. The groove is half filled with construction adhesive, then FRP bar is pressed inside the grove such that half of the circumferential perimeter of the bar is covered with adhesive. The groove is then completely filled with adhesive. This strengthening process was carried out while the bridge was in service and it took a short time period to improve the flexural capacity of the bridge girder by 29% (Nanni et al., 1999).

NSM-FRP has thus been suggested as a promising technique for improving the performance of structurally deficient RC structure, because of its ease of installation. However research showed that the performance of this technique is strongly dependent on the bond performance between epoxy-concrete and epoxy-FRP bar (Laura De Lorenzis & Nanni, 2002; T. K. Hassan & Rizkalla, 2004). Even when a full development length is provided for the CFRP bar, strength rupture of FRP is highly unlikely as the bar observes a stress level of 60%-70% of its ultimate strength. The failure of NSM-FRP typically takes place by de-bonding of NSM-FRP from the surrounding adhesive. The beam acts further as a convectional (RC) Beam. Recent studies (Badawi & Soudki, 2009; Wahab, Soudki, & Topper, 2011, 2012) have shown that the fatigue performance of NSM-FRP retrofitted structures is not very efficient under cyclic loading. The flexural member is safe to observe no more than 45% of its capacity under cyclic loading. The

failure mode for fatigue is also in bond. Typically in NSM-FRP strengthened RC beams, flexural failure can take place in two modes: de-bonding of the bar and bar rupture. As the bar does not experience more than 60%-70% of its ultimate strength, de-bonding is the typical governing failure. De-bonding can be experimentally simulated using two ways, direct pullout test and beam pullout test. In the current study beam the bond was investigated experimentally under beam pullout fixture.

RC beams experience shear loads in addition to the flexural loads. When a beam becomes structurally deficient with respect to the applied loads, the RC beam members will require shear strengthening, flexural strengthening or both. Shear strengthening of RC beams using FRP has been widely examined and approved as an acceptable method in most design codes. The different techniques used currently are, NSMFRP-shear strengthening and U-wrap FRP shear strengthening using wet-layup technique. The performance of FRP-U wrap shear strengthening was extensively instigated (Chajes, Januszka, Mertz, Thomson Jr, & Finch Jr, 1995; Kachlakev & McCurry, 2000; Malvar, Warren, & Inaba, 1995; Norris, Saadatmanesh, & Ehsani, 1997). Currently, in typical RC beam strengthening, NSMFRP for flexural strengthening and FRP U-wrap shear strengthening techniques are widely acceptance techniques. The design considerations of ACI-440 2R-08 code treats NSMFRP flexural strengthening and U-wrap shear strengthening as two separate design techniques and thus, there are no guidelines on possible RC beam behavioral change if the two techniques are combined. Figure 1.1 illustrates the two techniques treated separately by ACI-440 2R-08. This thesis examines this concern.

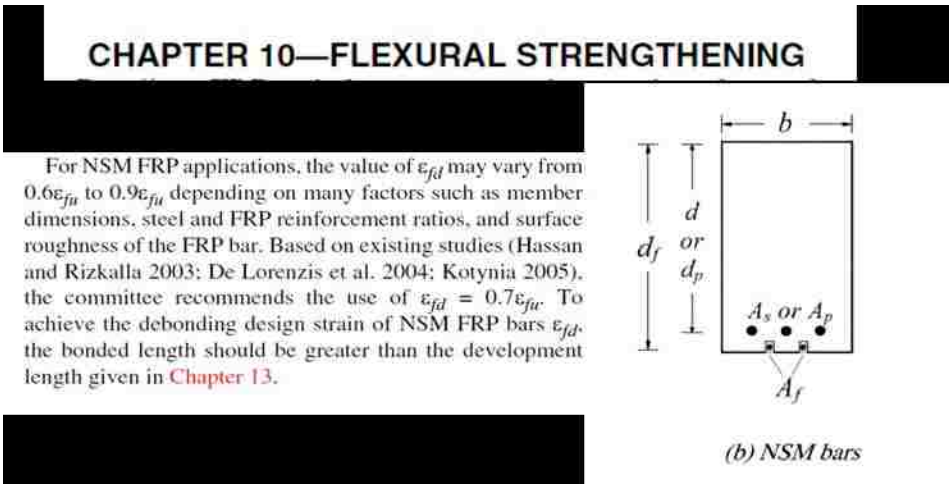

(a)

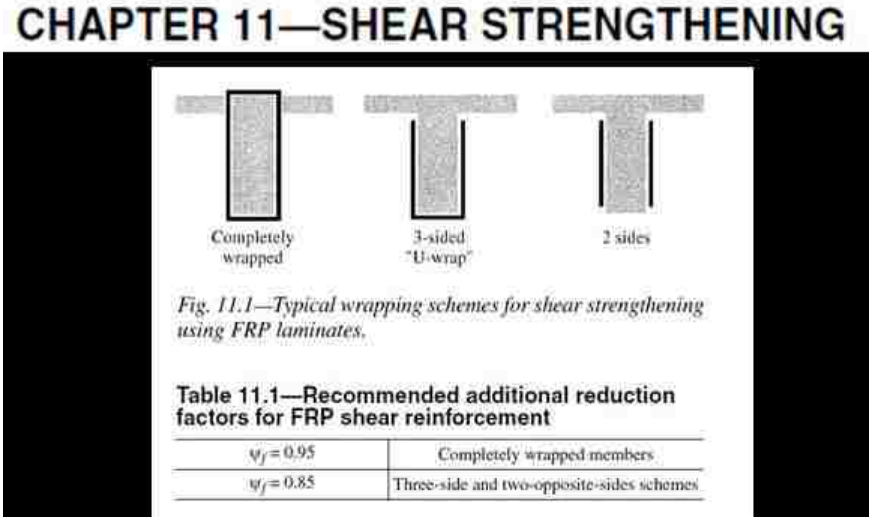

(b)

Figure 1.1: Figures (a) and (b) from ACI-440 2R-08 treating NSM-FRP flexural strengthening and U-wrap shear strengthening as two separate techniques

1.2. Contribution

The aim of this study is to examine the combined effect of NSM-FRP flexural strengthening and U-wrap shear strengthening using FRP sheets. Presently, NSM-FRP flexural strengthening and U-wrap FRP shear strengthening are used together in the industry but the combined behavior of these two systems was never studied. This study focuses on this aspect to experimentally investigate the combined NSMFRP flexural and U-wrap FRP shear strengthening technique. As failure of NSM-FRP strengthened beams is typically governed by bond between FRP bar and surrounding adhesive, it would be interesting to observe the effect of potential confinement by U-wrap shear strengthening on bond strength of NSM-FRP. The hypothesis in using the U-wrap shear strengthening is that shear strengthening might improve the bond and stress of NSM-FRP bars such that the FRP bar may rupture. The combination of these two techniques might lead to loss of NSM bar ductility and this risk of abrupt failure of RC-beams strengthened with NSM-FRP.

An experimental program is executed to test this hypothesis. A typical three-side FRP U-wrap was employed to provide RC shear strengthening for NSM-FRP bars. U-wrap is a typical method used for shear strengthening of RC beams. A test matrix of 25 beams, a set of 5 beams per type was tested under static loading to failure. Set-1 of convectional RC beam without NSM-FRP, set-2 of RC-beams with U-wrap only, set-3 of RC-beams with NSM-FRP only, set-4 of RC-beams with NSM-FRP along with FRP U-wrap shear strengthening. Set 5 of RC-beams with NSM-FRP along with partial U-wrap shear strengthening only in the shear zone of the beam.

1.3. Thesis outline

Chapter 2 discusses relevant literature to date on flexural strengthening techniques of RC beams. Moreover, brief relevant literature on FRP's will be discussed.

Chapter 3 discusses the complete experimental method employed for this study. We describe the different materials used, the method of preparation of the different beams and the test setup.

Chapter 4 presents the results and comparisons of different NSM – FRP strengthening configurations. Detailed analysis of moment-curvature, stress-strain behavior and the effect of confinement on NSM-FRP are presented. Finally, the conclusions from the study and some recommendation for future studies are presented in Chapter 5.

Chapter 2 Literature Review

2.1 RC beams Strengthening

Typically RC Beams are strengthened flexurally, by increasing the area of cross section there by adding additional reinforcement steel. The arrangement of the additional reinforcement steel is on the tension side by casting additional concrete to achieve complete composite action. Other methods include, using grouted steel reinforcement on tension side and externally bonding steel plate on tension side of the beam. In 1948, bridge slabs were (Asplund, 1949). In late 1960's development of structural adhesives in South Africa lead pathway for use of externally bonded steel plates on the tension side of the beam (Fleming & King, 1967). Use of steel plates for strengthening of beams has gained acceptance since then and proved to be an effective technique for flexural strengthening of beams (Toutanji, Zhao, & Zhang, 2006). Steel being a highly corrosive material, external exposure of steel makes it vulnerable for corrosion. This will directly affect the durability of the structure. Hence, the need for an alternative material, which is resistant to corrosion, made pathway for use of FRPs as a material for strengthening techniques in late 1980's (Saadatmanesh & Ehsani, 1990).

2.2 Fiber Reinforced Polymers (FRP)

Fiber Reinforced Polymer (FRP), as the name indicates polymer matrix reinforced with different types of fibers. Based on the type of fiber used as reinforcement the type of FRP laminate is determined. Following world-war- ii, the growing petro-chemical industry made available the earliest FRP material, which used glass fibers with polymeric resins as the reinforcement (Bakis et al., 2002). The different types of fibers used are glass, carbon, aramid and boron because of their high strength, high stiffness and low-density properties (Bakis et al., 2002). Generally, Glass Fiber

Reinforced Polymers (GFRP) and Carbon Fiber Reinforced Polymers (CFRP) are most commonly used materials in construction industry. Another classification is based on the orientation of the fiber direction within the polymer matrix. Unidirectional FRP, all the reinforcement fibers are oriented in the same direction within the polymer matrix. Bi-directional FRP, the reinforcement fibers are oriented in two mutually perpendicular directions within the polymer matrix.

FRP have a high strength to weight ratio and highly resistant to corrosion. These properties made it a suitable material for space explorations and aircraft industry in 1960's and 1970's. Efforts were made to reduce the manufacturing costs of FRP during 1970's and 1980's (Bakis et al., 2002). During the period of late 1980's through 1990's FRP gained acceptance in the field of construction, recognized not only for its noncorrosive nature, but for FRP tensile and fatigue capacities dominated steel (Bakis et al., 2002). Though, FRPs are non-corrosive in nature, they are sensitive to other environmental conditions like humidity and temperature, which makes it necessary to consider some design guidelines for durability and ductility for strengthening of RC structures (Garner, 2011).

2.3 Flexural Strengthening of RC beams using FRP

Generally flexural strengthening of RC Beams can be conducted either by reaching the tension flange of the beam or by reaching the compression flange of the beam. Mostly, strengthening for the beams is done by reaching tension side of the beam, but for exceptional cases where reaching the tension side of the beam is not possible, strengthening can be carried out from the compression flange.

2.3.1 Flexural strengthening from compression flange

In cases where a water stream is flowing under the beam, height of the column is very high making it very difficult to reaching the tension flange and other cases where reaching the tension flange is difficult, this methodology for flexural strengthening of RC beams and slabs can be used. RC beams strengthened by using FRP and Ultra High Performance concrete (UHPC) reaching the compression side of the beam was presented by (Genedy, 2014). Generally in this technique, some part of the concrete on the top is removed, then the FRP sheets are bonded to the surface, later the top of the beam is filled with UHPC overlay. The main reason to use the UHPC overlay is to push the neutral axis more onto the compression side, so that the FRP that is placed acts as the tension reinforcement thereby increasing the flexural capacity of the beam (Garner, 2011; Genedy, 2014; Kim, Noh, Reda Taha, & Mosallam, 2013).

2.3.2 Flexural strengthening from tension Flange

Reaching the compression side of the beam for retrofitting is an expensive process in terms of both time and money, unless needed the above said procedure is not recommended. Typically there are two ways to strengthen an RC beam from tension flange using FRP. Directly bonding FRP sheets onto the tension side of the beam using a polymeric epoxy, this process is widely known as Externally Bonded (EB) FRP technique. Second technique is widely known as the Near Surface Mounted (NSM) FRP, where a saw cut groove is made on the tension flange which is half filled with epoxy, later a FRP bar is placed acting as the tension reinforcement such that surface of the bar is immersed into the epoxy, later the rest of the groove is completely filled with epoxy. After the epoxy hardens the beam is under complete composite action with increased flexural capacity. This current study focuses on the bond performance of the NSM-FRP technique. The

ease of installation and noncorrosive nature of the materials made these techniques as efficient way to strengthen RC beams for flexure.

2.3.3 Shear strengthening using U-wrap FRP for beams

Wrapping is a technique, where FRP fabric is saturated in the polymeric epoxy and the fabric is applied on to the desire surface of the beam and this technique is named as the wet layup technique. The shear strengthening using wrapping can be performed in 3 different ways and is illustrated in the experimental studies on shear strengthening of existing beams and columns were conducted by (Chajes et al., 1995; Kachlakev & McCurry, 2000; Malvar et al., 1995; Norris et al., 1997)

2.4 NSM-FRP technique

The earliest literature on NSM technique dates back to 1948, where same procedure as NSM-FRP was used to flexurally strengthen RC-Beam, the only difference was that the reinforcement material used was steel and cement grout was used instead of polymeric epoxy (Asplund, 1949). Later in 1999, NSM technique was used to strengthen Highway bridge decks using FRP as the reinforcement material; this study presented that FRP material can be effectively used to strengthen bridge decks flexurally (Nanni et al., 1999). A study on bond development, size of the groove, surface configuration was presented under beam pullout fixture (Laura De Lorenzis, Nanni, & La Tegola, 2000; T. K. Hassan & Rizkalla, 2004). With beam pullout fixture, it is difficult to have a slip control failure and measure loaded end slip; hence bond strength was investigated under direct pullout configuration (Yan et al. 1999; Warren, 2000). A study on type of FRP material, surface preparation effects and groove filling material was presented using direct pull out configuration (Laura De Lorenzis, Rizzo, & La Tegola, 2002).

Typically, CFRP and GFRP are the most commonly used materials for NSM-FRP flexural strengthening technique. CFRP is preferred over GFRP as CFRP has better modulus of elasticity and tensile properties over GFRP, thereby CFRP for the same cross-section as GFRP gives better tensile strength limiting the groove size of the for NSM-FRP technique for RC beams (L De Lorenzis & Teng, 2007). FRP is now available in different shapes making it possible to use square, round, rectangular, oval shaped FRP as reinforcement for flexural strengthening (L De Lorenzis & Teng, 2007). Typically, the round FRP bars are readily available making it easier for the industry level strengthening. RC beams strengthened flexurally using NSM-FRP rectangular strips was studied by conducting flexural tests (El-Hacha & Rizkalla, 2004; T. Hassan & Rizkalla, 2003; Teng et al., 2006). The significance of using same amount of reinforcement between FRP round bars and strips was studied. the authors concluded that strip form of reinforcement performed better in bond achieving the rupture of FRP strip reinforcement (El-Hacha & Rizkalla, 2004). This current study focuses on using GFRP spirally wound sanded round bars.

Investigations on bond were performed by (Yan, Miller, Nanni, & Bakis, 1999), using Carbon Fiber Reinforcement Polymer (CFRP) sand blasted rods for NSM under direct pull out fixture. The specimen used was a concrete block of dimensions 152x152x203 mm^3, with a groove made on the opposite faces filled with epoxy and NSM CFRP rod. A steel frame was used to restrain the concrete surface, while the load was applied on the bar to pullout. The main issue associated with this setup is possible eccentricity between the grooves; eccentricity may change the bond behavior by inducing flexural effects on the specimen. The Author presented two different failure modes; shorter embedment length specimens had a failure associated with cracking of concrete on the edge, whereas the longer bond length specimens experienced failure in bond between CFRP surface and epoxy. (Laura De Lorenzis & Nanni, 2002), critiques that the

failure in concrete edge is because of, not providing adequate distance between edge of the concrete and the top of the groove. A more realistic modified direct pull study addressing the problems of eccentricity from previous test configurations was developed with a test matrix of 34 specimens (Laura De Lorenzis, Lundgren, & Rizzo, 2004). The assed variables in the test program were material for groove filling (between epoxy and Cement based expansive paste), size of the groove (varied between 1.24 and 2.5 times the bar diameter), Bond length varied between 4 and 24 times the bar diameter, surface configuration of the bar (spirally wound and ribbed). The test results have shown that the groove size greater 1.5 times diameter of the bar is optimum but 2.0 times diameter of the bar is recommended. Spirally wound bars seem to have higher bond strength compared to deformed bars, epoxy performed better compared to the cement paste as the groove filling material. A Finite Element Model has been developed analyze bond in NSM FRP (Laura De Lorenzis et al., 2004). The model could validate the experimental results of bond strength.

Bond under beam pull out fixture was investigated in various studies with shorter embedment length, but most likely the epoxy cover develops cracks associated with flexural cracks making it very difficult to investigate bond under this fixture (L De Lorenzis & Teng, 2007). Lorenzis and Nanni (2001), examined the bond under beam pullout fixture for NSM. Inverted T-beam specimens with adequate concrete in tension were used with a plastic hinge at the mid span on the compression side and a saw cut groove was made on the tension side. One NSM FRP rod was placed for each beam with desired development length. The bond strength was examined for different development lengths as a function of the diameter of the bar. 6, 12 and 18 times the diameter of the bar were determined as the bonded lengths to examine the bond stress. The effect of size of the groove was examines for 12 times the diameter of the bar bond length. Different groove sizes used were 0.5in, 0.75in, 1in, where width of the groove, b_g and depth of the groove,

d_g of the groove are equal. All the specimens except 1in groove size had a failure in splitting of epoxy cover and the specimen with 1in groove experienced failure by cracking of concrete surrounding the groove. This change in mode of failure is mainly because of the additional resistance offered by the epoxy cover to splitting. A comprehensive experimental and analytical investigation was performed to develop equation for bond development length for two cases, bond between epoxy-concrete interface and epoxy-FRP interface (T. K. Hassan & Rizkalla, 2004). Bond strength for different bond lengths was investigated experimentally and FEA model was developed to understand the stress transfer for different groove sizes, thereby developing a design chart with a factor called G_1, G_2 and G_2' based on the C/d ratio. Where, C corresponds to the cover of epoxy from bottom of the bar and d corresponds to the diameter of the bar.

The equation for development length given by T. K. Hassan and Rizkalla (2004),

L_dFor concrete-epoxy interface,

$$L_d = G_1 \frac{d}{4} \frac{f_{FRP}}{\mu f_{ct}} \quad \textbf{(2.1)}$$

L_dFor concrete-epoxy interface,

$$L_d = G_2 \; or \; G_2' \frac{d}{4} \frac{f_{FRP}}{\mu f_a} \quad \textbf{(2.2)}$$

where, L_d is development length required for the stress transfer, G_1, G_2 and G_2' are the coefficient from design charts based on unit radial pressure, d is diameter of the bar, f_{FRP} is the stress in FRP bar, μ is the coefficient of friction, f_{ct} is tensile strength of concrete and f_a is tensile strength of epoxy.

The possible failure modes for RC beam flexurally strengthened with NSM-FRP technique; crushing of concrete after the yielding of tension steel, FRP-rupture after yield of tension steel and deboning of NSM FRP(L De Lorenzis & Teng, 2007). Though a full development length is provided for the NSM-FRP bar T. K. Hassan and Rizkalla (2004) concluded that it is highly unlikely that strength rupture of FRP bar will occur. The debonding failure can be further categorized to: Debonding between FRP bar and epoxy interface, this mode of failure mainly depends on the surface configuration of the bar when mechanical interlock between the epoxy and the bar is lacking. The other reason for debonding is flexural cracks created in the RC beam create longitudinal splitting cracks in the epoxy, which makes it easy for the debonding of NSM-FRP bar with surrounding adhesive(L De Lorenzis & Teng, 2007). Separation of concrete cover is the next possible mode of failure, in which generally cracks are formed roughly at 45° angle with respect to the beam axis on the bottom side (L De Lorenzis & Teng, 2007; Teng et al., 2006). These cracks propagate upwards at an angle of 45°, when these cracks intersect steel, the crack can propagate horizontally to separate concrete. Because of this debonding can occur at different forms: End cover separation of FRP bar, generally for RC beams with NSM-FRP is not provided along all longitudinal section giving excessive distance from support there by crack initiates from the cutoff section (Teng et al., 2006). Cover separation localized, in this mode of failure triangular wedges or trapezoidal wedges are formed at the maximum flexural moment area, however this may coincide with the previously formed flexural cracks. The pictures of this mode of failure are given (Barros & Fortes, 2005; L De Lorenzis & Teng, 2007; Teng et al., 2006). Other modes are cover separation induced by flexural cracks and cover separation from beam edge. The cover separation from beam edge is caused because of using multiple bars for NSM-FRP flexural strengthening and the edge FRP bar can get detached from concrete cover near the edge (L De Lorenzis & Teng,

2007). Other notable debonding modes are, debonding of epoxy from concrete interface (T. Hassan & Rizkalla, 2003) and localized splitting of epoxy, where the epoxy cover separates completely, which will clearly show FRP bar (L De Lorenzis & Teng, 2007).

Though debonding is the main mode of failure, predicting the flexural capacity is simple by underestimating tensile strain capacity of the bar. The procedure for flexural design is given in ACI-440 (ACI-440, 2008).

Chapter 3 Experimental Methods

This chapter discusses experimental methodology used for the current study starting with the experimental program followed by the different materials used and their material properties. Later, dimensions of the beams, casting of concrete, NSM-FRP, U-wrapping and curing process are discussed. In conclusion, description of test setup and preparation are given.

3.1 Experimental Program

Twenty five rectangular beams were tested in four point bending. These twenty-five beams were classified into five groups and description of all the beam types are given in **Table 3.1.**

Table 3.1: Description of all beam types and number of beams tested.

Name	Beam Type	Number Tested
C	Simple RC Beam Control	5
U	RC Beam U-wrap only	5
N	RC Beam with NSM only	5
NU	RC Beam with NSM and U-wrap	5
NUS	RC Beam with NSM and U-wrap only in shear zone	5

3.2 Materials

The concrete used has a maximum nominal aggregate size of 12.7mm. The observed slump of the concrete was 100mm and the 28day compressive strength of 44MPa. The slump test conducted abiding to the ASTM (ASTM-C143, 2015). The concrete properties are further discussed in Chapter 4. Steel was used as reinforcement for all 25 beams with nominal diameter of 10mm. The yield strength of steel used is 414MPa according to the manufacturer. GFRP spirally wound deformed bar with nominal diameter of 10mm was used for NSM reinforcement. The ultimate tensile capacity of the GFRP bar is 827MPa, tensile modulus of elasticity of 46GPa and ultimate strain of 1.79%. The epoxy used for NSM technique is Dural LPL MV and the Euclid

chemical company manufactured it. This epoxy has a modulus of elasticity of 1172MPa, tensile strength of 21MPa, compressive strength of 69MPa and bond strength of 14MPa. U-wrapping was performed using 1mm thick unidirectional GFRP fabric by wet-layup procedure. The epoxy and GFRP fabric for wet-layup was supplied by Fyfe chemicals. The composite system is named "Tyfo SEH-51A" Composite using "Tyfo S Epoxy". Composite gross laminate properties according to the manufacturer are; Ultimate tensile strength in the primary fiber direction 575MPa, elongation at break 2.2%, tensile modulus of elasticity 26.1GPa and has a nominal laminate thickness of 1.3mm.

3.3 Beam dimensions and reinforcement

The beam length is 763mm and the span between the supports is 660.4mm. The beams were loaded under four point bending with two concentrated loads following ASTM standards. The spacing between two concentrated loads is 152mm. The cross section of the beam is a square with a depth of 152mm. All beams were reinforced with four #3 steel bars with a nominal diameter of 10mm. Of four longitudinal bars, two bars were used as compression reinforcement and two bars were used as tension reinforcement. #3 with nominal diameter of 10mm, stirrups were used to resist the shear reinforcement and spaced at 76mm. **Figure 3.1** shows the beam longitudinal section showing the reinforcement detailing and the dimensions of the beam and **Figure 3.2** shows the cross-section of the different beam types. All the specifications mentioned above are applicable to the beams of the groups in the **Table 3.1**.

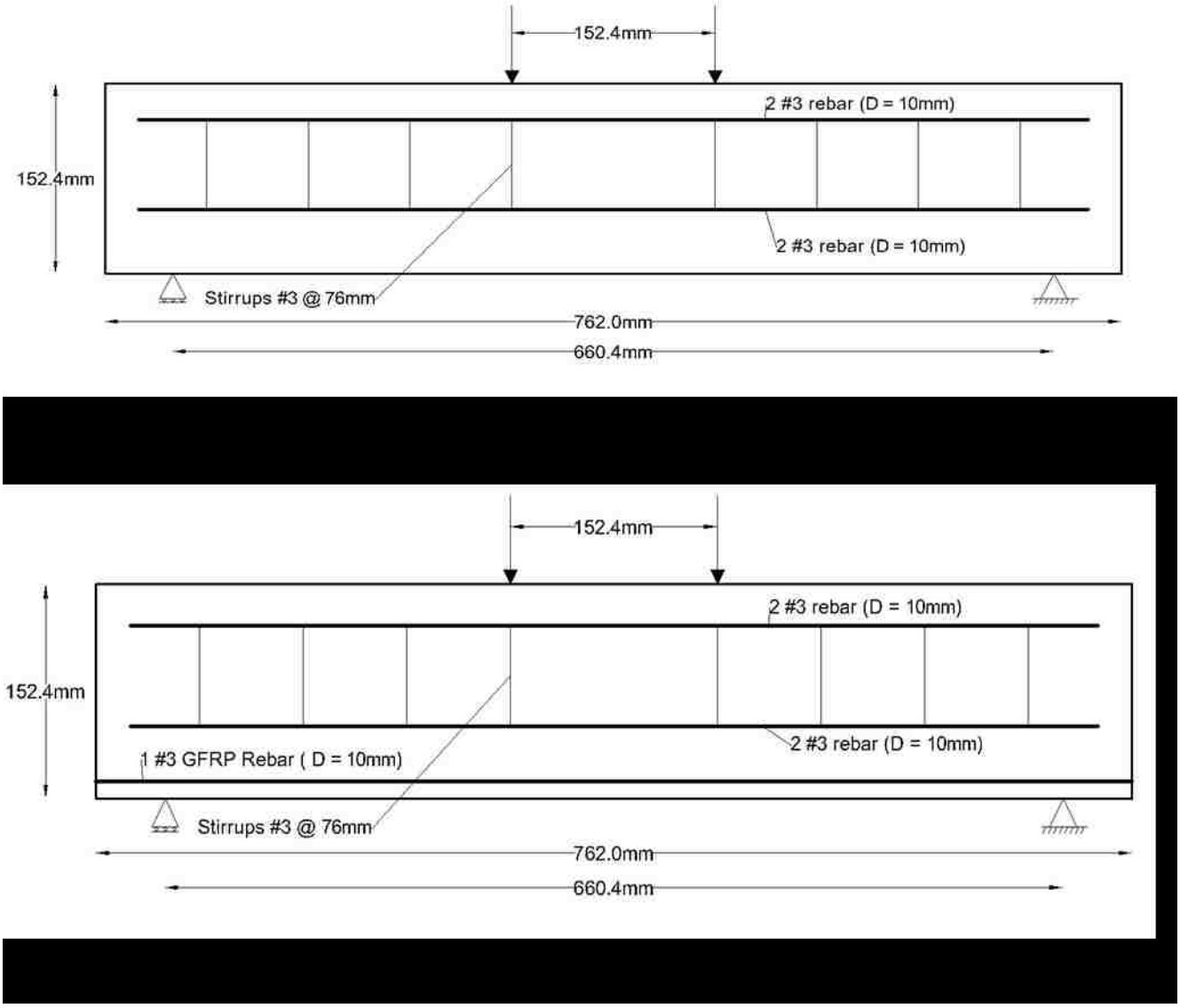

Figure 3.1: Longitudinal section of the beam; a.) Beam Control 'C' and beam with U-wrap only 'U'; b.) Beam with NSM only 'N', Beam with NSM and U-wrap 'NU' and Beam with NSM and U-wrap in shear zone only 'NUS'

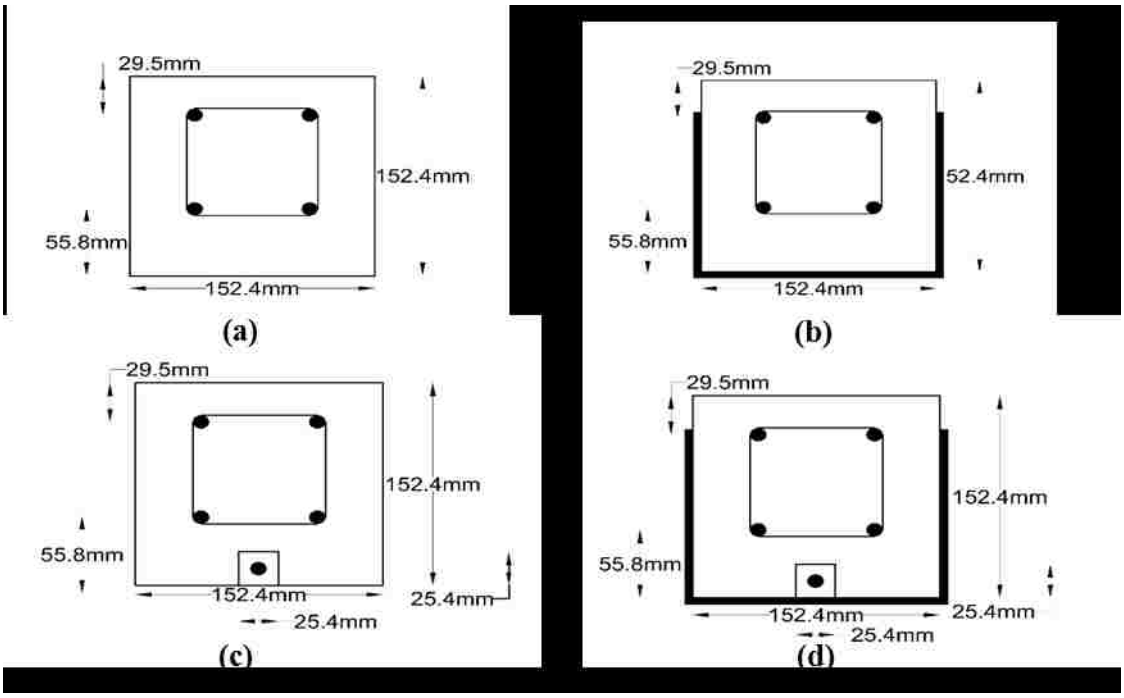

Figure 3.2: Cross section of (a) Beam-C (b) Beam-N (c) Beams-C (d) Beam-U and Beam-NUS

3.4 Strain Gauges

Strain gauges used were manufactured by omega Engineering Inc. OMEGA KFH-10-120-C1-11L3M3R strain gauge model with gauge length 10mm and resistance of 120Ω has been used. Concrete and steel strain gauges were installed at mid-span. Strains were measured at the top of the beam concrete in compression, compression steel, tension steel and GFRP for NSM specimens. **Figure 3.3** shows the different locations and placement of strain gauges.

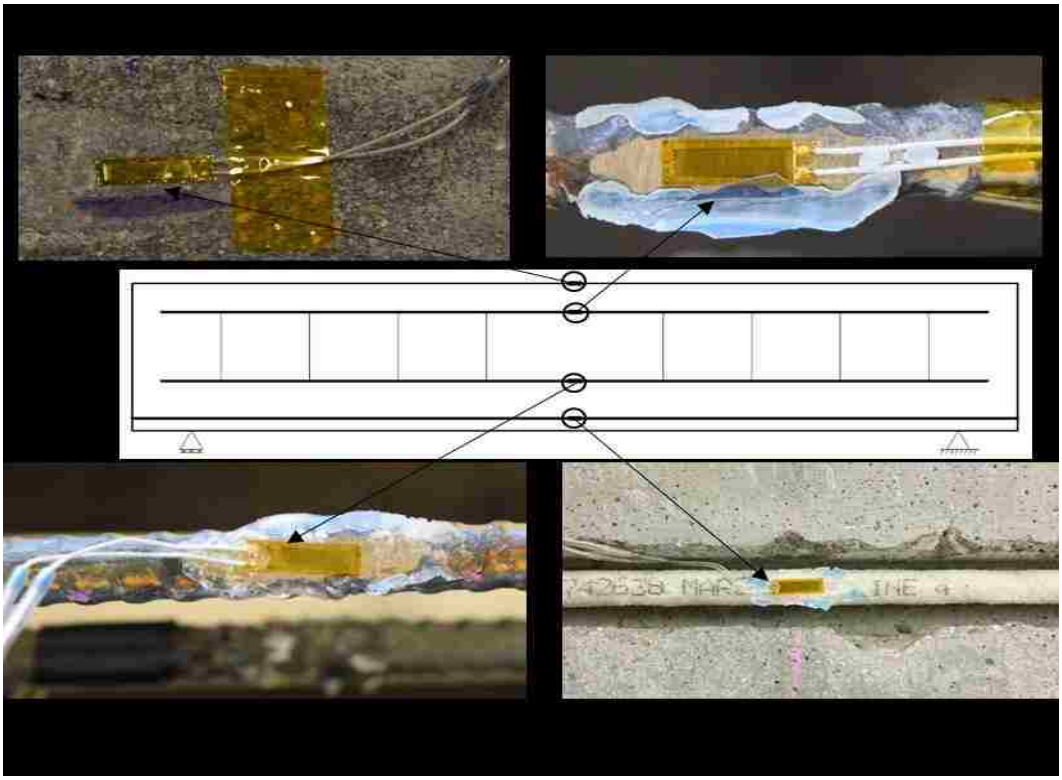

Figure 3.3: Schematic and pictures depicting the location and strain gauge fixture (a) Concrete compression fibers on top; (b) Compression steel; (c) Tension Steel; (d) Tension in NSM GFRP bar

3.5 Concrete Casting

Five steel molds with inner dimensions equal to the dimensions of the beam were used to cast the concrete beams. Reinforcement cages with compression and tension steel along with the stirrups were built in the lab according to the dimensions given in **Figure 3.4.** Plastic chairs available in the market with the height of 50mm were used, so that the clear cover is 50mm from bottom. A foam piece with dimensions 25mm width and depth was placed on the form bonded with a two-side adhesive tape to allow formation of groove on tension side of the beam in order to facilitate NSM flexural strengthening. **Figure 3.4 and Figure 3.5** showing steel molds after placing the cage and foam piece to have a precast NSM groove for flexural strengthening.

After placing the reinforcement steel cages into the forms, concrete was poured into the molds in 3 layers. After each layer concrete was vibrated using a needle vibrator to ensure perfect compaction removing any voids in the concrete. The mold was completely filled until the top of the form to have depth of 152.4mm and concluded by surface finishing. **Figure 3.6** shows the compacting process of the concrete while pouring. The molds were unmolded after twenty-four hours from pouring of concrete and set to cure for twenty-eight days(ASTM-C192/C, 2015). Concrete batching and curing was done following ASTM (ASTM-C192/C, 2015).

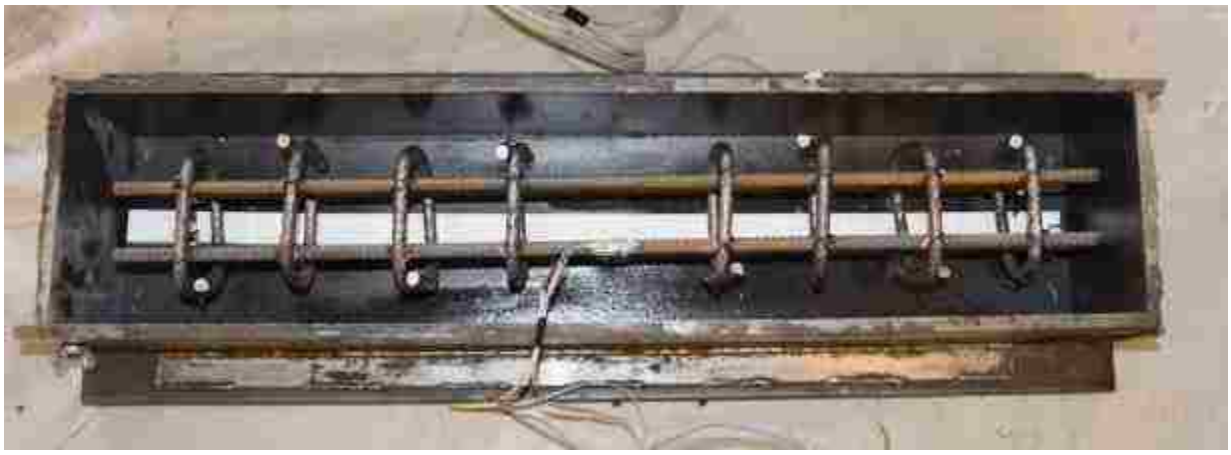

Figure 3.4: Reinforcement cage and foam piece to precast NSM groove

Figure 3.5: Prepared molds before pouring concrete

Figure 3.6: Concrete compaction using vibrator

3.6 NSM Flexural Strengthening

A square foam piece with side dimension of 25mm was used to make a precast groove on tension side of the concrete, the groove formed was a square groove with side dimension of 25mm

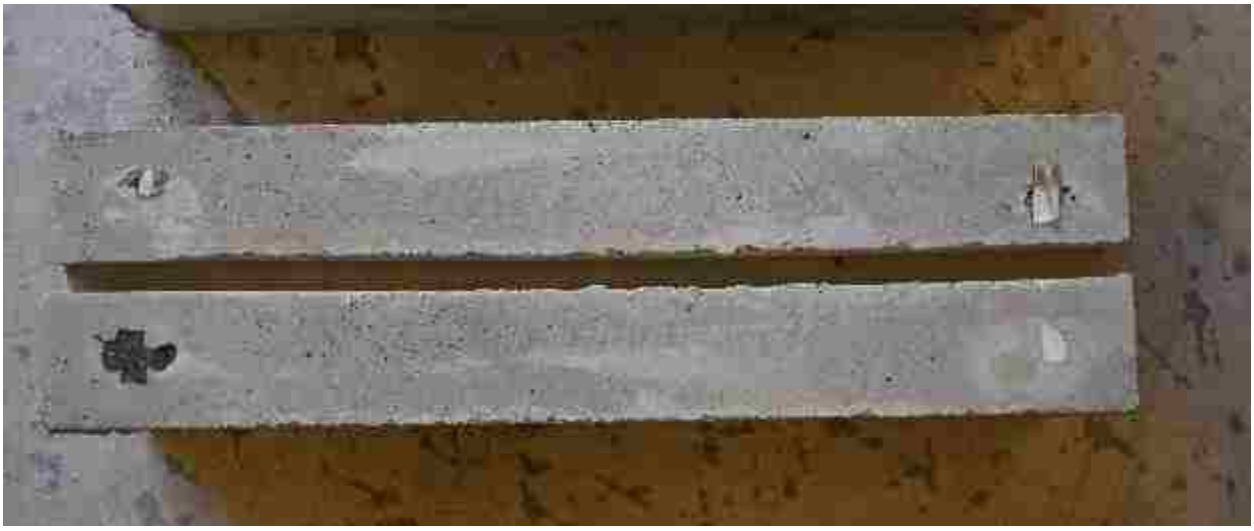

Figure 3.7: Beam NSM groove after cleaning

all along the length of the beam on tension side. Acetone was used as a solvent to remove all the foam from the groove, later a wire brush has been used to completely remove all the debris from the surface. The surface was then roughened using a sand paper, then cleaned using a water jet and then allowed to air dry for twenty-four hours to remove all the moisture from the groove. Later compressed air was used to remove any dust particles from NSM groove. These steps were performed to make sure that NSM groove was free of any dust, moisture and unwanted material on the groove surface. **Figure 3.7** shows beam with cleaned NSM groove.

Figure 3.8: NSM groove with GFRP bar before pouring the adhesive

After cleaning the groove, the GFRP bar was placed inside the groove extending outside the groove on both sides with supports of 139.7mm height to have it exactly at the center of the groove, then ends of the grooves on either sides were sealed completely using silicon sealant and allowed to completely harden for twenty four hours to form a perfect seal. After sealing the ends

with the bar the groove is filled with epoxy. The epoxy viscosity allowed it to completely fill the groove with epoxy and the epoxy is allowed to cure. Care was taken in surface preparation to have a rough surface to ensure mechanical bond between epoxy and concrete avoiding the failure

Figure 3.9: NSM groove being filled with epoxy

between epoxy and concrete. **Figure 3.8** shows the NSM groove with GFRP bar before pouring epoxy, **Figure 3.9** shows the NSM groove while pouring the epoxy. After complete hardening of epoxy, the beam is flexurally strengthened.

3.7 GFRP three side U-wrapping with wet layup

A three side U-wrapping is a technique employed for shear strengthening of concrete beams (ACI 440). Beams U, NU and NUS were strengthened using this GFRP wrapping technique. Beams NU and NUS were wrapped after strengthening with NSM-GFRP bars.

The surface preparation and installation was performed according to the manufacturer's guidelines and ACI standards (ACI 440). A one layer unidirectional glass fiber fabric with a wet-layup epoxy was used. The direction of the fibers was in the direction perpendicular to longitudinal direction of the beam, so that this wrapping does not contribute for flexural strength of the beams.

An angle grinder has been used to grind of the top concrete layer for removing any dust particles and have a rough surface. This step makes sure that the surface between GFRP and concrete does not form any air pockets after wrapping. The grinded surface was cleaned using compressed air and then by use of water jet. The beams were allowed to air-dry for twenty-four hours to remove all the moisture on the surface of the beams. Finally, it was made sure that the surface is clean, dry and free from any protrusions. **Figure 3.10** shows grinded beams ready for wrapping. **Figure 3.11** showing RC beam rounded edge prior to GFRP wet-layup application.

Figure 3.10: Grinded RC beams ready for FRP wrapping

Figure 3.11: RC Beam showing rounded edge prior to GFRP wet-layup application

The GFRP fabric was cut to the desired dimensions; 406mm in the direction of the fibers going along the two sides and the bottom of the beam and a length of 660mm opposite to the direction of fibers which is equal to the length between the two supports for the beam. The wet-layup epoxy is mixed accordingly in the ratio of 100 parts of component A to 34.5 parts of component B by weight and mixed for five minutes with a low speed mixture at 400-600RPM until a uniform mix is achieved. **Figure 3.12** showing mixing of epoxy.

Figure 3.12: Mixing of epoxy for wet-layup

Figure 3.13: Prime coat with adhesive before GFRP wet-layup

One prime coat of the epoxy was applied on the concrete substrate by using a roller. The GFRP fabric was saturated in the epoxy and then wrapped by hand. A roller was used to ensure correct orientation of the fibers. Using the same roller, any entrapped air was completely rolled out. **Figure 3.13** showing the prime coat on the beam, **Figure 3.14** showing GFRP fabric being impregnated in epoxy and **Figure 3.15** showing the beam after wrapping in wet-layup procedure.

This U-wetlayup shear strengthening for beams was carried out in two configuration, for beam series NU, the 3-side U-wrapping was carried out along the length of the beam and beam series NUS U-wrapping has been carried out only in the shear area of a four point bending configuration.

Figure 3.14: GFRP fabric saturated in adhesive

Figure 3.15: Beam after U-wrapping with GFRP fabric for shear strengthening

3.8 Curing Procedures

All the concrete beams after de-molding were used for 28days in a temperature controlled curing room at 24℃ ± 2℃ and a relative humidity of 97% was maintained (ACI 318 curing). Beams that were flexurally strengthened with NSM technique, the epoxy was allowed to cure for 14 days at room temperature to have the epoxy completely hardened. Beams BD and BE were U wrapped. This wrapping was performed 3 days after the NSM technique was performed and then these beams were allowed to cure for 14 days at room temperature to enable complete hardening of wrapping and have composite action with the beams. By this, both NSM epoxy and wrapping epoxy have passed the required curing time of 15days and the specimens were ready to test.

3.8 Flexural testing of beams

All the beams in the current study were tested under four point bending configuration with two concentrated loads spaced at 152mm at the mid span following ASTM standards. The two supports were spaced at 660mm leaving 50mm edge distance on both sides of the beam. One support is restrained in both vertical and horizontal direction acting as a hinge, but the other support was restrained only in vertical direction acting as a roller support. Instron MPT machine was used to load all the beam specimens to failure. The experiment was conducted under displacement control, the rate of displacement was 1mm/minute up to 15mm and later increased to 3mm/minute. The machine has a built in Linear Variable Deferential Transducers (LVDT), and a load cell connected to MTS 793 controller. **Figure 3.16** shows the section view of bending setup.

Figure 3.16: Four point bending test configuration

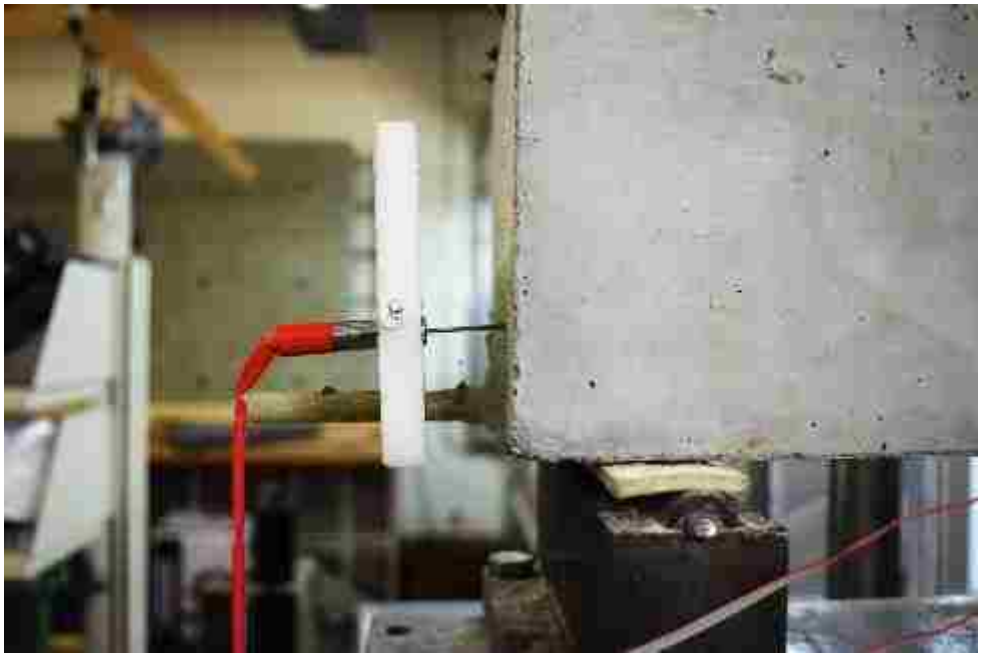

Figure 3.17: LVDT fixture to measure NSM bar debonding

For beams, two LVDTs were used to measure the slip in GFRP rebar caused by the de-bonding of the bar with epoxy substrates. In-order to facilitate the fixation of LVDTs, a square plastic plate with side 100mm and thickness 12mm was used. A hole equal to the bar diameter was drilled into the plate and this plate was coaxially inserted through the rebar on either ends and bonded it using epoxy, the by fixing the plate. Another hole was drilled through the plate with diameter equal to thickness of LVDT holder and this holder was inserted into this hole. This hole was also provided with another provision using a tapping screw such that the LVDT holder can fixed using the screw. As this plate is now completely fixed to the rebar, the LVDT needle tip is bonded to beam face using quick set epoxy such that any bar slip is recorded. **Figure 3.17** shows the LVDT fixture to measure end slip. **Figure 3.18** shows the LVDT fixture while testing.

Figure 3.18: LVDT fixture while test in progress showing slip of NSM GFRP bar

Two days before the test of the beams, the top surface was grinded to remove any excess epoxy and remove any irregularities on the top surface of the beams and a strain gauge was installed at the mid span of the beam to accurately measure the strain at top of the concrete. Accurate markings over the beams were made to mark the center, support area and two concentrated loading points to remove any discrepancies. For beams provisions for fixing the LVDTs were fixed using a 12.7mm thick plate before one day of testing. On the day of testing the beam was manually lifted and placed on the setup.

Load and deflection of the beam, strains in compression of concrete, strain in compression steel, strain in tension steel, strain in GFRP for NSM strengthened beams. End slip of GFRP was measured using LVDT's on either sides of the beam to measure the slip of the bar after de-bonding.

3.9 Summary

Beams C1 through C5 are simple RC beams and acts as control beams. **Figure 3.19** shows the five beams before testing.

Figure 3.19: Beams control C1 through C5 ready for testing

Beams U1 through U5 are simple RC beams with 3-side U-wrapping, these were prepared to see if there is any contribution in flexure by wrapping the beams. **Figure 3.20** shows the five beams before testing.

Figure 3.20: Beams with U-wrap shear strengthening only U1-U5 before testing

Beams N1 through N5 are the RC beams are flexurally strengthened with NSM GFRP technique. **Figure 3.21** shows the five beams before testing.

Figure 3.21: Beams with NSM flexural strengthening only N1-N5 before testing

Beams NU1 through NU5 are the RC beams are flexurally strengthened with NSM GFRP technique and shear strengthened using 3side U-wrap wet-layup technique. **Figure 3.22** shows the five beams before testing.

Figure 3.22: Beams with NSM flexural strengthening and U-wrap shear strengthening NU1-NU5 before testing

Figure 3.23: Beams with NSM flexural strengthening and U-wrap shear strengthening in shear zone only NUS2-NUS4 before testing, where NUS1 was already tested

Beams NUS1 through NUS5 are the RC beams are flexurally strengthened with NSM GFRP technique and confined using 3side U-wrap wet-layup technique in shear area only. **Figure 3.23** shows the 3 beams of 5 beams before testing. One of the beams failed because of the malfunction of the loading frame.

Chapter 4 Results and Discussion

This chapter will present the properties of normal concrete used followed by theoretical prediction of flexural capacity of the RC beams with and without FRP strengthening. Later, experimental observation of the RC beam series C, U, N, NU and NUS are presented. Followed by critical analysis and discussion of the results is presented by comparing the experimental observations of five beam batches.

4.1 Concrete properties

The concrete used was self-prepared in the structural laboratory in The University of New Mexico. The maximum nominal aggregate size used in the concrete mix was 12.7mm. The slump of the concrete used was 100mm±12mm as shown in **Figure 4.1**. The temperature of the concrete was measured immediately after mixing and it was 12℃ ± 1℃ (ASTM-C1064, 2012). 12 concrete cylinders 100mm diameter and 200mm height were cast. The compressive strength of the concrete was measured after 7 days and 28 days of curing following ASTM (ASTM-C39, 2015). The tensile strength and Young's modulus of the concrete at 28days were tested (ASTM-C469, 2014; ASTM-C496, 2011). **Table 4.1** presents the tested results of the normal concrete used in the current study. Stress strain curve of the concrete compression test is presented in **Figure: 4.2.**

Table 4.1 Properties of concrete at 7 days and 28 days

	Mean Value [MPa]	Standard Deviation [MPa]
Compressive strength (7 days)	44.1	3.2
Compressive strength (28 days)	54.8	2.5
Modulus of Elasticity	41335	-
Tensile strength (28 days)	4.6	0.7

Figure 4.1: Slump of concrete

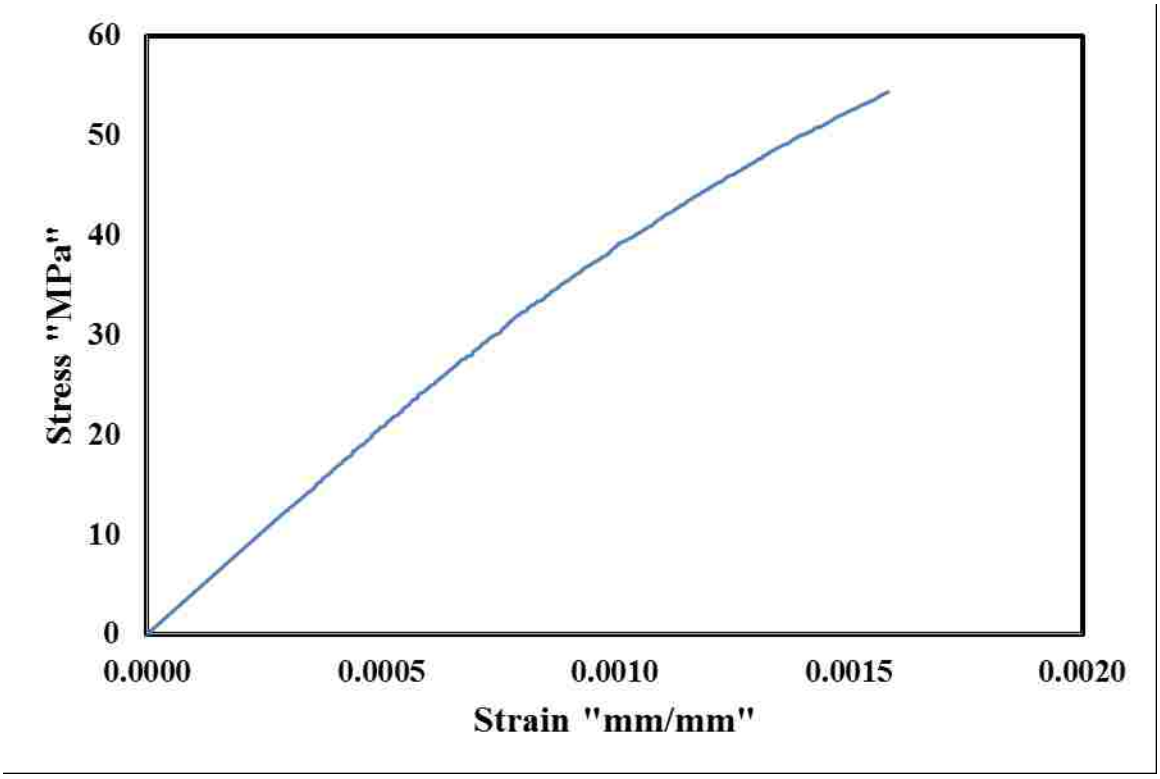

Figure 4.2: Stress vs Strain concrete

4.2. Predicted RC beam capacity

This section, presents the theoretically predicted behavior of all the beam types. All the beams were tested in 4-point bending configuration. Generally, flexural performance is dominant in 4-point bending fixture, it also contributes to zero shear force between two loading points. This 4-point bending configuration is shown in **Figure: 4.3**. The bending moment diagram and shear force diagrams are shown in **Figure: 4.4** and **Figure: 4.5** respectively.

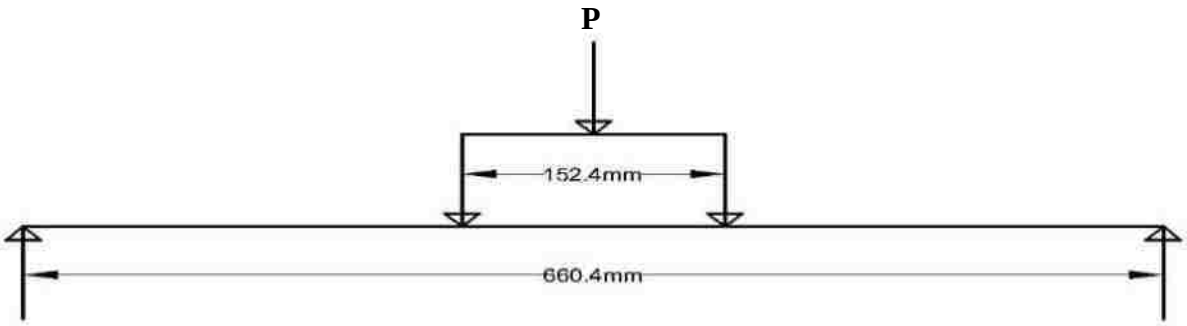

Figure 4.3 Schematic to show four point bending

0.127P (kN.m)

Figure 4.4 Bending moment diagram

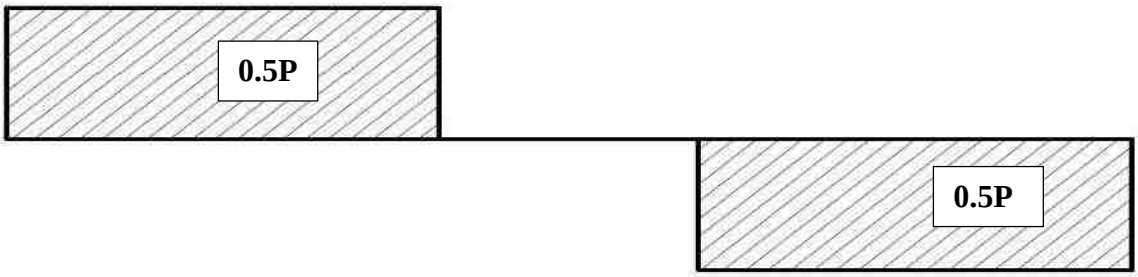

Figure 4.5 Shear force diagram

4.2.1. Predicted behavior

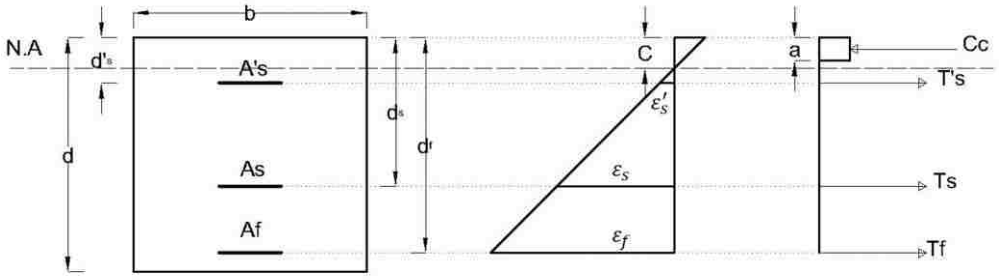

Figure 4.6 Schematic showing beam cross section

The moments of the beams were calculated based on the **equation 4.1** and the cracking moment corresponding to the beam has been calculated using the **equation 4.2.** All the flexural calculations were calculated following ACI 318-14 (ACI-318, 2014).

$$M = 0.127P \quad \textbf{(4.1)}$$

Where:

M = Bending Moment (kN.m)

P = Load Applied (kN)

4.2.2 Service state behavior

$$M_{cr} = \frac{f_t * I_g}{y_t} 10^{-6} \quad \textbf{(4.2)}$$

Where:

M_{cr}= Cracking moment (kN.m)

f_t= Tensile strength of concrete (MPa)

I_g = Gross moment of inertia (mm^4)

y_t = Distance of neutral axis from bottom of the beam

In order to calculate the gross moment of inertia the modular ratio between steel-concrete was considered for RC beams – control C and RC beam shear strengthened with FRP U-wrap shear strengthening U and modular ratio between steel-concrete and GFRP-concrete was considered for RC beams flexurally strengthened with NSM-FRP N, RC beam strengthened flexurally with NSM-FRP and U-wrap shear strengthening NU and RC beam strengthened with NSM-FRP and U-wrap shear strengthening in shear area only NUS. The modular ratio between U-wrapped GFRP is neglected, because the orientation of fibers does not contribute for flexural capacity of the beam. The equations 4.3 and 4.4 are used to calculate the distance from centroid to bottom of the beam. Equation 4.3 corresponds to RC beams C and U and equation 4.4 corresponds to beams – N, NU and NUS.

$$y_t = \frac{(A_g * d_g) + ((n_s - 1) * A'_s * d'_s) + ((n_s - 1) * A_s * d_s)}{A_g + ((n_s - 1) * A'_s) + (n_s - 1) * A_s} \quad \textbf{(4.3)}$$

$$y_t = \frac{(A_g * d_g) + ((n_s - 1) * A'_s * d'_s) + ((n_s - 1) * A_s * d_s) + ((n_f - 1) * A_f * d_f)}{A_g + ((n_s - 1) * A'_s) + (n_s - 1) * A_s + (n_f - 1) * A_f} \quad \textbf{(4.4)}$$

Where:

A_g: Gross correctional area (mm^2)

y_g: Distance from centroid of section to the bottom of the beam (mm)

n_s: Modular ratio between modus of elasticity of steel and modulus of elasticity of concrete

A'_s: Area of compression steel used for reinforcement (mm^2)

d'_s: Distance from center of the compression steel to the bottom of the beam (mm)

A_s: Area of tension steel used for reinforcement (mm^2)

d_s: Distance from center of the tension steel to the bottom of the beam (mm)

A_f: Area of tension GFRP reinforcement using NSM technique (mm^2)

n_f: Modular ratio between modus of elasticity of GFRP and modulus of elasticity of concrete

d_s: Distance from center of the GFRP to the bottom of the beam (mm)

y_t: Distance from the neutral axis to the bottom of the beam (mm)

4.2.3 Ultimate flexural capacity

Based on the compressive strength of concrete and the reinforcement ratio, the nominal flexural capacity and nominal shear capacity were calculated in order to facilitate the calculations, the compressive strain at ultimate was assumed to be -0.003 for all the beams (ACI-318, 2014). The calculation procedure for flexural capacity and shear capacity for all the beam types are given bellow.

The nominal flexural capacity for beams C and U are given by:

$$C_c + C_s = T_s \quad \textbf{(4.5)}$$

Where:

C_c: Compression force in concrete (kN)

C_s: Compression force in compression steel (kN)

T_s: Tension force in tension steel (kN)

The **equation 4.5** can be expanded as bellow

$$0.85 f_c' B \beta_1 C + A_s' * f_y = A_s * f_y \quad \textbf{(4.6)}$$

Where:

f_c': Characteristic compressive strength of concrete (MPa)

a: compression block depth (mm)

B: width of the beam (mm)

f_y: Yield stress of steel (MPa)

C: Depth of compression zone from force equilibrium

β_1: Concrete stress block coefficient

Based on ACI 318-14 the value for β_1 is considered as 0.65 for 50MPa concrete.

Equation 4.5 can be rewritten as equation 4.6:

$$C = \frac{A_s * f_y - A_s' * f_y}{0.85 f_c' B \beta_1} \quad \textbf{(4.7)}$$

From equation 4.6 depth of compression zone can be calculated. In order to facilitate the calculation we assume that the tension steel yields. We develop an equation in terms of ε_s strain in steel.

$$f_s = E_s * \varepsilon_s \leq f_y \quad \textbf{(4.8)}$$

Where:

ε_s: Strain in compression steel

E_s: Modulus of elasticity of steel

Using the concept of similar triangles equation 4.9 is developed:

$$\varepsilon_s = \frac{\varepsilon_{cu} * (C - d_s)}{C} \quad \textbf{(4.9)}$$

Where:

ε_{cu}: Compressive strain in concrete ultimate

d_s: distance centerline of steel rebar to top of the concrete.

Now equation 4.7 can be rewritten as:

$$0.85 f_c' B \beta_1 C = A_s * f_y - A_s' * E_s * \frac{\varepsilon_{cu} * (C - d_s)}{C} \quad \textbf{(4.10)}$$

The equation 4.10 can be written in second degree quadratic equation form:

$$aC^2 + bC + d = 0 \quad \textbf{(4.11)}$$

Where:

a: $0.85 f_c' B \beta_1$

b: $A_s' * E_s * \varepsilon_{cu} - A_s * f_y$

d: $A_s' * E_s * \varepsilon_{cu} * d_s$

$$C = \frac{-b \pm \sqrt{b^2 - 4ad}}{2a} \quad \textbf{(4.12)}$$

Once the compression block depth (C) is calculated the strain in tension and compression steel can be checked and confined to yield. Using the depth of the compression block, the nominal moment capacity is calculated using **equation 4.14.**

$$M_n = A_s f_y (d_s - \frac{a}{2}) + A_s f_y (d'_s - \frac{a}{2}) \quad \textbf{(4.13)}$$

The equations 4.11, 4.12 and 4.14 can be rewritten as following for Beams, N, NU and NUS:

$$0.85 f'_c B \beta_1 C = A_s * f_y + A_f * f_f - A'_s * E_y * \frac{\varepsilon_{cu} * (C - d_s)}{C} \quad \textbf{(4.14)}$$

Where:

A_f: GFRP bar area

f_f: Stress in GFRP bar

It is assumed that the deboning between FRP bar and surrounding epoxy will take place at 60% of its ultimate capacity base ACI 440.2R-08.

The equation 4.10 can be written in second degree quadratic equation form:

$$aC^2 + bC + d = 0 \quad \textbf{(4.15)}$$

Where:

a: $0.85 f'_c B \beta_1$

b: $A'_s * E_y * \varepsilon_{cu} - A_s * f_y - A_f * f_f$

d: $A'_s * E_y * \varepsilon_{cu} * d_s$

$$C = \frac{-b \pm \sqrt{b^2 - 4ad}}{2a} \quad \textbf{(4.16)}$$

After calculating the compression zone (C), depth of the compression block is calculated. Using the depth of the compression block, the nominal moment capacity is calculated using **equation 4.14.**

$$M_n = A_s f_y (d_s - \frac{a}{2}) + A_f f_f (d_f - \frac{a}{2}) - A_s f_y (d_s' - \frac{a}{2}) \quad \textbf{(4.17)}$$

$$f_f = \varepsilon_f * E_f \quad \textbf{(4.18)}$$

$$\varepsilon_f = \epsilon_c (\frac{d_f - c}{c}) \quad \textbf{(4.19)}$$

Where:

d_f: Distance from centerline of GFRP bar to top of the concrete

4.2.3 Ultimate state shear capacity

The nominal shear capacity V_n for the beams is calculated based on ACI 318. The **equation 4.18** is used for beams C, N and equation 4.19 is used for beams U, NU and NUS.

$$V_n = (V_c + V_s) \quad \textbf{(4.20)}$$

$$V_n = (V_c + V_s + V_f) \quad \textbf{(4.21)}$$

Where:

V_c: Shear contribution from concrete following ACI 318

V_s: Shear contribution from steel stirrups following ACI 318 abiding to assumption that the steel yields.

V_f: Shear contribution from GFRP U-wrapping following ACI-440

$$V_c = \frac{\sqrt{f_c'}}{6} b_w d \quad \textbf{(4.22)}$$

$$V_s = \frac{A_v f_y d}{s} \quad \textbf{(4.23)}$$

$$V_f = \frac{A_{fv} f_{fe} d_{fv}}{s_f} \quad \textbf{(4.24)}$$

$$\varepsilon_{fe} = k_v \varepsilon_{fu} \quad \textbf{(4.25)}$$

$$k_v = \frac{k_1 k_2 L_e}{11900 \varepsilon_{fu}} \quad \textbf{(4.26)}$$

$$L_e = \frac{23300}{(n t_f E_f)^{0.58}} \quad \textbf{(4.27)}$$

$$k_1 = (\frac{f_c'}{27})^{2/3} \quad \textbf{(4.28)}$$

$$k_2 = \frac{d_{fv} - L_e}{d_{fv}} \quad \textbf{(4.29)}$$

Where:

b_w: Width of the beam (mm)

d: depth of the beam (mm)

A_v: Area of steel for shear stirrups (mm^2)

f_y: yield stress of steel (MPa)

d: Depth of reinforcement stirrups (mm)

s: Spacing between the stirrups (mm)

A_{fv}: Area of FRP shear reinforcement (mm^2)

f_{fe}: Effective stress in the FRP (MPa)

$d_{fv:}$ Effective depth of FRP shear reinforcement (mm)

s_f: Spacing between the FRP laminates (mm)

k_v: Reduction factor for development length

k_1: Modification factor to account for concrete strength

k_2: Modification factor to account for wrapping scheme

E_f: Modulus of elasticity of FRP composite laminate (MPa)

ε_{fu}: Ultimate strain in tension for FRP laminate

ε_{fe}: Effective strain in tension for FRP laminate

n: number of laminates

Table 4.2: Predicted nominal flexural and shear capacities of all 4 beam series

Beams	C	U	N	NU	NUS
I_g (*10^7 mm^4)	4.66	4.66	4.67	4.67	4.67
Cracking Moment (kN.m)	2.78	2.78	2.79	2.79	2.79
Cracking force (kN)	21.8	21.8	21.9	21.9	21.9
Ultimate flexural capacity (kN.m)	5.97	5.97	5.97	5.97	5.97
Maximum flexural load (kN)	47	47	91.8	91.8	91.8
Ultimate shear capacity (kN)	107	218	107	218	174
Maximum shear load capacity (kN)	214	436	214	436	348

4.3 Experimental Results

This section presents the results of experimental program conducted by testing the beams under four-point bending fixture.

4.3.1 Beam Control (C)

Control five beams have been tested designated as C1 through C5. These beams are simple RC beams with steel as the reinforcement. As the beams were loaded two vertical cracks appeared near the two loading points and these were the only two cracks appeared all along the testing until failure. The two cracks appeared simultaneously at the same point corresponding to a load of 18.2kN ± 2.2kN for all 5beams. The corresponding moment was calculated to be 2.3kN.m ± 0.2kN.m. These flexural cracks are shown **in Figure 4.7**

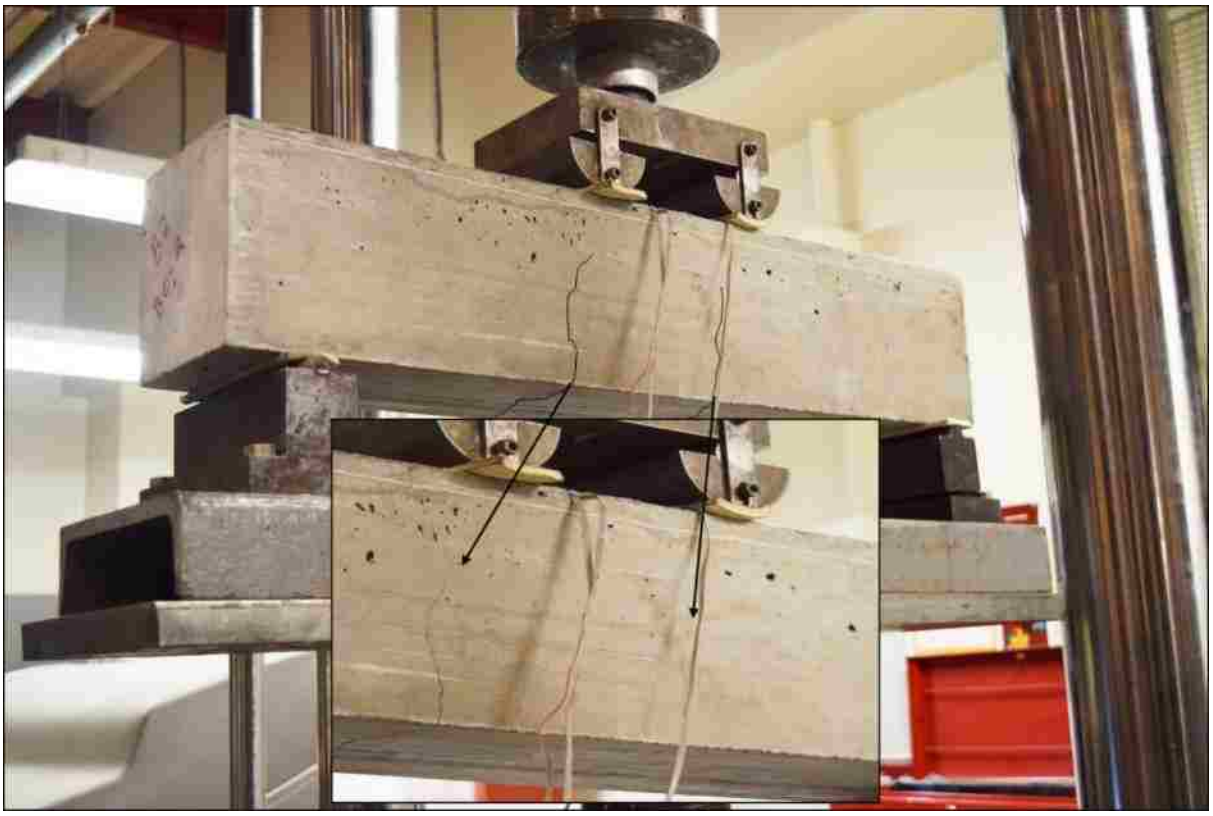

Figure 4.7: Beam control showing initial cracks at the loading points

Table 4.3: Experimental results control RC beams

	Linear- Elastic			Failure		
	Force	Deflection	Moment	Force	Deflection	Moment
	kN	mm	kN.m	kN	mm	kN.m
C1	51.2	4.4	6.5	65.4	10.9	8.3
C2	50.6	4.5	6.4	62.9	10.1	8.0
C3	50.1	4.4	6.4	65.3	11.4	8.3
C4	54.4	4.7	6.9	70.2	10.3	8.9
C5	55.2	4.6	7.0	72.6	10.2	9.2
Mean	52.3	4.5	6.6	67.3	10.6	8.5
Stdev	2.3	0.1	0.3	4.0	0.5	0.5

The beams C1 to C5 could carry a mean load of 67.3kN ± 4.0 kN. The corresponding mean moment at failure was calculated to be 8.5 kN.m ± 0.5 kN.m. **Table 4.3** presents the maximum loads and moments corresponding to each beam. The load deflection behavior for beams C was linear-elastic up to a mean load 52.3kN corresponding to mean mid-span deflection of 4.5mm. This linear behavior was until the strain in tension steel reached 0.0021 which is the linear elastic limit or yield strain of the steel rebar. The load deflection curves of all five beams are shown in **Figure 4.8.**

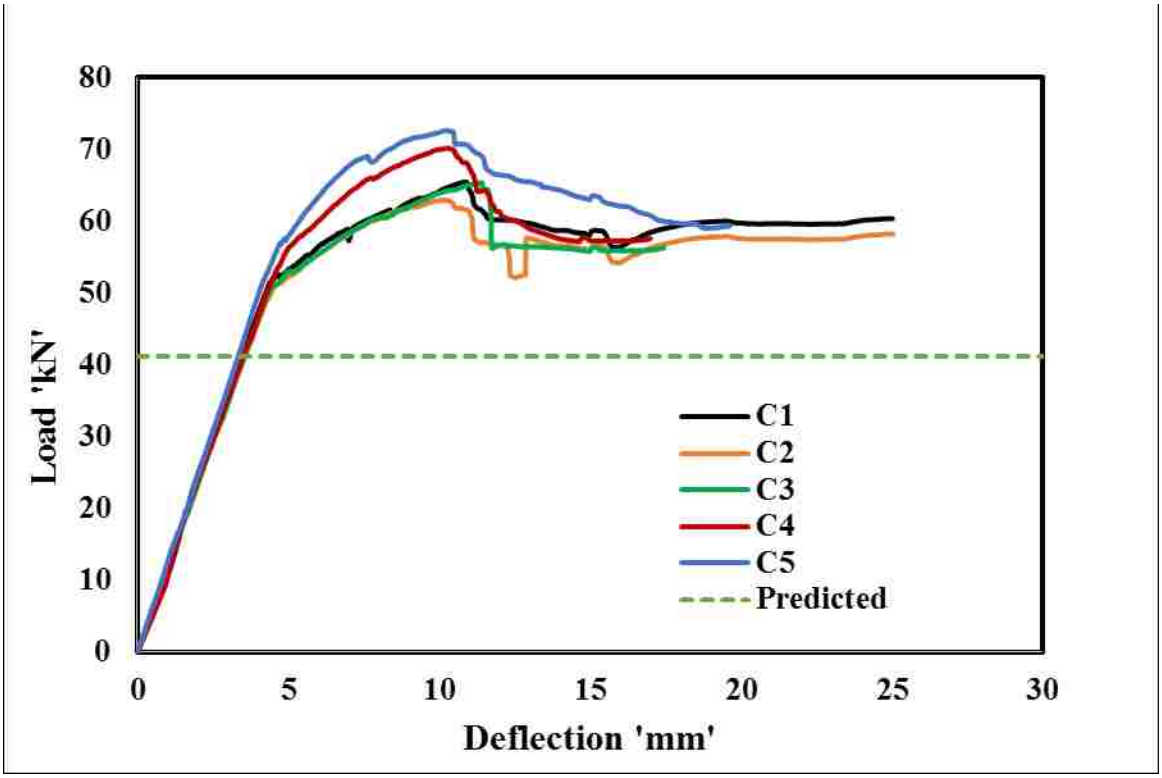

Figure 4.8: Load deflection behavior of control RC beams

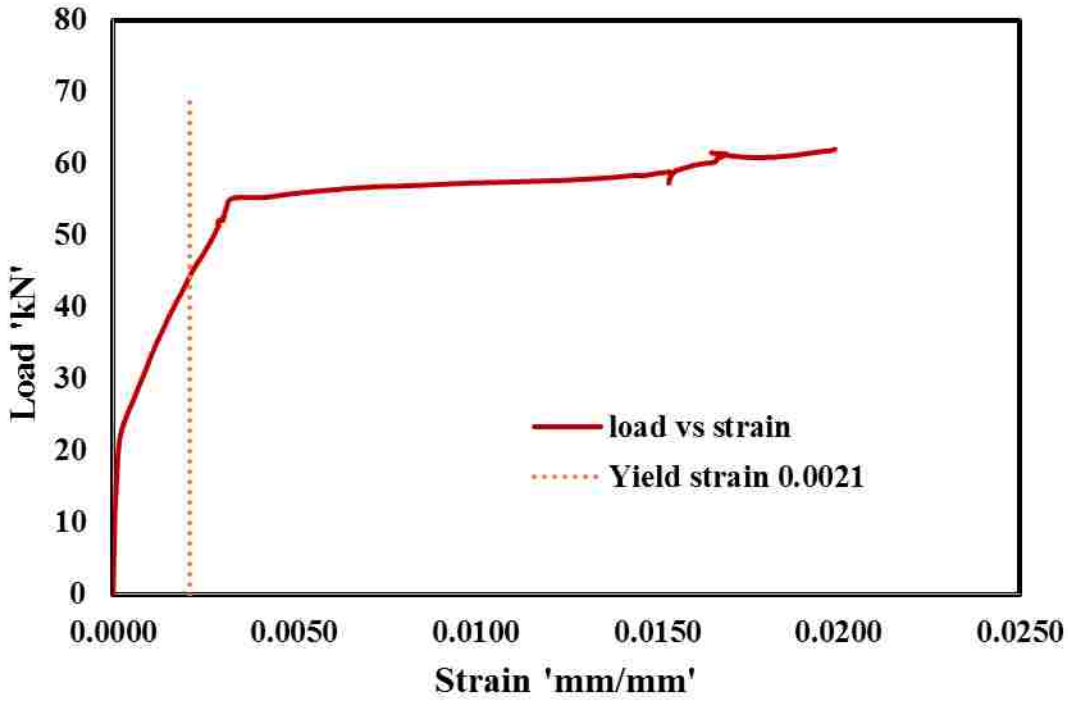

Figure 4.9: Load vs strain in tension steel for control RC Beam – C1

Strains in concrete top compression fibers, compression steel and tension steel were measured using strain gauges for beam C1. Load vs strain in tension steel bar had been plotted and shown in **Figure 4.9.** It could be observed that the rebar reached 0.0021 yield strain at a load of 44.4kN and the corresponding mid-span deflection was measured to be 3.7mm for beam C1. The strain gauge stopped reading at a strain of 0.015 and the corresponding load to this strain is 62.9kN. At this same point of steel maximum strain, the strain in top compression fibers reached 0.003 and increased up to 0.0042 there by beam failed in crushing of concrete. The load corresponding to strain 0.0042 was recorded to be 62.9kN and the corresponding mid-span deflection is 9.1mm. **Figure 4.10** shows the plot between load and the strain in top compression fibers. Crushing of concrete failure is shown in **Figure 4.11.**

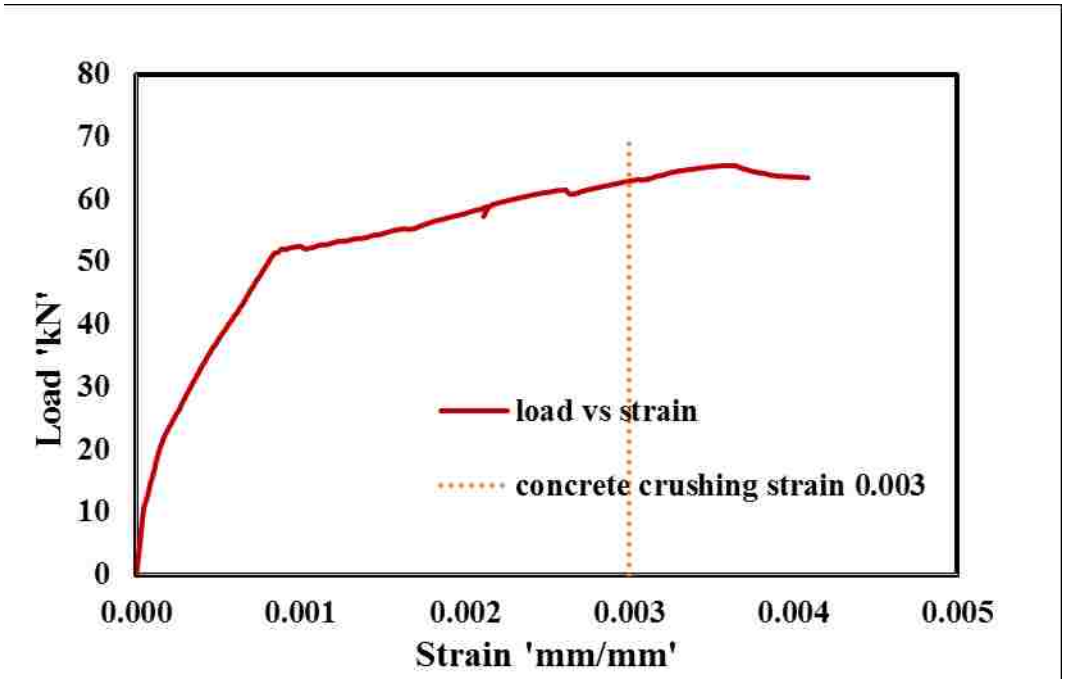

Figure 4.10: Load vs Strain in concrete top compression fibers for control beam C1

Figure 4.11 Control beam C-3 after failure showing concrete crushing

Using the concept of similar triangles, concrete compression (c) zone can be computed from the strain distribution diagram. The strain distribution diagrams at different load intervals up to a maximum load are presented in **Figure 4.13.** This c value was used to compute the moment curvature. Moment curvature plot is presented in **Figure 4.12**.

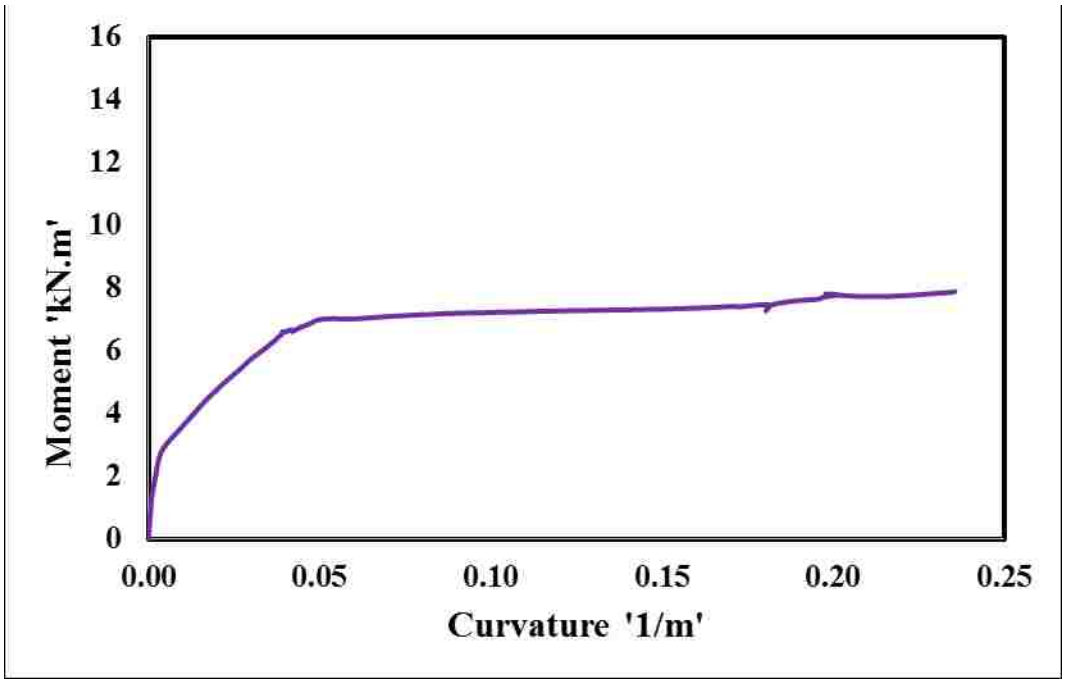

Figure 4.12: Moment curvature curve for beam C1

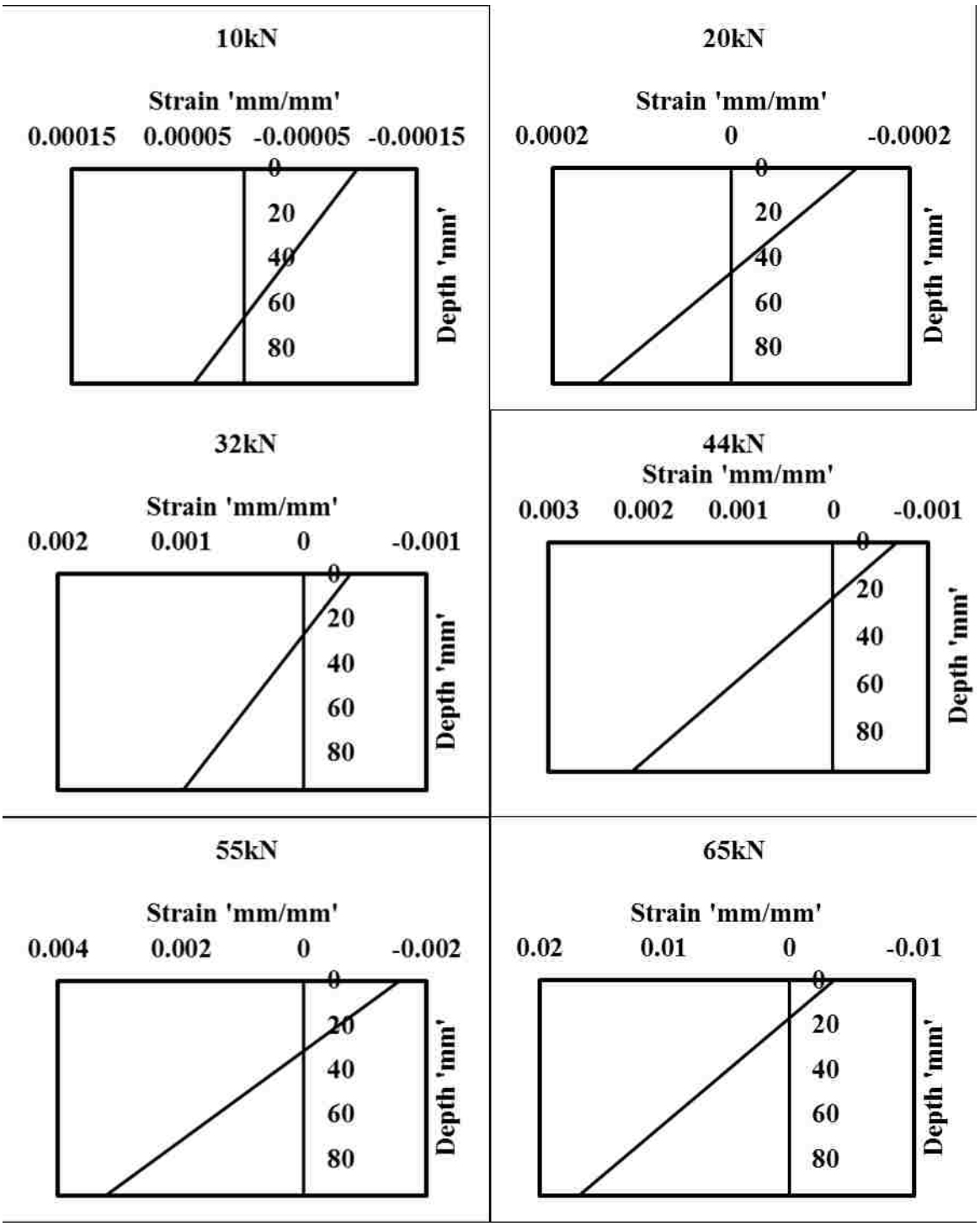

Figure 4.13: Strain distribution for different load levels for RC Beam Control C

4.3.2 Beam U-Wrapped (U)

Five FRP U-wrapped beams have been tested designated as U1 through U5. These beams are simple RC beams with steel as the reinforcement and shear strengthened with GFRP 3-side U-wrapping. The significance of this beam batch is to observe, if the GFRP shear strengthening will contribute to the flexural strength. The appearance of the flexural cracks was at a higher load compared to the control beams as the wrapping was covering the beam making it not possible to observe the crack when it first formed. **Figure 4.14.** Showing beam U-wrapped while loading on the Instron loading frame.

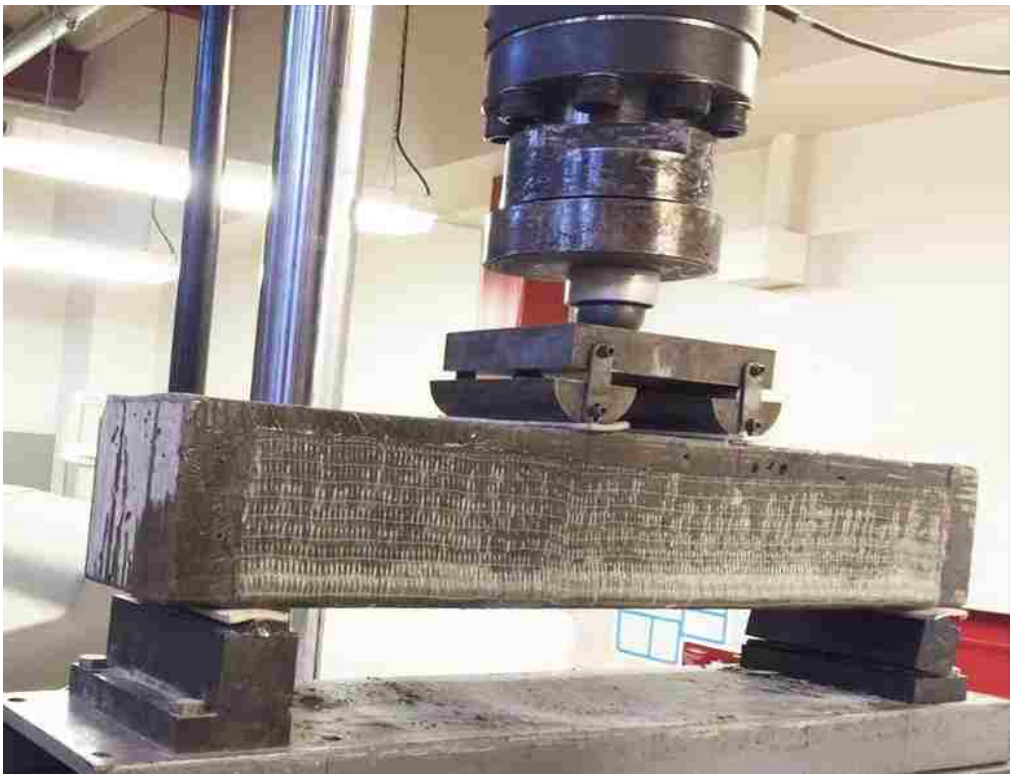

Figure 4.14: FRP U-wrapped beam (U) while loading

Beams FRP U-wrapped U1 to U5 could carry a mean load of 72.1kN ± 1.7kN. The corresponding mean moment at failure was computed to be 9.2kN.m ± 0.2kN.m. **Table 4.5** presents the corresponding loads and moments carried by each beam. The load deflection curves

of all 5 beams are shown in **Figure 4.15**. The load deflection behavior was identical to the beams C, which is linear-elastic up to a mean load of 52.7kN ± 4.6kN with a corresponding deflection at mid-span is 4.38mm ± 0.55mm. This linear elastic behavior continued until the strain in tension steel reached 0.0021 which is the linear elastic limit of the steel bar.

For the strains looking into beam U1, which is the only beam to have the strain gauges. The strains are measured on top concrete fibers, compression steel and tension steel. When the strain in tension steel reached 0.0021, the corresponding load was measured to be 44.3kN with a deflection of 3.39mm which is close to the theoretical predicted load value. The maximum recorded strain in tension steel was 0.019 at a load of 68.04kN and the beam failed at a load of 73kN. The load vs strain in tension steel is presented in **Figure 4.17**. The strain in concrete compression is 0.003 when the load was 68.04kN the same point when the maximum strain in tension steel was recorded. The maximum strain recorded in concrete top compression is 0.0035 with a corresponding load of 70.5kN and a deflection of 10.9 was measured at this point. There by with a slight increase in load to 73kN, the beam failed. **Figure 4.16** shows the failed beam clearly showing crushing of concrete. For the hypothesis, the beam went on linear elastic in the beginning, later becoming non-linear because of the steel yielding, the two flexural cracks developed and when strain in concrete compression increased over 0.0035, the beam failed in concrete crushing. The load vs strain in top compression fibers of concrete is presented in **Figure 4.17.**

The strain distributions for various load stages are presented in **Figure 4.19.** This strain distribution values were used to compute the actual compression (c) zone using the concept of similar triangles. Also the moment vs curvature for FRP U-wrapped beam is presented in **Figure 4.18**.

Table 4.4: Experimental results of beams U

	Linear- Elastic			Failure		
	Force	Deflection	Moment	Force	Deflection	Moment
	kN	mm	kN.m	kN	mm	kN.m
U1	58.4	4.7	7.4	73.0	9.3	9.3
U2	56.1	5.0	7.1	72.7	9.2	9.2
U3	52.8	4.7	6.7	72.5	9.2	9.2
U4	48.6	4.0	6.2	73.3	9.3	9.3
U5	47.7	3.7	6.1	69.2	8.8	8.8
Mean	52.7	4.4	6.7	72.1	9.2	9.2
Stdev	4.6	0.6	0.6	1.7	0.2	0.2

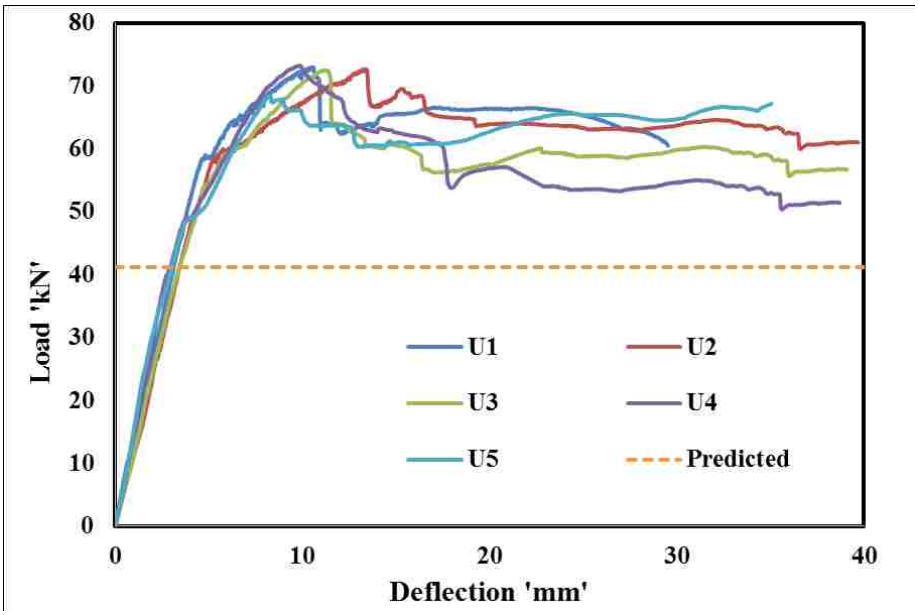

Figure 4.15: Load deflection curves of RC beams strengthened with FRP U-wrap shear strengthening (U)

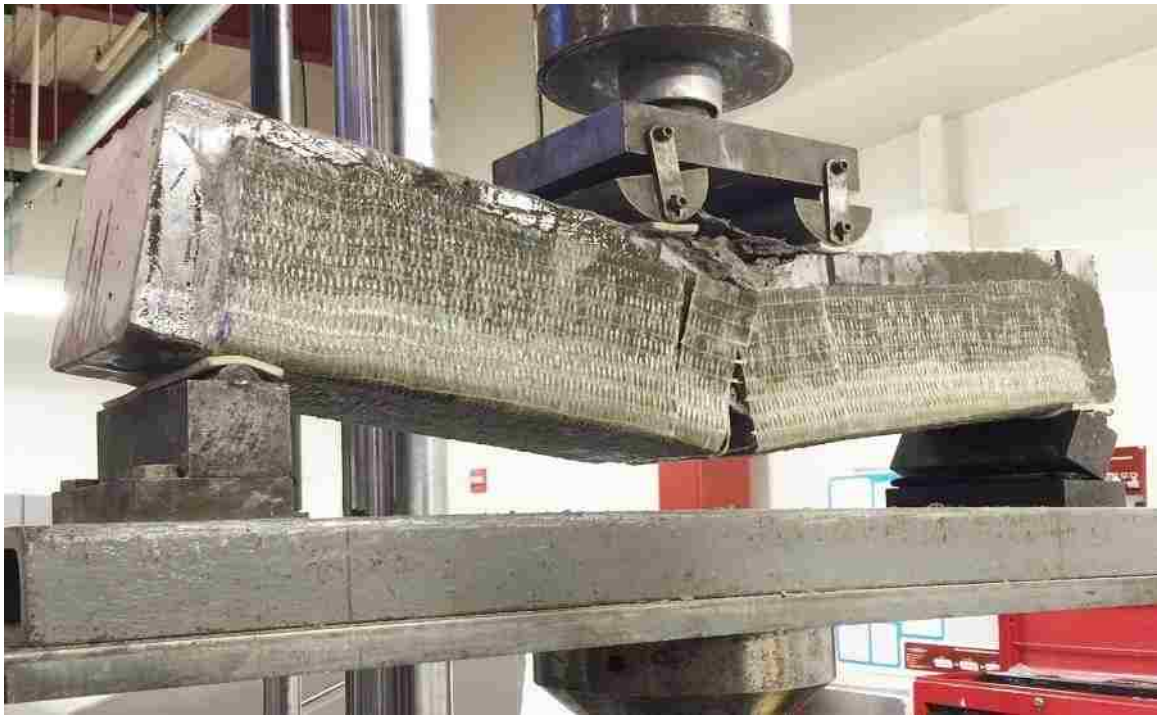

Figure 4.16: RC Beam U3 after failure

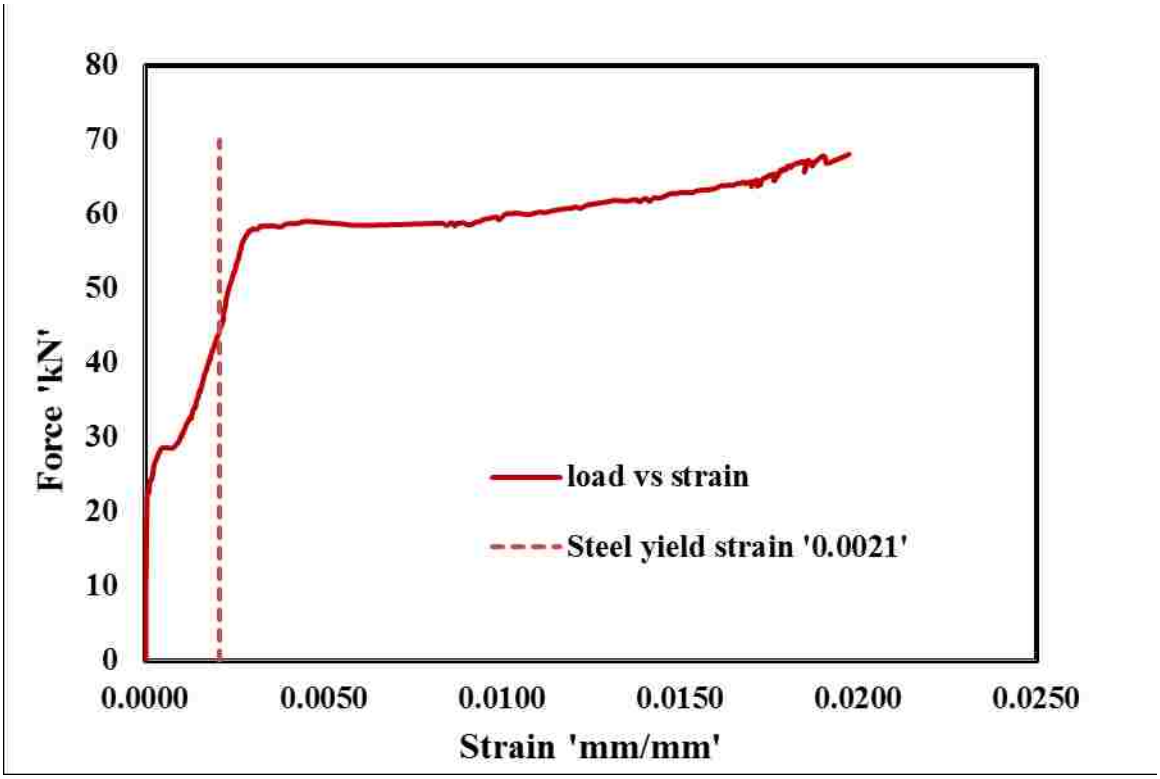

Figure 4.17: Load vs strain in tension steel for RC beam U

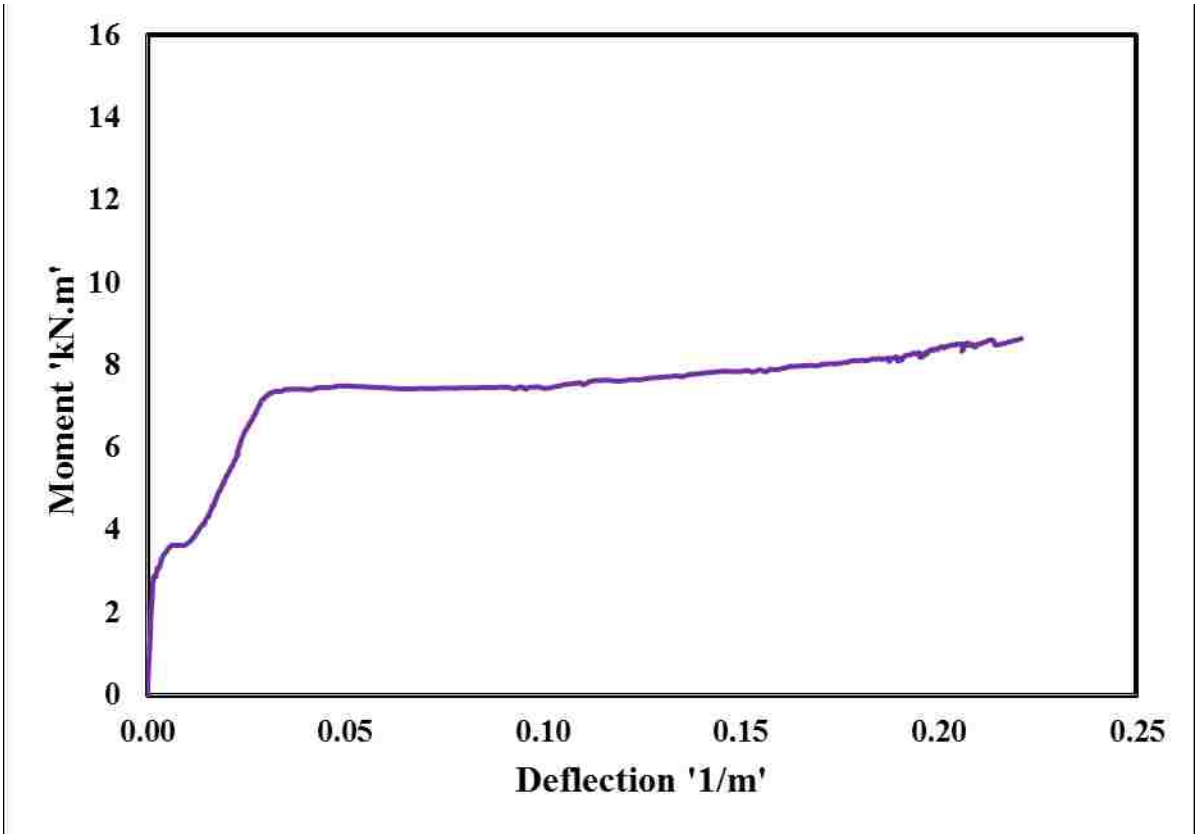

Figure 4.18: Moment curvature for beam U

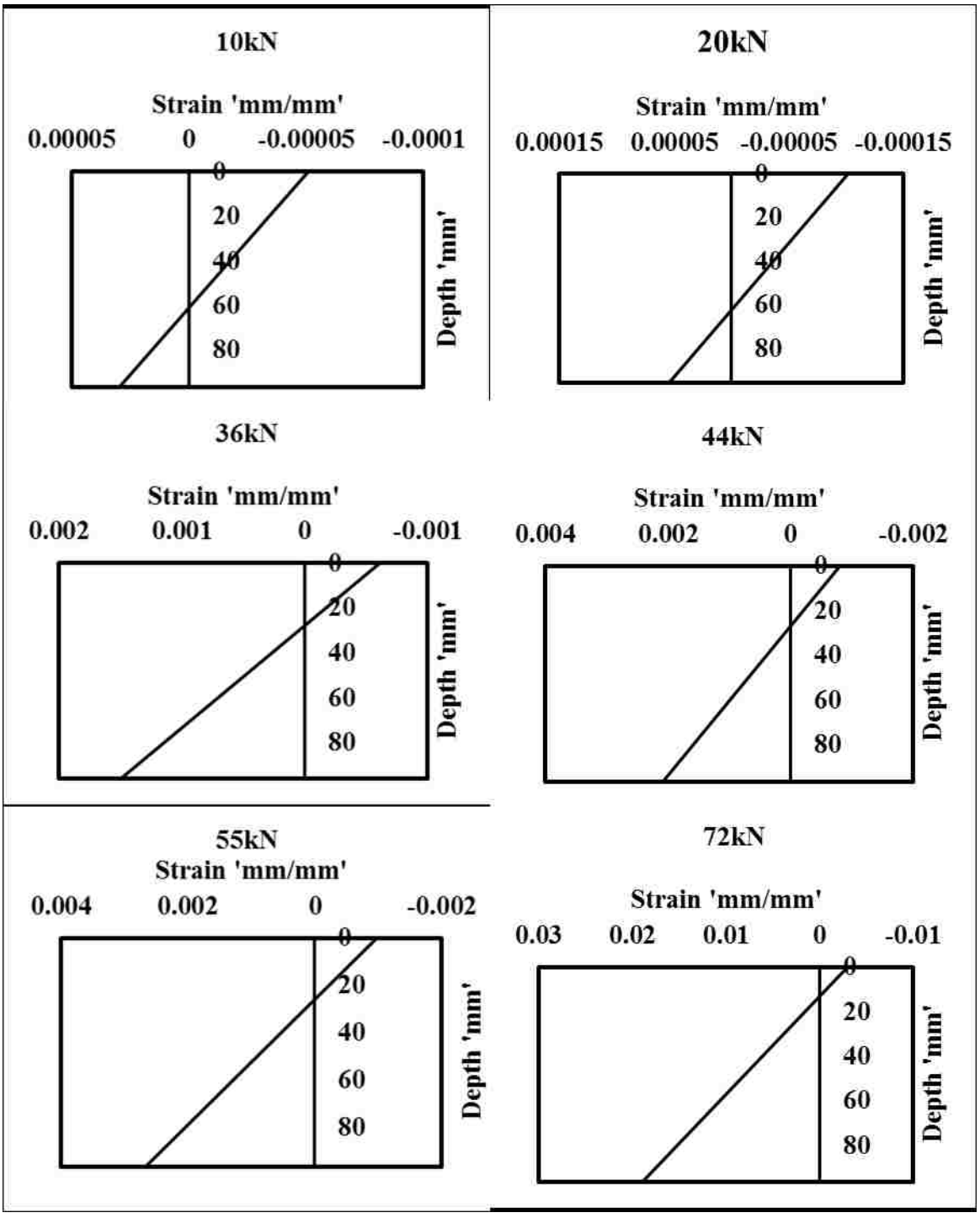

Figure 4.19: Strain distribution diagrams at different load levels for RC-beam U-wrapped with FRP for shear strengthening

4.3.3 Beams strengthened with NSM (N)

Five RC beams strengthened flexurally with NSM-FRP have been tested designated as N1 through N5. These beams are simple RC beams with steel as the reinforcement and strengthened with NSM-FRP flexural strengthening technique using one 10mm diameter GFRP bar using epoxy as bonding material. The significance of these beams is to observe, the bond behavior of the NSM-FRP technique experimentally.

Figure 4.20: NSM-FRP beam showing flexural shear cracks before failure, at this point the bar already started slipping.

As the beam was loaded, two cracks developed near the two loading points, later several flexural shear cracks developed near the loading points. **Figure 4.20** clearly shows the developed cracks. **Figure 4.21** shows the completely failed beam with crushing of concrete. Beams N1 to N5 could carry a mean load of 98.8kN ± 2.9kN. The corresponding mean moment at failure was computed to be 12.5kN.m ± 0.3kN.m. **Table 4.6** presents the corresponding loads and moments carried by each beam. The load deflection curves of all 5 beams are shown in **Figure 4.22** The

Figure 4.21: NSM-FRP beam post failure showing crushing of concrete

load deflection behavior was different compared to the beams C and U, which is linear-elastic up to a mean load of 69.1kN ± 4.6kN with a corresponding deflection at mid-span is 4.8mm ± 0.1mm. Beyond this point there is a change in slope but continued to be linear until the failure. It can be said that the load deflection behavior is bilinear. The failure mode was deboning of the bar from the surrounding epoxy for all the five beams. Once the load response to the displacement started to fall, slip of GFRP bar could be observed, this was even more evident in **Figure 4.27** this figure not only shows load vs displacement but also shows corresponding strain to the same slip. Load vs slip is plotted for all the beams showing that all beams had a failure caused by deboning. It can be inferred from the figure that, once the de-bonding started causing bar slip, the strain increased significantly in concrete and causing failure by crushing of concrete. It was also recognized from

the data, change in slope of the load vs deflection curve was observed when the strain in tension steel reached 0.0021 which is the linear-elastic limit of steel.

Table 4.5: Experimental results of NSM beams N

	Linear- Elastic			Failure		
	Force	Deflection	Moment	Force	Deflection	Moment
RC-Beam	kN	mm	kN.m	kN	mm	kN.m
N1	68.9	4.8	8.7	98.0	9.3	12.5
N2	72.7	5.1	9.2	94.2	7.8	12.0
N3	67.6	4.8	8.6	99.9	10.4	12.7
N4	66.3	4.7	8.4	100.6	11.2	12.8
N5	69.8	4.9	8.9	101.7	10.8	12.9
Mean	69.1	4.9	8.8	98.9	9.2	12.6
Stdev	2.4	0.1	0.3	2.9	1.4	0.4

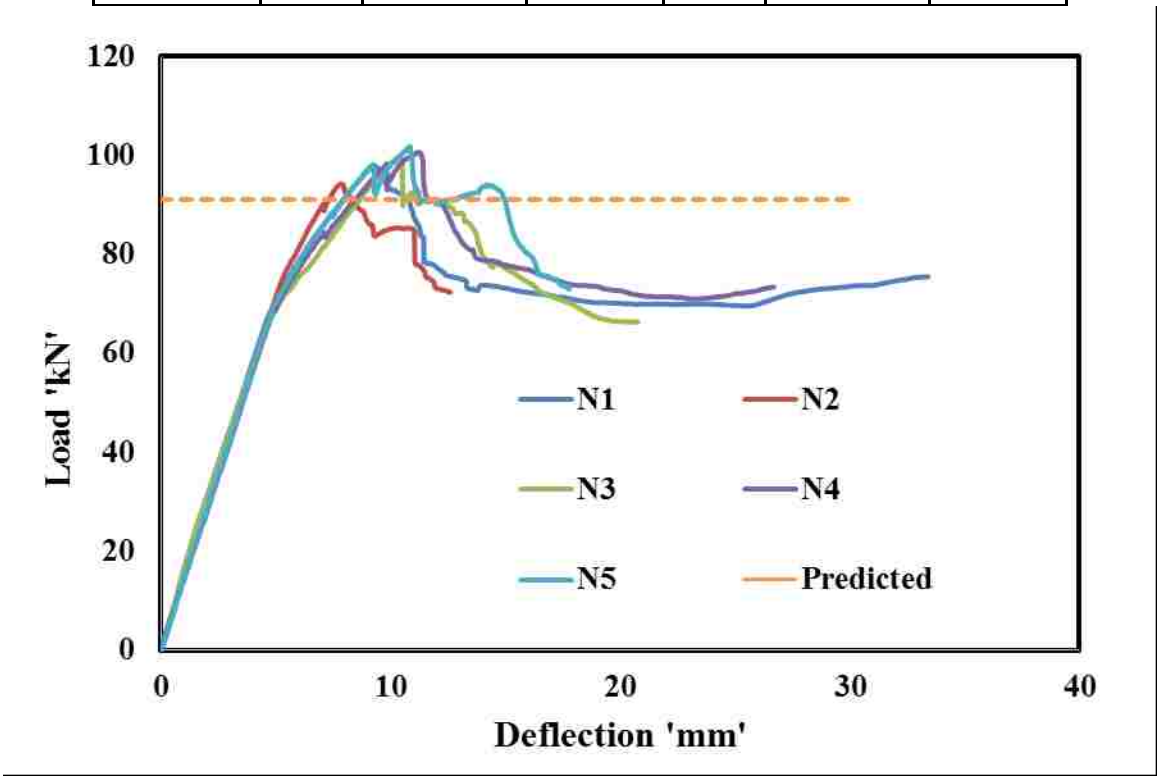

Figure 4.22: Load Vs deflection curves for RC beam flexurally strengthened with NSM-FRP (N)

For the strains looking into beam strengthened with NSM (N1), which is the only beam to have the strain gauges. The strains are measured on top concrete fibers, compression steel, tension steel and GFRP rebar. When the strain in tension steel reached 0.0021, the corresponding strain in GFRP bar is 0.0028, load was measured to be 50.3kN with a corresponding mid-span deflection of 3.4mm. The maximum recorded strain in tension steel was 0.03 at a load of 74kN and the beam failed at a load of 98kN the strain in steel at this point was measured to be 0.0102. The load vs strain in tension steel is presented in **Figure 4.24.** The maximum recorded strain in concrete compression was 0.0024 the corresponding load is 98kN, which is the maximum load for this beam later failed by de-bonding first and then crushing of concrete. The maximum recorded strain in the GFRP bar is 0.010 which is 60% of the ultimate strain capacity of the bar. The beam reached its maximum capacity at this strain there by failure took place by de-bonding of the bar with surrounding epoxy. **Figure 4.28** shows the failed beam clearly showing displaced bar. For the hypothesis, the beam went on linear-elastic in the beginning, later with a change in slope continued linear until failure happened by de-bonding between GFRP bar and surrounding epoxy. The load vs strain in tension steel is presented in **Figure: 4.24.** The load vs strain in top compression fibers of concrete is presented in **Figure 4.25.** The load vs strain in NSM GFRP bar is presented in **Figure: 4.26**.

The strain distributions for various load stages are presented in **Figure 4.29** this strain distribution values were used to compute the actual compression (c) zone.

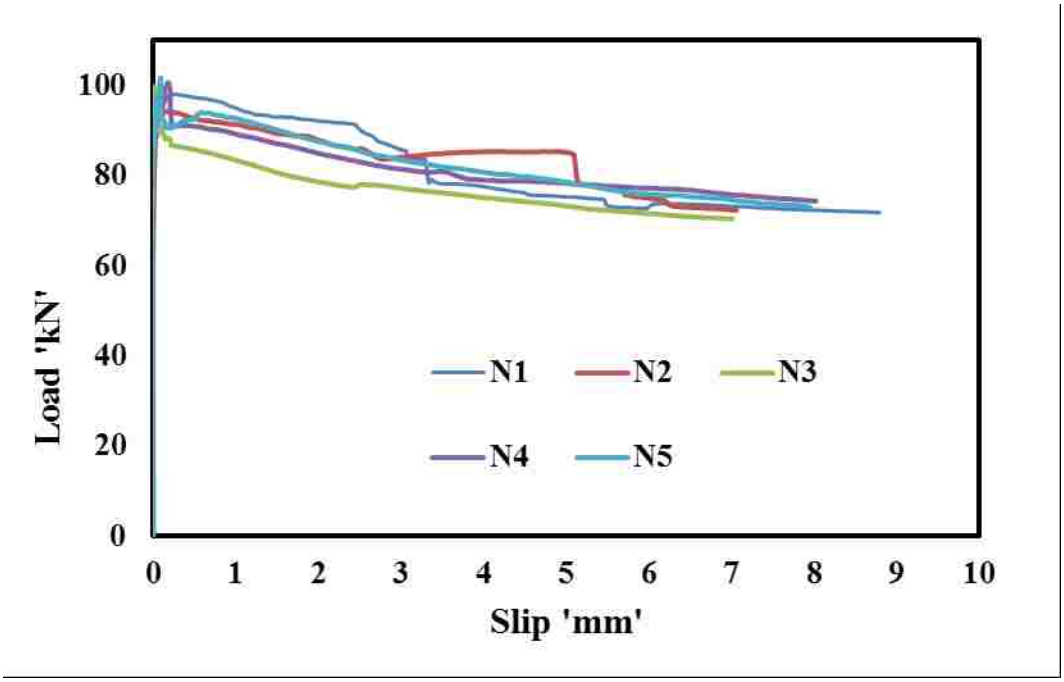

Figure 4.23: Evidence to show that all RC beam flexurally strengthened with NSM-FRP (N) have GFRP bar debonded with surrounding adhesive

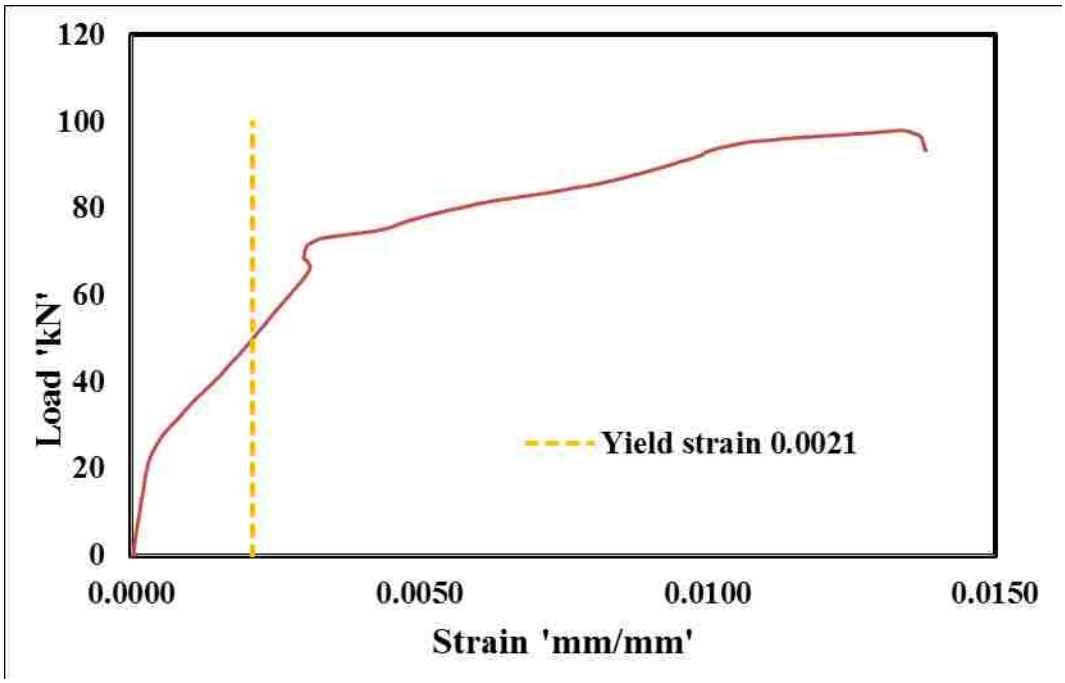

Figure 4.24: Load vs strain in tension steel for RC beam flexurally strengthened with NSM-FRP (N)

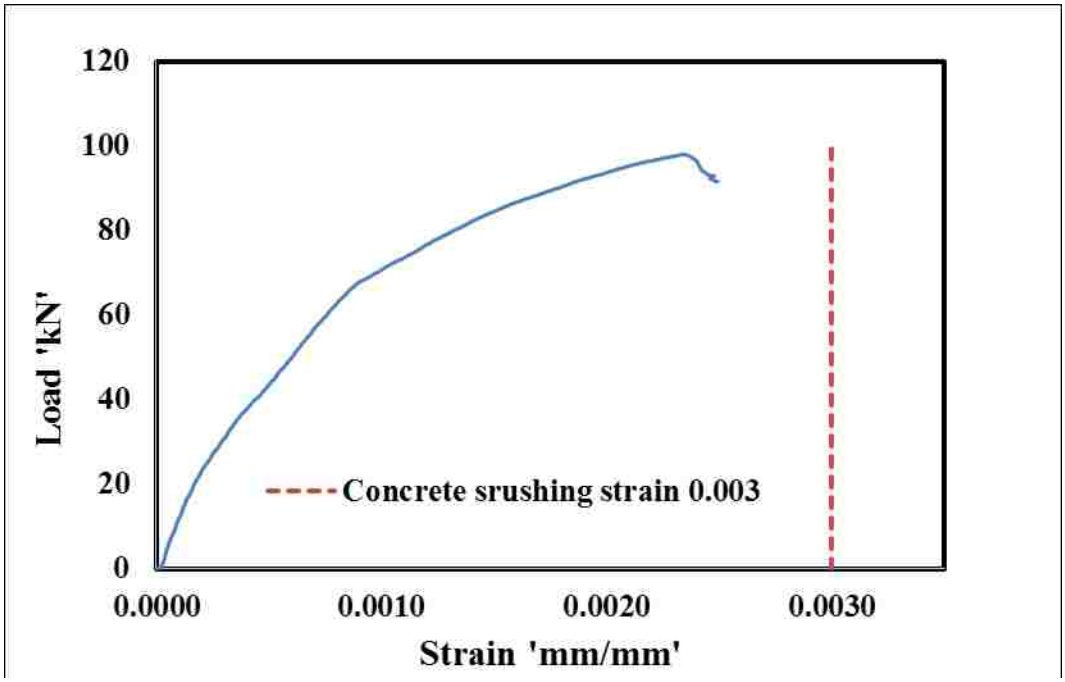

Figure 4.25: strain in top concrete fibers for RC beam flexurally strengthened with NSM-FRP (N)

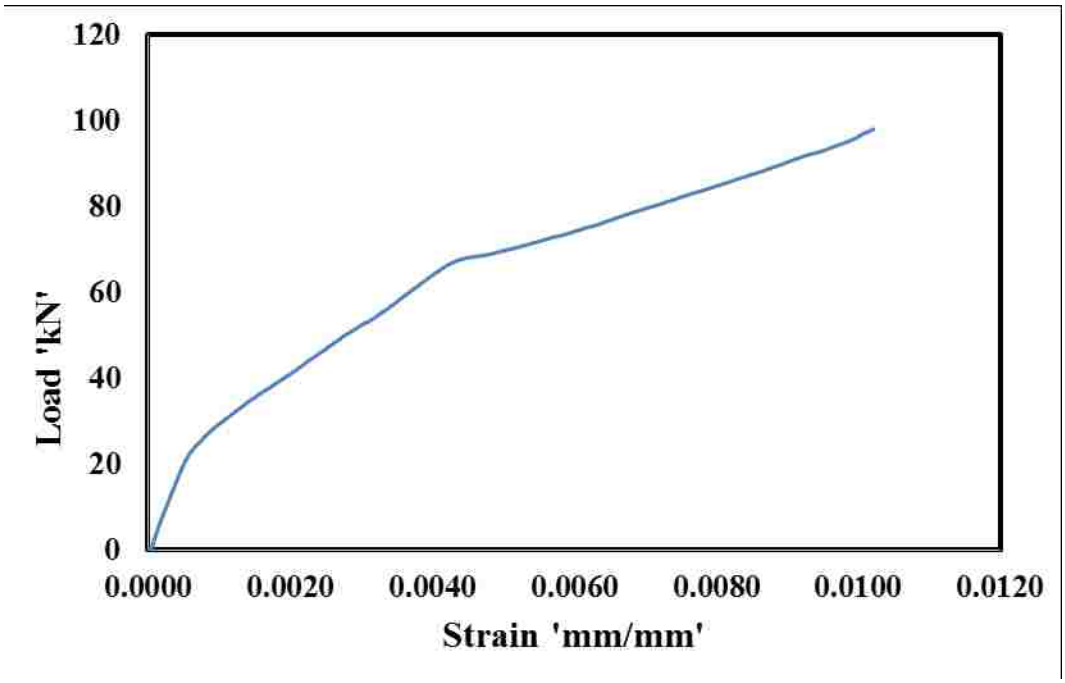

Figure 4.26: Strain in NSM GFRP bar for RC beam flexurally strengthened with NSM-FRP (N)

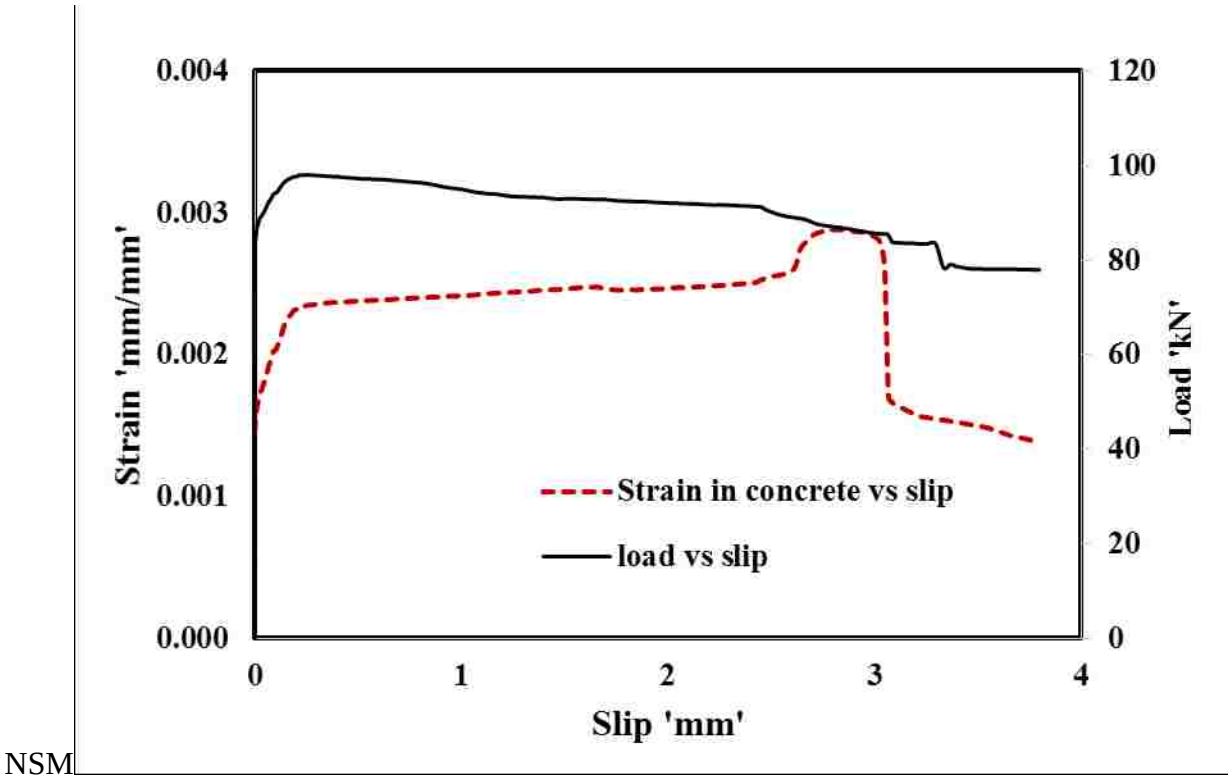

NSM

Figure 4.27: Strain and load vs slip for RC beam flexurally strengthened with NSM-FRP (N) to show that debonding happened first and later failed in concrete crushing

Figure 4.28: NSM-GFRP bar slip (a) before failure (b) after failure

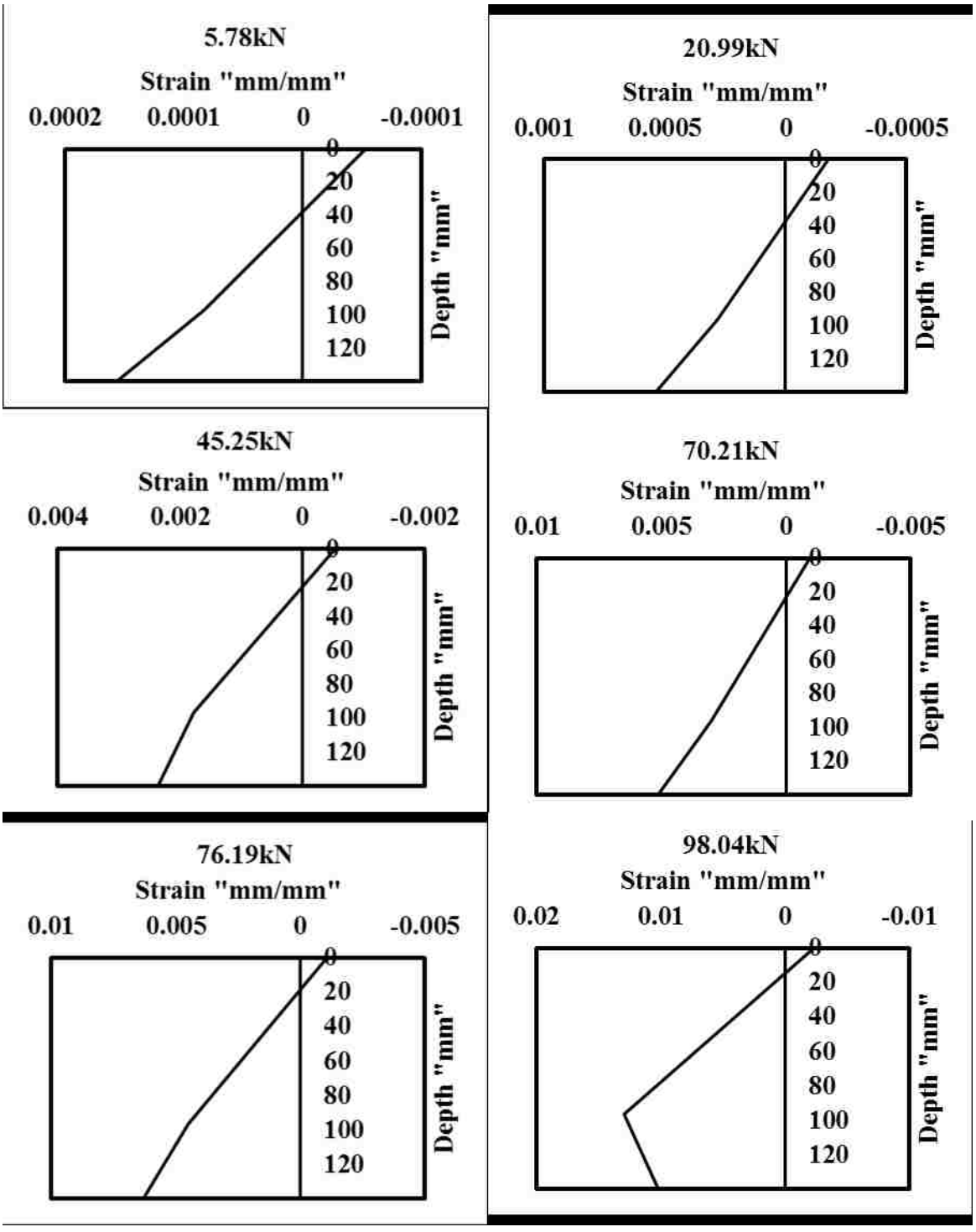

Figure 4.29: Strain distribution diagrams at different load levels for RC beam flexurally strengthened with NSM-FRP (N)

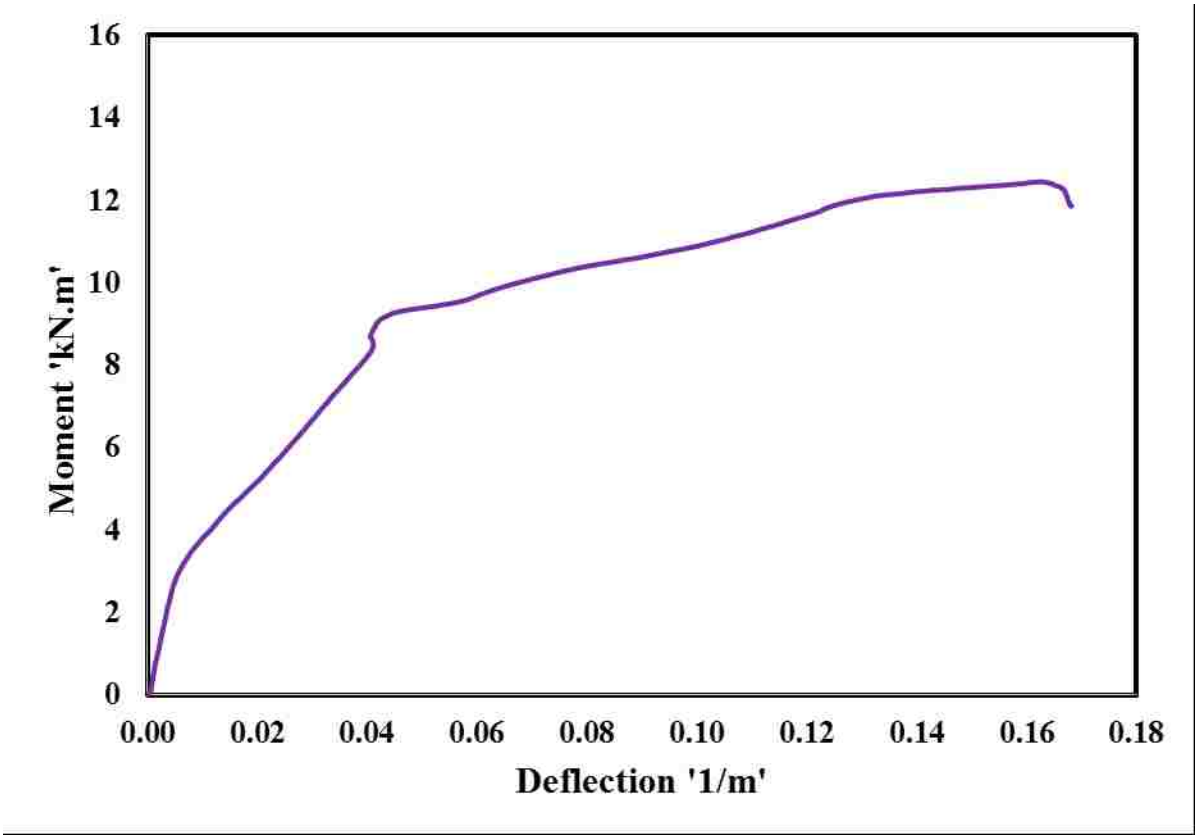

Figure 4.30: Moment vs Curvature for RC beam flexurally strengthened with NSM-FRP (N)

4.3.4 Beams strengthened with NSM and U-wrap shear strengthening (NU)

Five beams have been tested designated as NU1 through NU5. These beams are simple RC beams with steel as the reinforcement and strengthened with NSM-FRP flexural strengthening technique using one 10mm diameter GFRP bar using epoxy as bonding material and also strengthened with GFRP wet layup U-wrap shear strengthening. The significance of these beams is to investigate, the combined effect of NSM-FRP flexural strengthening technique and GFRP U-wrap shear strengthening technique.

Figure 4.31: RC Beam flexurally strengthened with NSM-FRP and shear strengthened with U-wrap FRP Showing flexural cracks while loading of the beam

As the beam was loaded, two cracks developed near the two loading points which could be observed in **Figure 4.31** shows the developed cracks. Beams N1 to N5 could carry a mean load of

119.1kN ± 2.6kN. The corresponding mean moment at failure was computed to be 15.1kN.m ± 0.3kN.m. **Table 4.7** presents the corresponding loads and moments carried by each beam.

Table 4.6: Experimental results for beams NU

	Linear- Elastic			Failure		
	Force	Deflection	Moment	Force	Deflection	Moment
RC-Beam	kN	mm	kN.m	kN	mm	kN.m
U1	82.0	5.4	10.4	120.8	12.6	15.3
U2	83.8	5.8	10.6	118.1	12.2	15.0
U3	81.6	5.8	10.4	119.6	17.4	15.2
U4	80.7	5.7	10.3	115.2	15.6	14.6
U5	82.6	5.6	10.5	121.8	13.3	15.5
Mean	82.1	5.7	10.4	119.1	9.2	15.1
Stdev	1.1	0.2	0.1	2.6	2.2	0.3

The load deflection curves of all 5 beams are shown in **Figure 4.32.** The load deflection behavior is linear-elastic up to a mean load of 82.1kN ± 1.1kN with a corresponding deflection at mid-span is 5.6mm ± 0.1mm. Beyond this point there is a change in slope but continued to be linear until the failure similar to NSM-FRP flexural strengthened beams (N) specimens. But the noted difference between NSM-FRP flexural strengthened specimens and beams strengthened with NSM-FRP flexural strengthening and U-wrap FRP shear strengthening combine beams is that failure is a sudden failure and all the NU specimens were lacking ductility compared to NSM-FRP ‘N” specimens. Also a flexural strength increase of 20% was noted for NU specimens compared to N specimens.

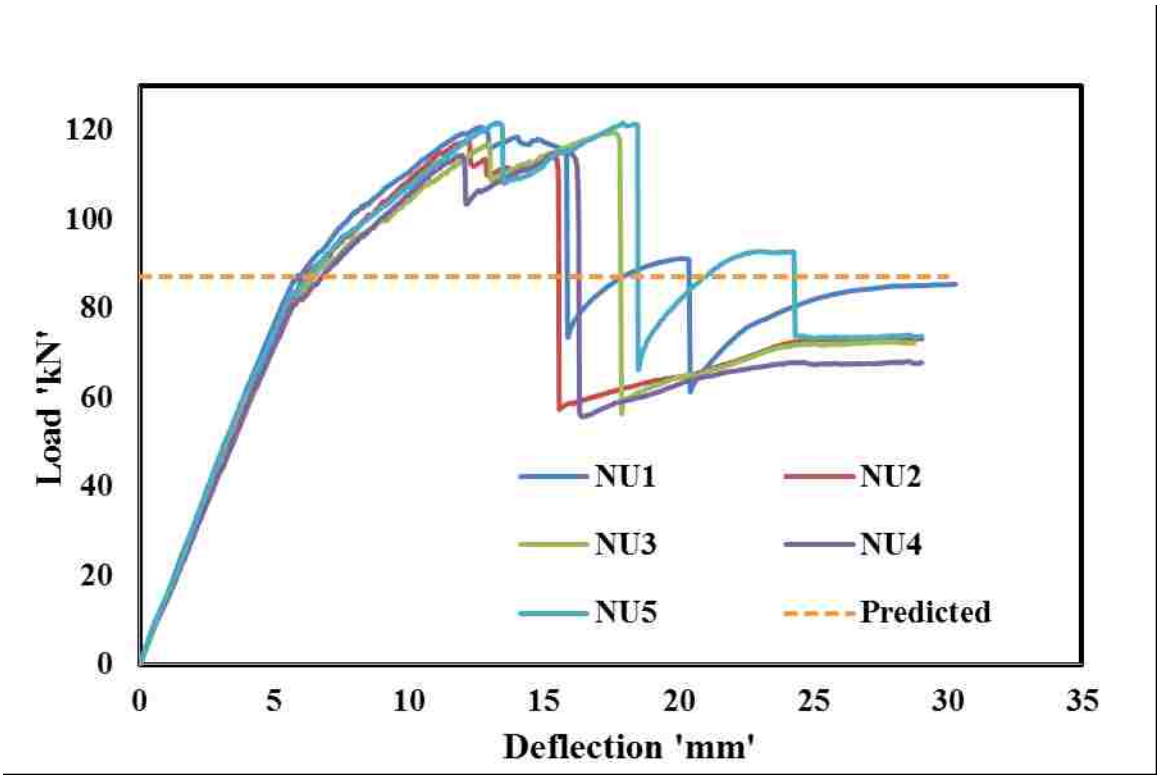

Figure 4.32: Load deflection behavior of RC Beams flexurally strengthened with NSM-FRP and shear strengthened with U-wrap FRP (NU)

For the strains looking into beam NU4, which is the only beam to have the strain gauges. The strains are measured on top concrete fibers, compression steel, tension steel and GFRP rebar. When the strain in tension steel reached 0.0021, the corresponding strain in GFRP bar is 0.0034, load was measured to be 73.4kN with a corresponding mid-span deflection of 5.1mm. The maximum recorded strain in tension steel was 0.016 at a load of 108kN and the beam failed at a load of 114kN the strain in steel at this point was measured to be 0.0082. The load vs strain in tension steel is presented in **Figure 4.35. Figure 4.37** presents the strain concrete top compression fibers. The maximum recorded strain in concrete compression was 0.0026 the corresponding load is 113.8kN, which is just before reaching maximum load for this beam later failed by strength

rupture of GFRP bar. The rupture of bar caused a sudden failure. The maximum recorded strain in the GFRP bar is 0.014 which is close to 80% of the ultimate strain capacity of the bar. However bar rupture proves that the bar reached its ultimate strain capacity. The GFRP bar strength rupture is shown in **Figure: 4.40**. The strain in NSM GFRP bar is presented in **Figure: 4.36**. Out of the five beams tested, only one beam showed bar slip and this is the only beam to not have bar rupture, whereas the rest of the four beams failure was caused by bar rupture, the evidence to show no slip is given in **Figure: 4.33**. **Figure 4.34** shows the failed beam by strength rupture of GFRP bar. The failure modes and the behavioral changes are further discussed in **section 2.2.2.**

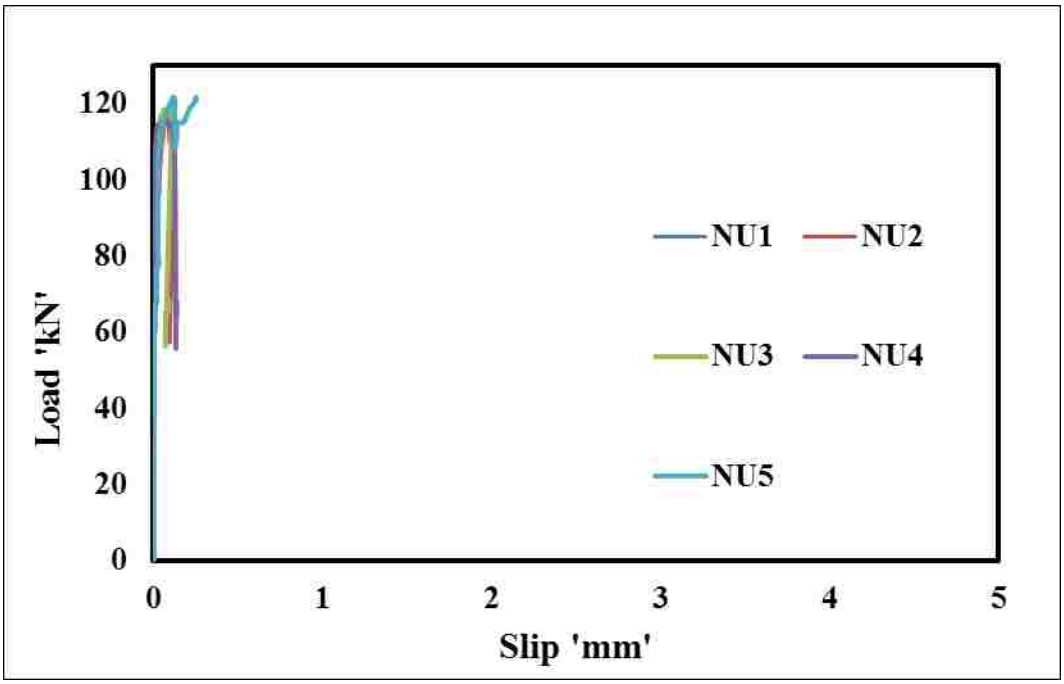

Figure 4.33: Force vs GFRP slip of RC beams strengthened flexurally with NSM-FRP and shear strengthened with U-wrap FRP (NU)

Figure 4.34: RC Beam flexurally strengthened with NSM-FRP and shear strengthened with U-wrap FRP Showing flexural cracks while loading of the beam

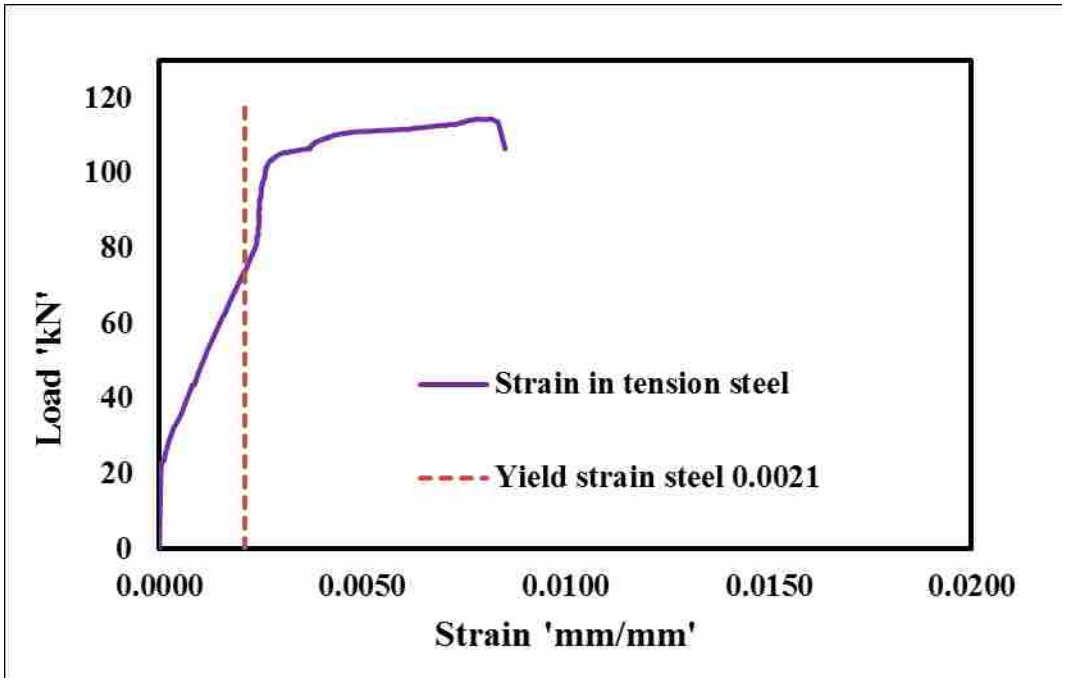

Figure 4.35: Strain in tension steel for RC Beam flexurally strengthened with NSM-FRP and shear strengthened with U-wrap FRP (NU)

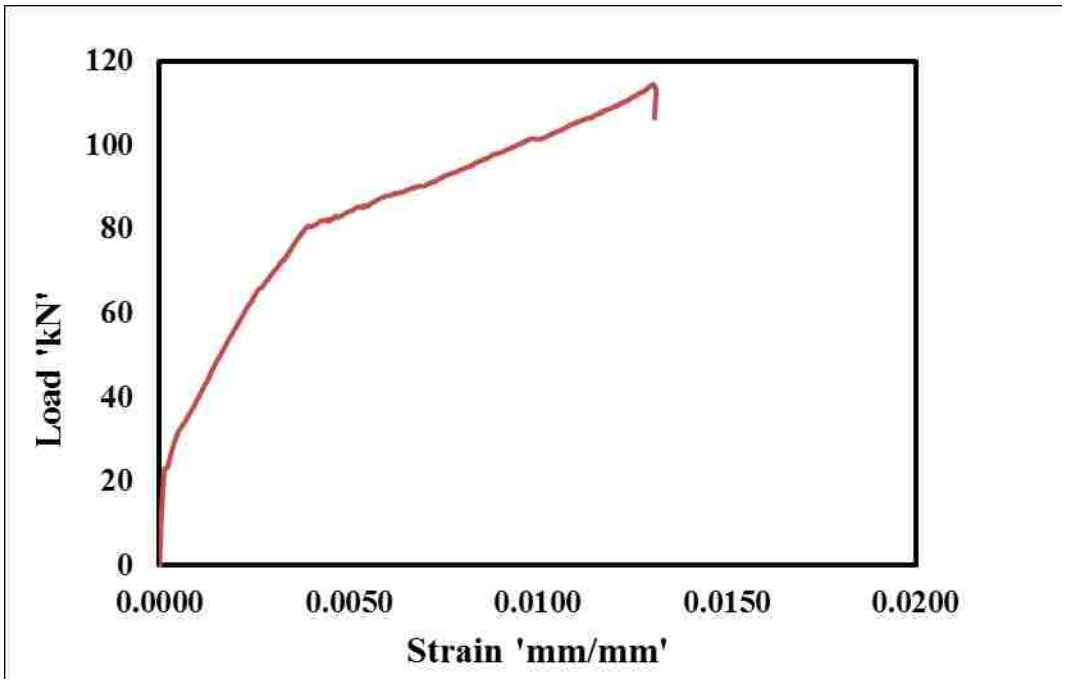

Figure 4.36: Strain in GFRP bar for RC Beam flexurally strengthened with NSM-FRP and shear strengthened with U-wrap FRP just before rupture of the bar

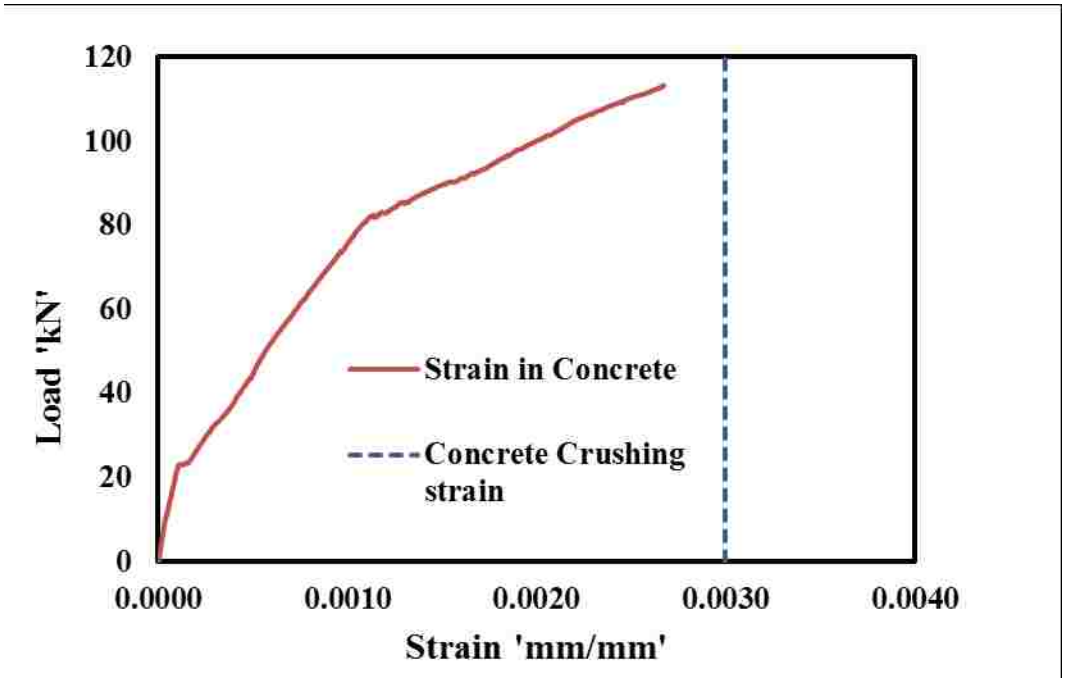

Figure 4.37: Strain in top concrete compression fibers for RC Beam flexurally strengthened with NSM-FRP and shear strengthened with U-wrap FRP

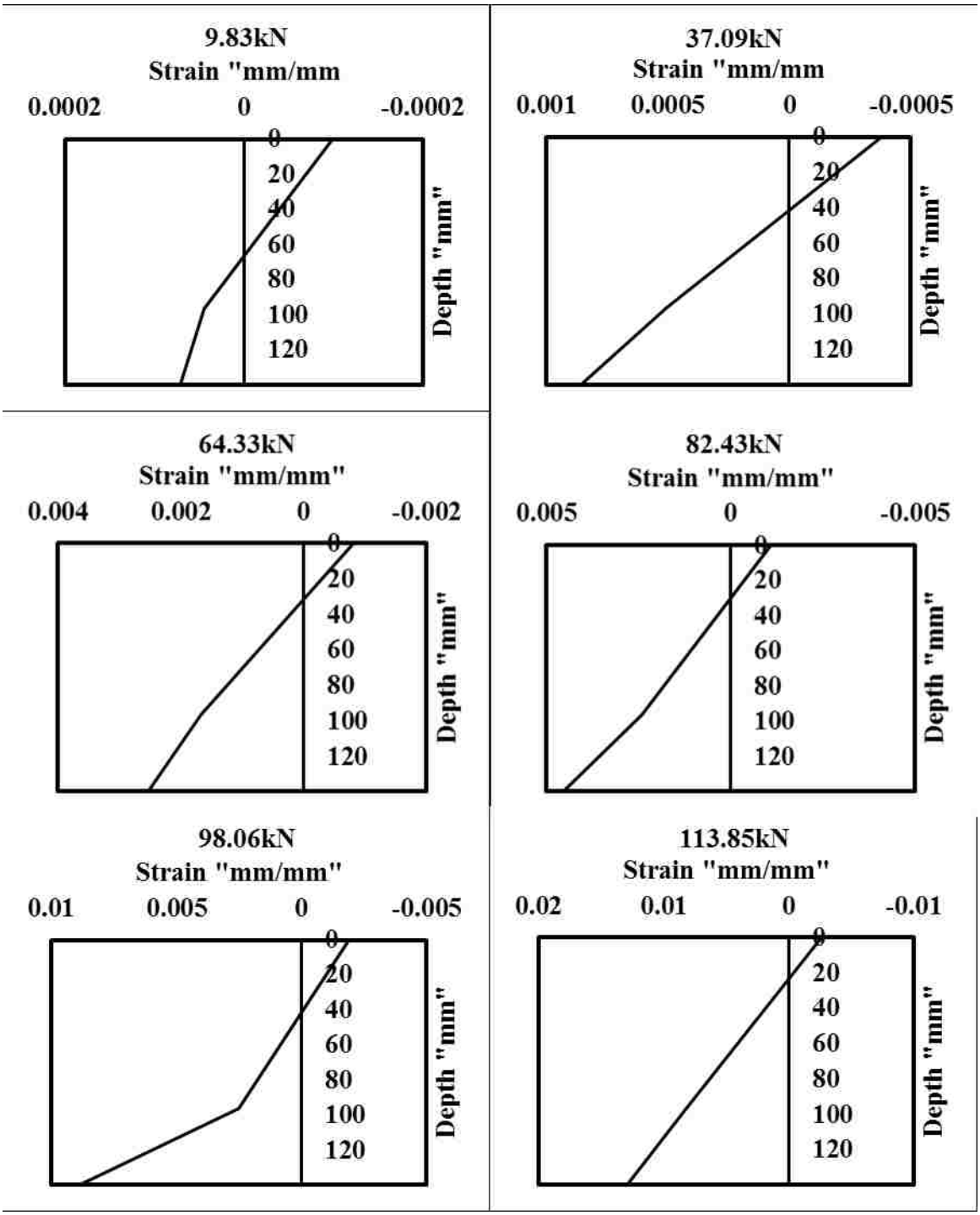

Figure 4.38: Strain distribution diagrams for RC Beam flexurally strengthened with NSM-FRP and shear strengthened with U-wrap FRP at different load levels.

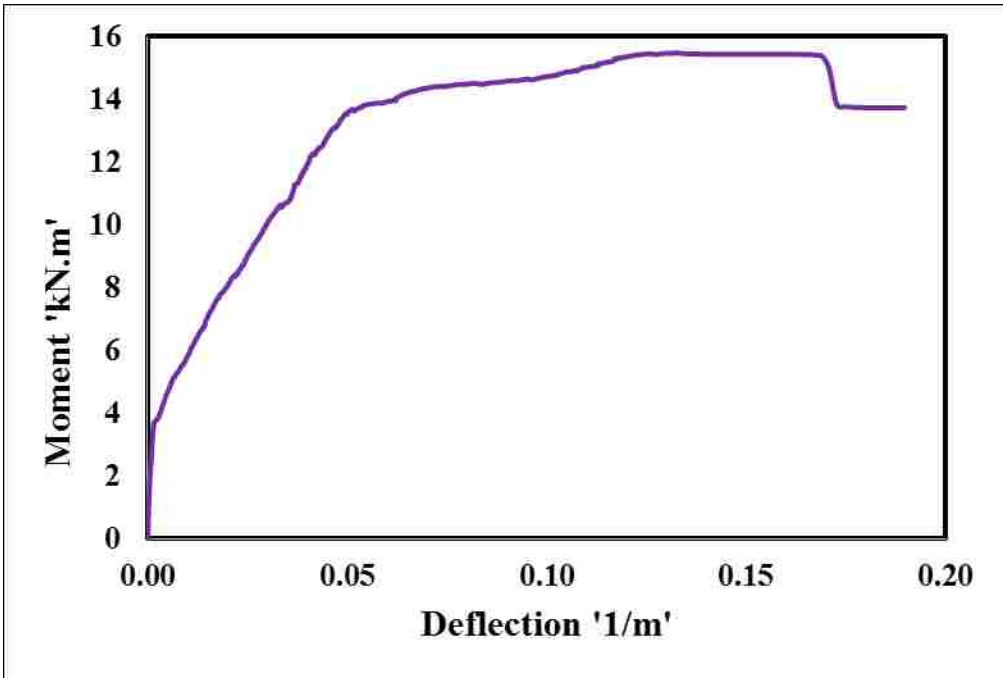

Figure 4.39: Moment vs curvature for RC Beam flexurally strengthened with NSM-FRP and shear strengthened with U-wrap FRP

Figure 4.40: Figure showing tension rupture of GFRP bar at failure

4.3.5 Beams strengthened with NSM flexural strengthening and U-wrap shear strengthening in shear area (NUS)

Five RC beams strengthened flexurally with NSM-FRP and shear strengthened with FRP U-wrap shear strengthened with U-wrap in shear area have been tested designated as NUS1 through NUS5. These beams are simple RC beams with steel as the reinforcement and strengthened with NSM-FRP flexural strengthening technique using one 10mm diameter GFRP bar using epoxy as bonding material and also strengthened with GFRP wet layup U-wrap shear strengthening. The difference from the beams NU is that these beams are wrapped partially and only at the ends. The significance of these beams is to investigate, the combined effect of NSM-FRP flexural strengthening technique and GFRP U-wrap shear strengthening technique when wrapped only in the shear zone. One of the five beams did not work due to machine mall function.

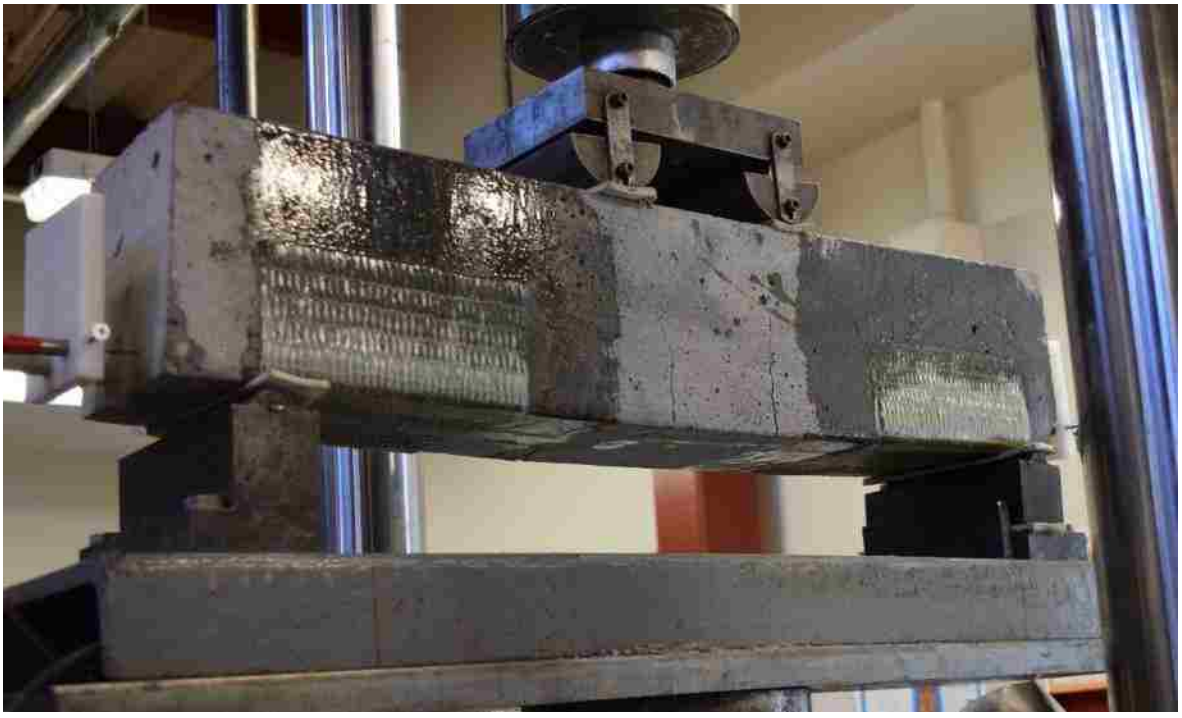

Figure 4.41: RC Beam flexurally strengthened with NSM-FRP and shear strengthened with U-wrap FRP in shear zone only showing flexural cracks while loading of the beam

As the beam was loaded, two cracks developed near the two loading points which could be observed in **Figure 4.41** shows the developed cracks. Beams NUS1 to NUS4 could carry a mean load of 111.8kN ± 4kN. The corresponding mean moment at failure was computed to be 14.2kN.m ± 0.32kN.m. **Table 4.8** presents the corresponding loads and moments carried by each beam. The load deflection curves of all 4 beams are shown in **Figure 4.42.** The load deflection behavior is linear-elastic up to a mean load of 70.7kN ± 1.1kN with a corresponding deflection at mid-span is 5.8mm ± 0.4mm. Beyond this point there is a change in slope but continued to be linear until the failure similar to N specimens. But the noted difference between NSM-FRP flexural strengthened and combined flexural strengthened NSM-FRP and U-wrap shear strengthened in shear area only specimens is that failure is a sudden failure and all the NUS specimens were lacking ductility compared to NSM-FRP 'N' specimens. Also a flexural strength increase of 13% was noted for NUS specimens compared to N specimens.

Table 4.7: Experimental results for RC beams strengthened in combination with both NSM-FRP flexural strengthening and FRP U-wrap shear strengthening in shear area

	Linear- Elastic			Failure		
	Force	Deflection	Moment	Force	Deflection	Moment
	kN	mm	kN.m	kN	mm	kN.m
NUS1	71.6	5.7	9.0	117.3	18.7	14.9
NUS2	76.5	6.5	9.7	107.7	12.0	13.6
NUS3	69.9	5.6	8.8	111.6	19.0	14.1
NUS4	65.0	5.3	8.2	110.5	17.1	14.0
Mean	70.7	5.8	8.9	111.8	16.7	14.2
Stdev	4.7	0.4	0.6	4.0	3.2	0.5

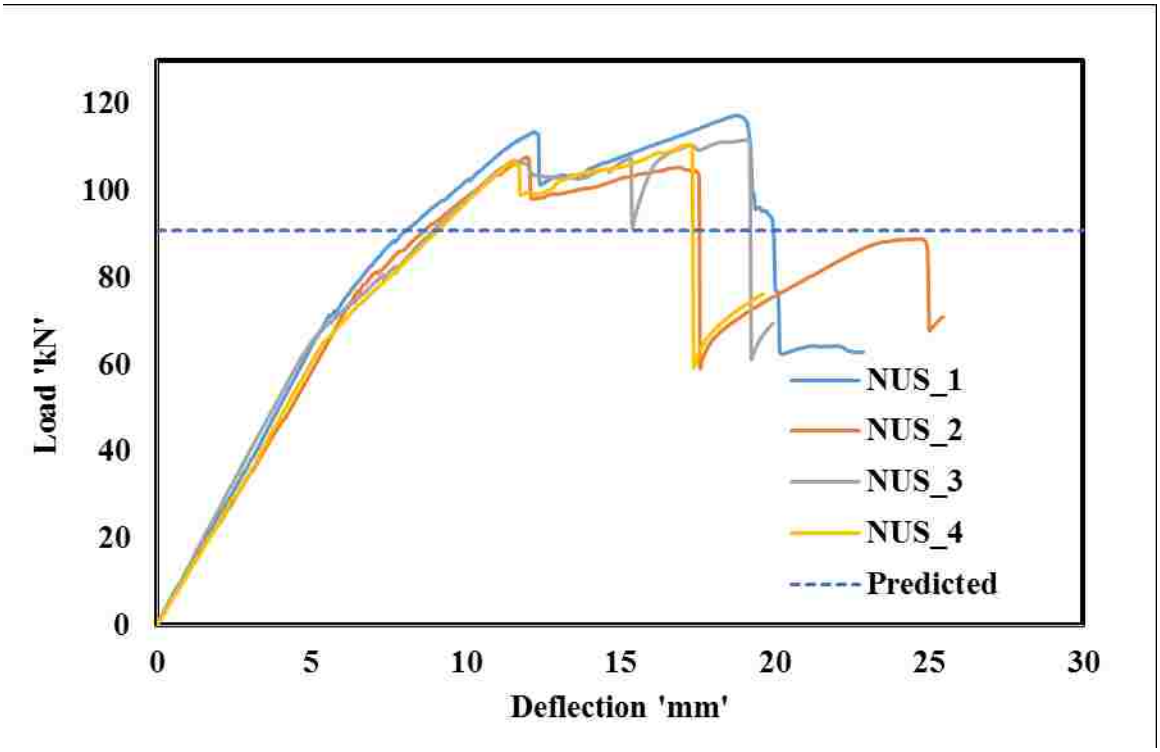

Figure 4.42: Load deflection behavior of beams RC beams strengthened in combination with both NSM-FRP flexural strengthening and FRP U-wrap shear strengthening in shear area

For the strains looking into RC beam strengthened in combination with NSM-FRP flexural strengthening and FRP U-wrap shear strengthening in shear area NUS3, which is the only beam to have the strain gauges. The strains are measured on top concrete fibers, compression steel, tension steel and GFRP rebar. When the strain in tension steel reached 0.0021, the corresponding strain in GFRP bar is 0.0034, load was measured to be 51.3kN with a corresponding mid-span deflection of 3.86mm. The maximum recorded strain in tension steel was 0.014 at a load of 106.4kN and the beam failed at a load of 114kN the strain in steel at this point was measured to be 0.0082. The load vs strain in tension steel is presented in **Figure 4.45.** The maximum recorded strain in concrete compression was 0.0029 the corresponding load is 105.2kN, which is just before reaching maximum load for this beam later failed by strength rupture of GFRP bar. The rupture of

bar caused a sudden failure. The maximum recorded strain in the GFRP bar is 0.018 which is beyond the ultimate strain capacity of the bar, this is mainly because at this point the bar did not rupture but failure happened by debonding caused because of sudden splitting of epoxy cover. However, only one of the four beams failed in GFRP bar strength rupture. The other three beams failed by sudden splitting of epoxy cover, there by debonding of the bar. The failure modes and the behavioral changes are further discussed in **section 4.3.5. Figure 4.44** showing strength rupture of GFRP bar.

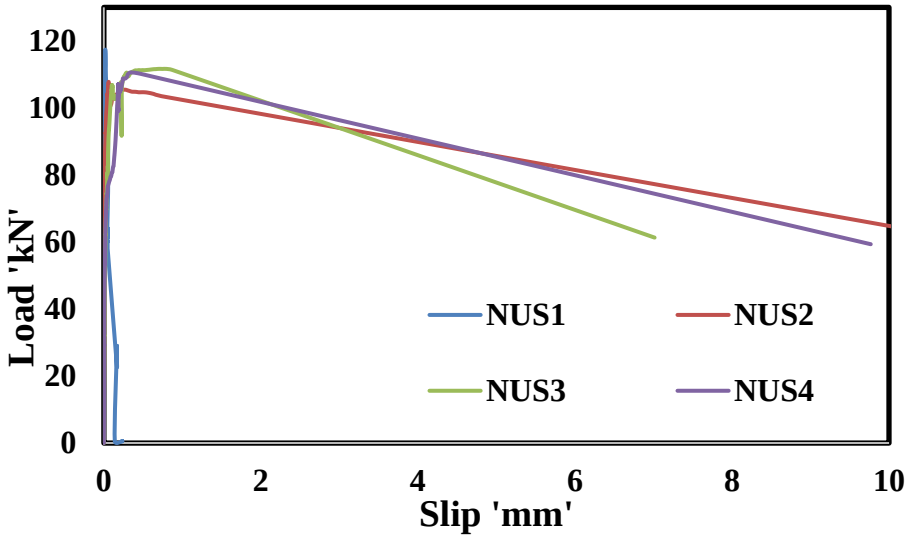

Figure 4.43: Load vs end slip of NSM GFRP bars NUS beams

(a)

(b)

Figure 4.44: Figure showing: (a) tension rupture of GFRP bar at failure; (b) Splitting of epoxy cover

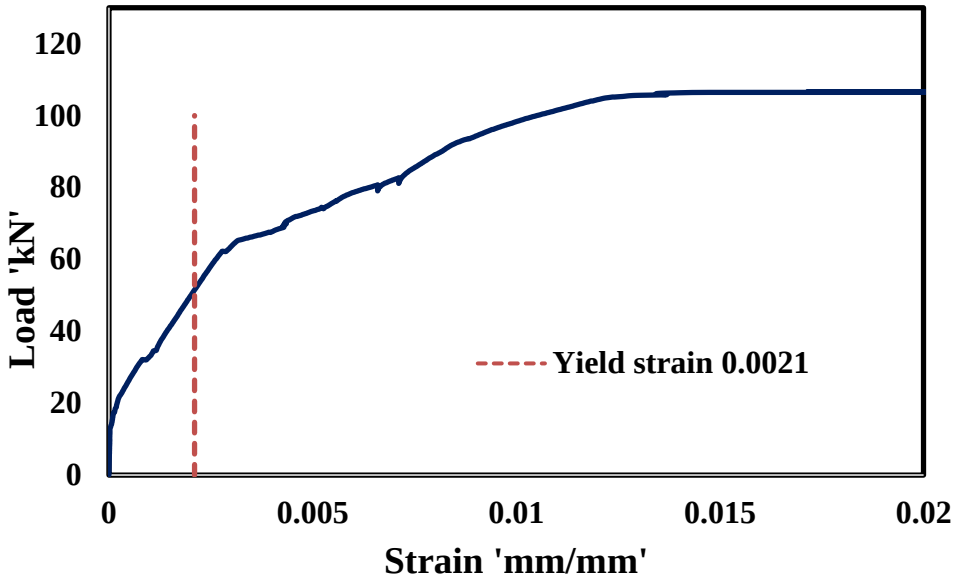

Figure 4.45: Strain in tension steel for beam NUS3

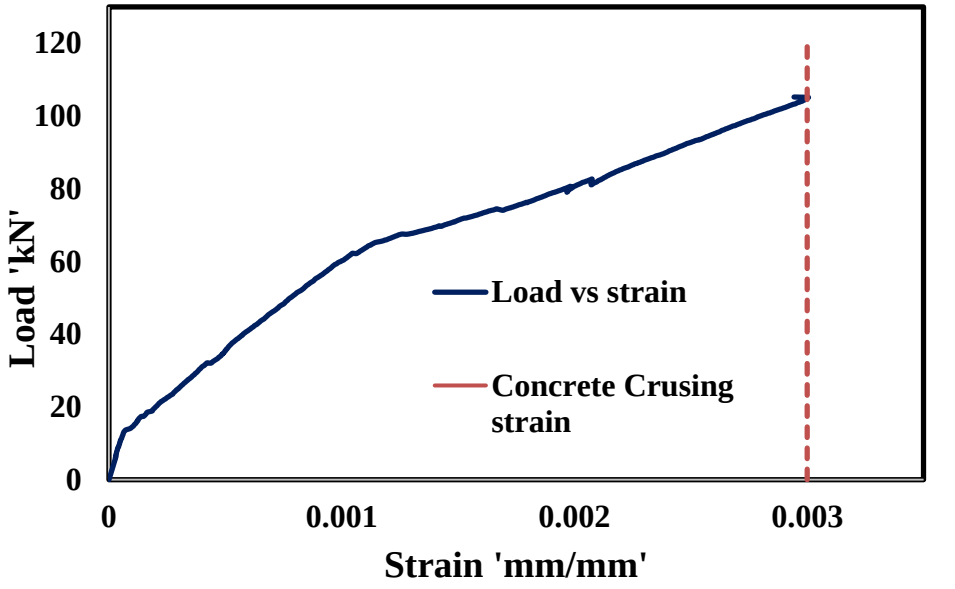

Figure 4.46: Strain in top compression fibers for beam NUS3

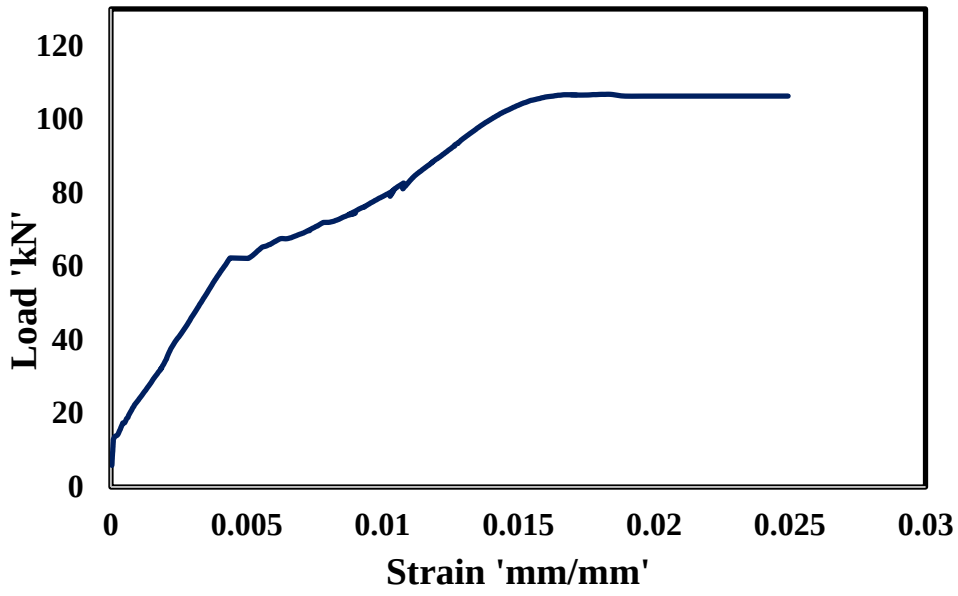

Figure 4.47: Strain in NSM GFRP bar for beam NUS3

Figure 4.48: RC Beam flexurally strengthened with NSM-FRP and shear strengthened with U-wrap FRP in shear area only after failure

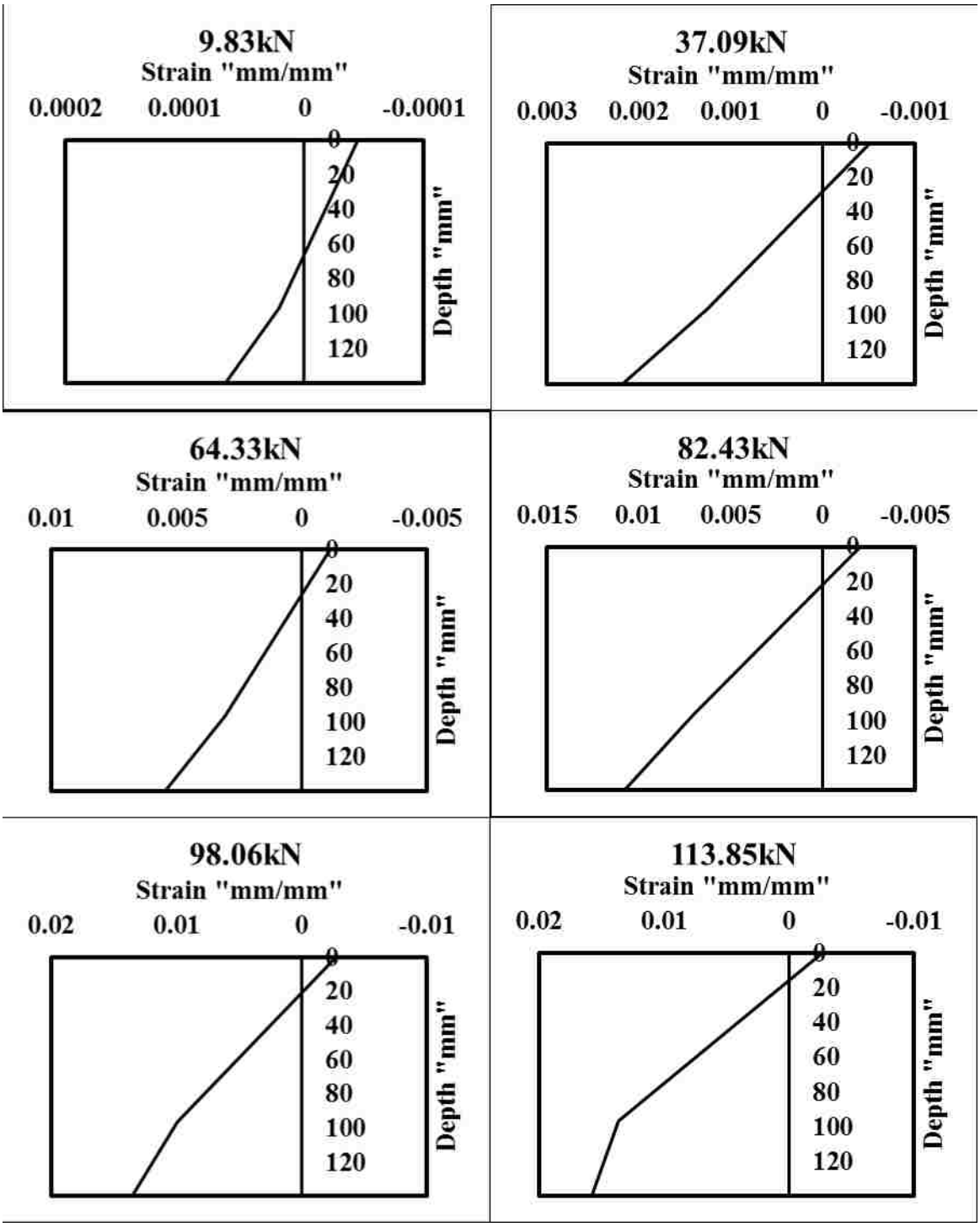

Figure 4.49: Strain distribution diagrams for different load levels of beam RC Beam flexurally strengthened with NSM-FRP and shear strengthened with U-wrap FRP in shear area only

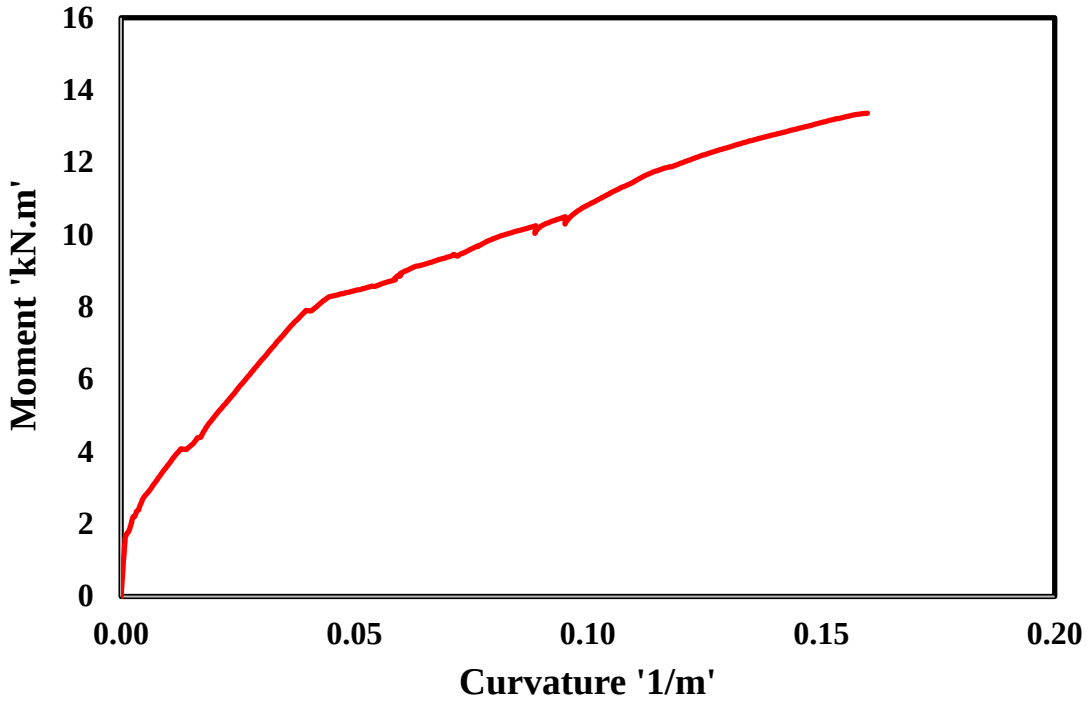

Figure 4.50: Moment curvature for RC Beam flexurally strengthened with NSM-FRP and shear strengthened with U-wrap FRP in shear area only

4.3 Comparison and Discussion

In this section, comparison between the control beams C and the other four beam types i.e., U, N, NU and NUS is presented. The main concentration will be to compare beams strengthened flexurally with NSM and the beams strengthened with NSM flexural and shear strengthened with U-wrap to observe the combined effect of NSM-FRP and U-wrap FRP. **Table 4.9** presents the summarized results for all five beam types.

Table 4.8: Summarized mean results at failure for all 5 beam types; Modes of failure CC- Concrete crushing after steel yielding, DB – debonding of NSM GFRP bar with surrounding epoxy, BR- strength rupture of GFRP bar, SE- sudden splitting of epoxy cover.

Beam	C	U	N	NU	NUS
Failure					
Mode	CC	CC	DB	BR	BR,SE
Load (kN)	67.29	72.1	98.9	119.1	111.8
Moment (kN.m	8.81	9.1	12.6	15.1	14.2
Mid-span deflection(mm)	10.6	9.1	9.2	9.2	16.74
Capacity over C		7%	47%	77%	66%
Capacity over N				20%	13%

It can be clearly observed NSM-FRP has a significant strength increase to the control specimens as given by the previous work (Laura De Lorenzis & Nanni, 2002; L De Lorenzis & Teng, 2007; El-Hacha & Rizkalla, 2004; T. K. Hassan & Rizkalla, 2004; Nanni et al., 1999). But, this study concentrates on the combined effect of NSM-FRP and U-Wrap FRP. The specimens NU had a strength increase by 20% compared to the N specimens with a TTEST statistical significance. The NUS specimens had a strength increase of 13% compared to that of the N specimens. Hence, it is clearly evident that U-wrap FRP shear strengthening has significant effect on the NSM-FRP flexural strengthened beams. The detailed results are given in **Table 4.9**. **Figure 4.51 and Figure 4.52** percentage increase of the average capacity of the beams. A beam from each beam type is

chosen based on its capacity close to the mean value and plotted for load deflection, which is presented **Figure 4.53.**

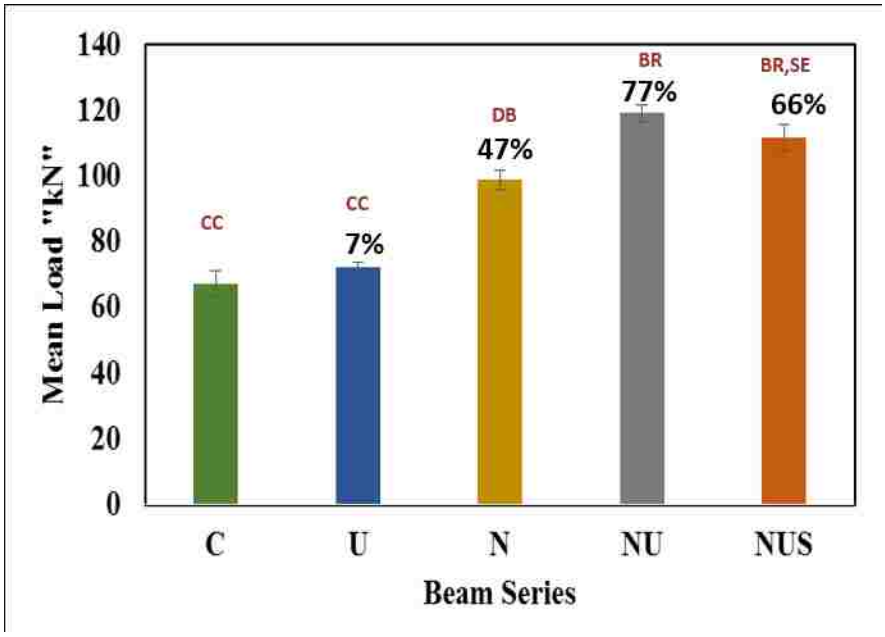

Figure 4.51: Error plot to show percentage average increase over the mean of the Control 'C' RC beam to other beam types

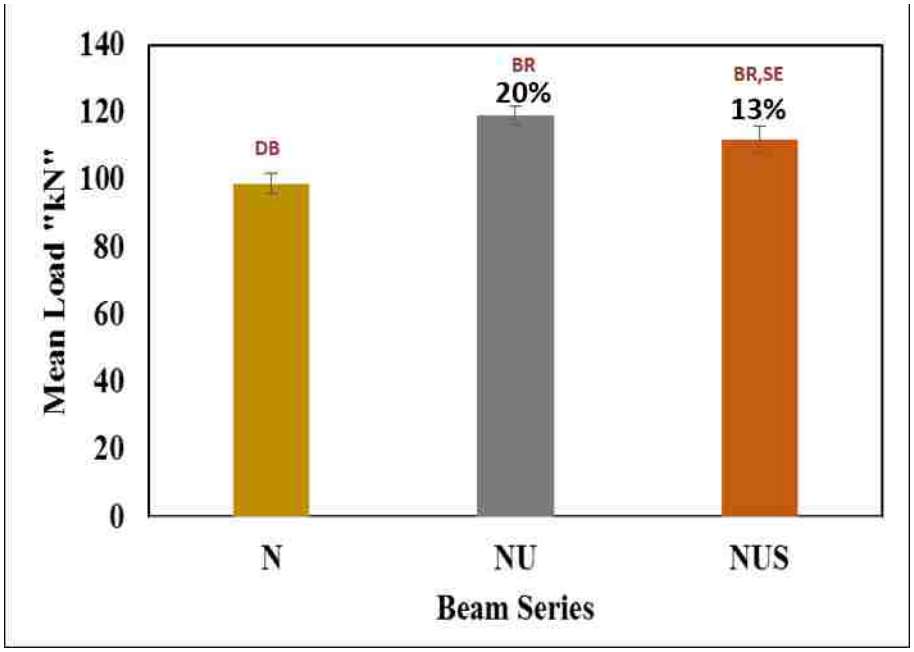

Figure 4.52: Error plot to show percentage average increase over the mean of the 'N' RC beam to other strengthened beam types

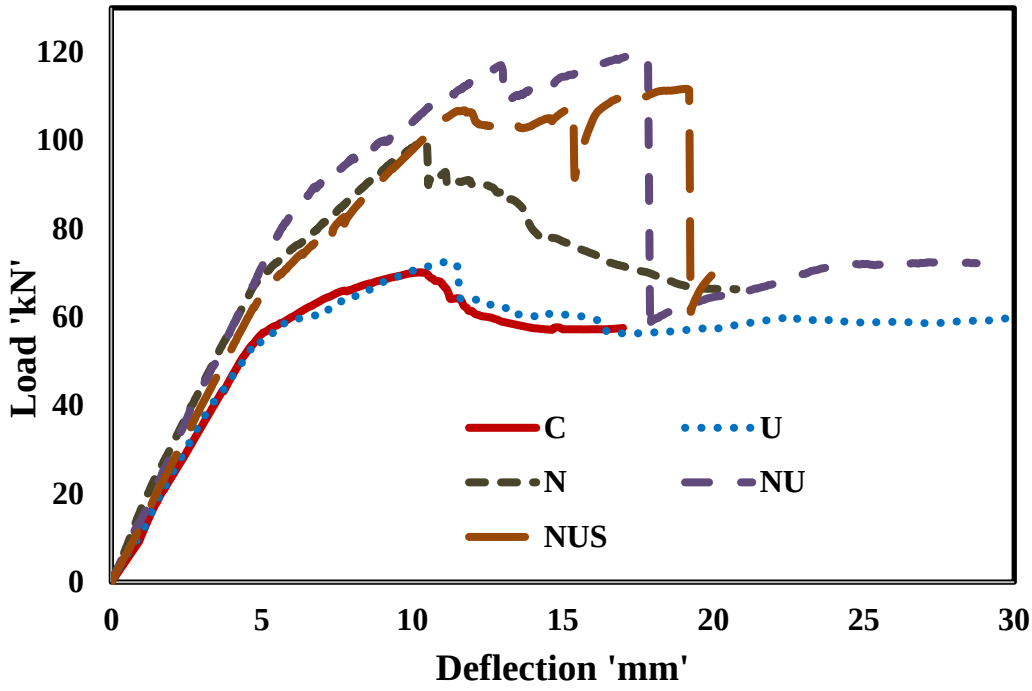

Figure 4.53: Median load deflection behavior of all five beam types

4.3.1 Comparison of Load vs Deflection of all beams:

It is clearly evident, that NSM-FRP could significantly increase the flexural capacity over the control beam but the main recognized mode of failure for all the N beams is debonding of NSM GFRP bar with the surrounding epoxy . However, combining NSM-FRP flexural strengthening and U-Wrap GFRP shear strengthening has also increased the flexural capacity significantly over RC bema strengthened flexurally with NSM-FRP 'N' specimens but a change in mode of failure has significantly affected the ductility of the beam. The mode of failure for five Beams is bar rupture which caused a sudden failure. The bar rupture increased the stain in top concrete fibers, making it a sudden abrupt failure. The beams NUS, which were partially wrapped only in the shear area also showed a similar effect of reduced ductility and sudden failure. Though, only one beam

had a strength rupture of GFRP bar, other three beams had sudden splitting of epoxy cover with a loud noise while conducting the experiment which also can be told as the sudden failure.

4.3.2 Statistical Significance:

Statistical significance was checked using the TTEST in Microsoft excel between the ultimate loads of the beam series. This statistical significance was checked between control beams 'C' and all the other beam series and achieved at least a 95% statistical significance. The statistical significance was checked between NSM-FRP flexural strengthened specimens 'N' only to combined strengthened beams 'NU' and 'NUS' and achieved a 99% statistical significance showing that the beam series are significantly different and valid. 97% statistical significance was achieved when TTEST significance was checked between NU and NUS making them significantly different from each other, though the difference between the average ultimate load values with these two beam series is only 6%.

4.3.3 Strains in GFRP:

Table 4.9: Strains of beams at failure

Beam	C	U	N	NU	NUS
Strain in concrete top fibers	-0.0036	-0.003	-0.0023	-0.0026	-0.0026
Strain in Steel tension	0.0169	0.019	0.013	0.0082	0.0136
Strain in NSM GFRP	NA	NA	0.01	0.0135	0.0158
Increase strain capacity in GFRP over N				35%	58%

Table 4.10 shows the strains at failure for all five beam types. Typically, for NSM-FRP s specimens, though given a full development length for bond, the main mode of failure is debonding of GFRP with the surrounding epoxy reaching a strain capacity of 50%-70% of the ultimate strain capacity. This was clearly observed for the N beams having GFRP bar reach 60%

of ultimate strain and failure mode is deboning. But the combined effect of NSM_FRP and U-wrapping has shown a significant increase of 35% for NU over N specimen and 58% for NUS over N specimens. This increase of strain capacity is mainly because of the confinement effect by the GFRP U-wrapping, which increasing the performance of bond changing the mode of failure to FRP- Bar rupture. NU specimens had a full U-wrapping, hence 4 of five beams had rupture but NUS specimens had a partial U-wrapping, which made a significant effect on bond but only one specimen failed in rupture FRP bar.

4.3.4 Slip of GFRP bar:

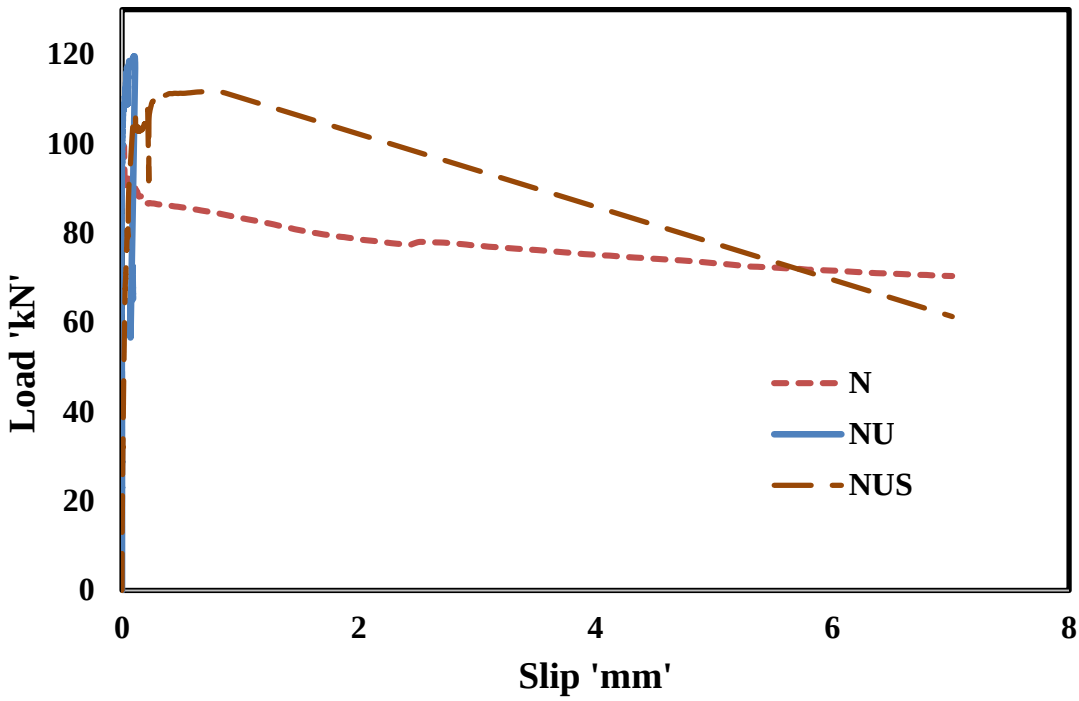

Figure 4.54: NSM GRP bar end slip for N, NU and NUS specimens

From the **Figure 4.54** it is clearly evident bond between NSM-GFRP bar and surrounding epoxy is significantly affected by FRP U-wrap shear strengthening. The RC beam strengthened only flexurally with NSM-FRP has failed by debondind and there for the slip of the bar is gradually increasing. Comparing this to the NU specimens which were strengthened both flexurally and for shear using FRP U-wrap did not have any slip of the bar as the failure mode is strength rupture of GFRP bar. Although the RC beam strengthened partially with FRP U-wrapping shows slip, this is a sudden slip resulted from sudden splitting of epoxy cover. This proves that FRP U-wrap shear strengthening technique has a significant effect on increasing bond performance of NSM-FRP flexural strengthening technique.

4.3.5 Criteria for ductility/deformability:

Generally, NSM-FRP flexurally strengthened beam sections will not have a sudden failure as debonding is the critical mode of failure (T. K. Hassan & Rizkalla, 2004). Although a balanced failure in which concrete crushing and FRP-rupture occur simultaneously was observed in the current study, is also an acceptable mode of failure for FRP strengthened flexural members (Reda Taha, Tromposch, Tadros, Mufti, & Klowak, 2003). Hence, Jaeger proposed a performance factor for ductility in order to check the ductile performance of concrete structures (Jaeger, Mufti, & Tadros, 1997). This ductility/deformability factor denoted by "J" can be calculated using **equation 4.21.**

$$J = \frac{\varphi_u M_u}{\varphi_{SE} M_{SE}} \qquad \textbf{(4.21)}$$

Where, φ_u and φ_{SE} are the curvatures of flexural members at ultimate and service moments M_u and M_{SE} respectively. In the current study the service moment is the moment

corresponding to a 0.001 strain in the tension steel and the ultimate moment is corresponding to the ultimate strain observed in the tension steel at failure.

Table 4.11, presents the J index for all beam series. It is evident that, there is a significant decrease in ductility for RC beam strengthened with both NSM-FRP flexural and shear strengthened with U-wrap shear strengthening (Beam NU). But the RC beam with partial shear strengthening has shown the same ductility using Jaeger's ductility index. **Figure 4.55** illustrates the drop in ductility deformability for NU beams.

Table 4.10: Deformability index (J) for all beam series

Beam		ε_s	Moment (M)	Curvature (φ)	J
C	Service	0.001	4.13	0.014	31
	Ultimate	0.019	7.88	0.230	
U	Service	0.001	3.83	0.012	43
	Ultimate	0.019	8.64	0.221	
N	Service	0.001	4.39	0.014	33
	Ultimate	0.013	12.45	0.163	
NU	Service	0.001	7.27	0.016	17
	Ultimate	0.01	15.46	0.131	
NUS	Service	0.001	4.23	0.016	33
	Ultimate	0.012	13.37	0.160	

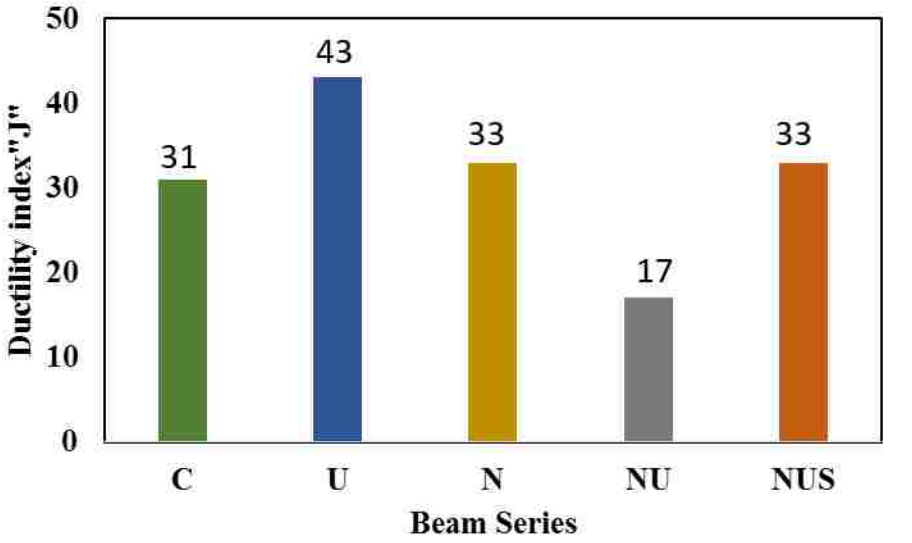

Figure 4.55: Plot to show Ductility/Deformability for five beam series

4.3.6 Modes of Failure:

RC Beams control C1-C5 and RC beams shear strengthened with FRP U-wrap shear strengthening U1-U5 failed by crushing of concrete in compression after the tension steel yielded. RC Beams flexurally strengthened with NSM-FRP failed by debonding caused by the local splitting of epoxy at 60% strain capacity of the FRP bar. The splitting of epoxy was mainly caused by flexural cracks intersection with the epoxy cover. **Figure 4.56** showing the splitting of epoxy failure.

RC beams strengthened with both NSM-FRP flexural and FRP U-wrap shear strengthening has shown significant improvement in bond and changed the mode of failure from debonding to the strength rupture of GFRP bar. The change in failure mode had a significant effect on ductility of the beam. **Figure 4.40** illustrates the failure mode rupture of GFRP bar.

RC beams strengthened with both NSM-FRP flexural and FRP U-wrap shear strengthening in shear area only NUS1-NUS has shown significant improvement in bond. One of the four beams

tested failed by strength rupture of GFRP bar. The other beams failed by debonding, but the failure was associated with sudden release of energy by splitting the epoxy cover, which made this a sudden failure. **Figure 4.44** illustrates both failure modes observed in the beam.

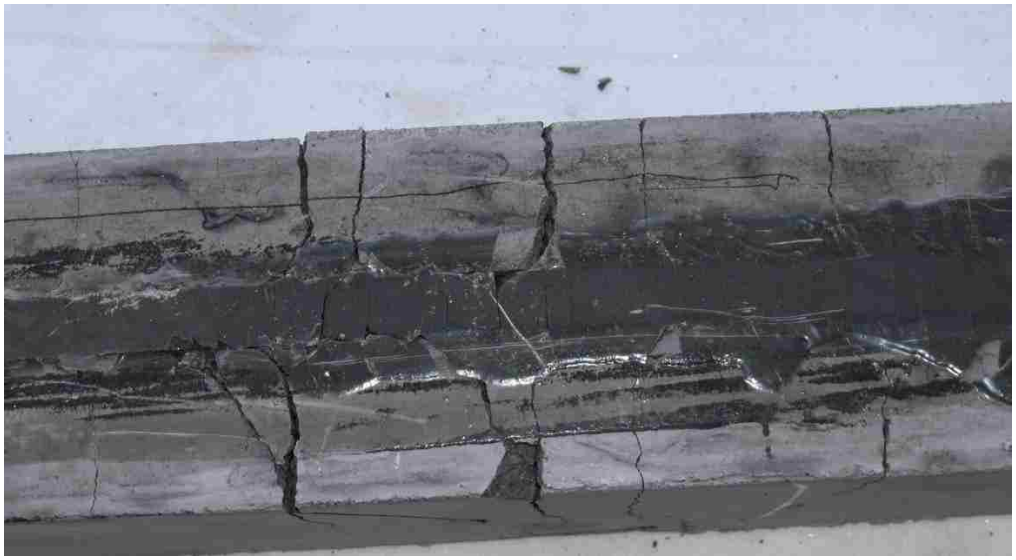

Figure 4.56: RC beam flexurally strengthened with NSM-FRP showing splitting of epoxy failure

Chapter 5 Conclusions and Recommendations

In the current study, combined effect of NSM-FRP flexural strengthening and U-wrap shear strengthening has been studied experimentally. This combination of strengthening systems is used currently in the industry but designed separately for flexural and shear strengthening. The design guidelines from ACI-440 are based on separate investigation of these two systems. The main focus of this research is to observe the behavior of flexural system, when the above said flexural and shear strengthening systems are combined. This chapter presents the conclusions based on the experimental observations and inferences made from the analysis of results followed by some recommendations for future work.

5.1 Conclusions

- The experimental results have shown that the RC beams flexural strengthening with NSM-FRP have shown a strength increase of 47% over beam control after strengthening the beam with NSM-FRP flexural strengthening technique. Failure of NSM-FRP flexural strengthening beams was due to debonding of the bar with surrounding epoxy.
- The combined effect of NSM-FRP flexural strengthening and U-wrap shear strengthening have shown an increase of 20% in the overall flexural capacity compared with RC beams strengthened only with NSM-FRP flexural strengthening. The U-wrap shear strengthening has shown an effect of confinement resisting the crack propagation within the epoxy cover and improving the bond performance between NSM-FRP bar and the surrounding epoxy. This resulted in changing the mode of failure from debonding of GFRP bar to GFRP bar rupture after reaching full tensile capacity of the bar.

- The combined effect of NSM-FRP flexural strengthening and U-wrap shear strengthening in shear area only have shown 13% increase in overall flexural capacity compared to the beam strengthened with NSM-FRP flexural strengthening only. The experimental observation has shown that, of the four beams tested one of the beams failed by GFRP bar rupture and the other three RC beams failed by sudden splitting of epoxy cover. However, strain readings have shown that the full tensile capacity of the bar was achieved, which proves the improved bond performance. Failure was caused by sudden release of stored energy by rupture of GFRP bar or sudden splitting of epoxy for both NU and NUS specimens. Both failure modes are abrupt and sudden reducing the ductility of the beam.
- The strain in GFRP NSM-bar for combined strengthened RC beams NU specimen has increased from 0.010 to 0.0135 over the beams strengthened flexurally with NSM-FRP only (N). RC Beams strengthen with NSM-FRP flexural and FRP U-wrap shear strengthened specimens have shown 35% increase in the strain at failure compared with RC beams strengthen with NSM-FRP flexural strengthening only. As the mode of failure was changed to GFRP bar rupture the strain at failure was much higher. The strain in GFRP-NSM bar for RC beams flexurally strengthened with NSM-FRP flexural strengthening and U-Wrap shear strengthening in shear area only specimen was recorded to be 0.0158 at failure corresponding to an increase of 58% over residual NSM-FRP flexural strengthened RC beams. It can be assumed that this strain value is accurate as the failure mode was splitting of epoxy cover beyond this point there is a sudden change in the strain value associated with debonding of strain gauge. The increased strain capacity indicates improved bond performance due to confinement.

- The combined effect has shown a significant improvement on bond performance which reflected on the overall flexural capacity of the RC beam. However, it is important to note the change in mode of failures from relatively ductile in NSM-FRP flexural strengthened RC beams to sudden and non-ductile. Bar rupture was observed as the failure mode for NSM-FRP flexurally strengthened RC beams when full U-wraps were used to improve the bond performance as a result of confinement.
- Deformability index following work by (Jaeger et al., 1997) has shown a significant loss in ductility/ deformability of RC beam when the combined NSM-FRP flexural strengthening and FRP U-wrap shear strengthening techniques are used for RC beams. No change in the deformability was observed after combining NSM with partially wrapped FRP U-wrap shear strengthening. Nevertheless, beam failure in this case occurred due to sudden failure associated with splitting of epoxy from RC beam.
- RC beam strengthened with U-wrap shear strengthening only have shown a strength increase of 7% compared to the control RC beam, proving that U-wrap shear strengthening does not affect the flexural strength of the RC beam.

5.2 Recommendations

ACI-440 2R-08 must consider the effect on combining NSM-FRP flexural strengthening and U-wrap shear strengthening. A limitation on use of these combined techniques of NSM-FRP flexural strengthening and U-wrap shear strengthening on the same flexural members must be placed. Further study of the combined system of NSM-FRP flexural strengthening and U-wrap shear strengthening system is required using CFRP bars. It would also be interesting to observe the fatigue behavior of the combined system. Studying the effect of confinement with varied

groove sizes would be an interesting aspect. An analytical model to evaluate the development length for the combined effect would be recommended. A full scale beam testing with varied development lengths is also recommended.

References:

ACI-318. (2014). Building Code Requirements for Structural Concrete and Commentary. U.S.A.

ACI-440. (2008). Guide for the Design and Construction of Externally Bonded FRP Systems for Strengthening Concrete Structures (Vol. 2R.08). American Concrete Institute, 38800 Country Club Drive, Farmington Hills, MI 48331, U.S.A.

Asplund, S. (1949). *Strengthening bridge slabs with grouted reinforcement.* Paper presented at the ACI Journal Proceedings.

ASTM-C39, A. C. C. M.-a. (2015). Standard Test Method for Compressive Strength of Cylindrical Concrete Specimens.

ASTM-C143, A. C. C. M.-. (2015). Standard Test Method for Slump of Hydraulic-Cement Concrete.

ASTM-C192/C, A. C. C. M.-. (2015). Standard Practice for Making and Curing Concrete Test Specimens in the Laboratory: ASTM.

ASTM-C469, A. C. C. M.-. (2014). Standard Test Method for Static Modulus of Elasticity and Poisson's Ratio of Concrete in Compression.

ASTM-C496, C. C. M.-. (2011). Standard Test Method for Splitting Tensile Strength of Cylindrical Concrete Specimens.

ASTM-C1064, A. C. C. M.-. (2012). Standard Test Method for Temperature of Freshly Mixed Hydraulic-Cement Concrete.

Badawi, M., & Soudki, K. (2009). Fatigue behavior of RC beams strengthened with NSM CFRP rods. *Journal of Composites for Construction, 13*(5), 415-421.

Bakis, C., Bank, L. C., Brown, V., Cosenza, E., Davalos, J., Lesko, J., . . . Triantafillou, T. (2002). Fiber-reinforced polymer composites for construction-state-of-the-art review. *Journal of Composites for Construction, 6*(2), 73-87.

Barros, J. A., & Fortes, A. (2005). Flexural strengthening of concrete beams with CFRP laminates bonded into slits. *Cement and Concrete Composites, 27*(4), 471-480.

Chajes, M. J., Januszka, T. F., Mertz, D. R., Thomson Jr, T. A., & Finch Jr, W. W. (1995). Shear strengthening of reinforced concrete beams using externally applied composite fabrics. *ACI Structural Journal, 92*(3), 295-303.

Charif, A. (1983). Structural behaviour of reinforced concrete beams strengthened by epoxy bonded steel plates.

De Lorenzis, L., Lundgren, K., & Rizzo, A. (2004). Anchorage Length of Near-Surface Mounted Fiber-Reinforced Polymer Bars for Concrete Strengthening? Experimental Investigation and Numerical Modeling. *ACI Structural Journal, 101*(2).

De Lorenzis, L., & Nanni, A. (2002). Bond between near-surface mounted fiber-reinforced polymer rods and concrete in structural strengthening. *ACI Structural Journal, 99*(2), 123-132.

De Lorenzis, L., Nanni, A., & La Tegola, A. (2000). *Strengthening of reinforced concrete structures with near surface mounted FRP rods.* Paper presented at the International Meeting on Composite Materials, PLAST 2000, Proceedings, Advancing with Composites.

De Lorenzis, L., Rizzo, A., & La Tegola, A. (2002). A modified pull-out test for bond of near-surface mounted FRP rods in concrete. *Composites Part B: Engineering, 33*(8), 589-603.

De Lorenzis, L., & Teng, J. (2007). Near-surface mounted FRP reinforcement: An emerging technique for strengthening structures. *Composites Part B: Engineering, 38*(2), 119-143.

Dussek, I. J. (1980). Strengthening of bridge beams and similar structures by means of epoxy-resin-bonded external reinforcement. *Transportation Research Record*(785).

El-Hacha, R., & Rizkalla, S. H. (2004). Near-surface-mounted fiber-reinforced polymer reinforcements for flexural strengthening of concrete structures. *ACI Structural Journal, 101*(5).

Fleming, C., & King, G. (1967). The development of structural adhesives for three original uses in South Africa. *Bulletin rilem, 1967*(37), 241-251.

Garner, A. P. (2011). *Strengthening reinforced concrete slabs using a combination of CFRP and UHPC.* (M.Sc Thesis, University of New Mexico).

Genedy, M. (2014). *A New CFRP-UHPC System for Strengthening Reinforced Concrete T-Beams.* (M.Sc Thesis, University of New Mexico).

Hassan, T., & Rizkalla, S. (2003). Investigation of bond in concrete structures strengthened with near surface mounted carbon fiber reinforced polymer strips. *Journal of Composites for Construction, 7*(3), 248-257.

Hassan, T. K., & Rizkalla, S. H. (2004). Bond mechanism of near-surface-mounted fiber-reinforced polymer bars for flexural strengthening of concrete structures. *ACI Structural Journal, 101*(6).

Jaeger, L., Mufti, A., & Tadros, G. (1997). *The concept of the overall performance factor in rectangular-section reinforced concrete members.* Paper presented at the Proceedings of the 3rd International Symposium on Non-Metallic (FRP) Reinforcement for Concrete Structures, Sapporo, Japan.

Kachlakev, D., & McCurry, D. (2000). Behavior of full-scale reinforced concrete beams retrofitted for shear and flexural with FRP laminates. *Composites Part B: Engineering, 31*(6), 445-452.

Kim, J. J., Noh, H.-C., Reda Taha, M. M., & Mosallam, A. (2013). Design limits for RC slabs strengthened with hybrid FRP–HPC retrofit system. *Composites Part B: Engineering, 51*, 19-27.

Klaiber, F. W., Dunker, K. F., Wipf, T. J., & Sanders Jr, W. W. (1988). *Methods of strengthening existing highway bridges*.

Klaiber, W. F., Dunker, K. F., & Sanders, W. W. (1982). Strengthening of single-span steel-beam bridges. *Journal of the Structural Division, 108*(12), 2766-2780.

Lorenzis, L. D., & Nanni, A. (2001). Characterization of FRP rods as near-surface mounted reinforcement. *Journal of Composites for Construction, 5*(2), 114-121.

Malvar, L., Warren, G., & Inaba, C. (1995). *Rehabilitation of navy pier beams with composite sheets.* Paper presented at the RILEM PROCEEDINGS.

Nanni, A., Alkhrdaji, T., Barker, M., Chen, G., Mayo, R., & Yang, X. (1999). *Overview of testing to failure program of a highway bridge strengthened with FRP composites.* Paper presented at the Proceedings of fourth international symposium on non-metallic (FRP) reinforcement for concrete structures (FRPRCS-4).

Norris, T., Saadatmanesh, H., & Ehsani, M. R. (1997). Shear and flexural strengthening of R/C beams with carbon fiber sheets. *Journal of structural engineering, 123*(7), 903-911.

Reda Taha, M., Tromposch, E., Tadros, G., Mufti, A., & Klowak, C. (2003). Performance Based Design for FRP Strengthening of the Roof Panels of Calgary Saddledome. *ACI Special Publication, 215*.

Saadatmanesh, H., Albrecht, P., & Ayyub, B. M. (1989). Experimental study of prestressed composite beams. *Journal of structural engineering, 115*(9), 2348-2363.

Saadatmanesh, H., & Ehsani, M. (1990). Fiber composite plates can strengthen beams. *Concrete International, 12*(3), 65-71.

Swamy, R., Jones, R., & Bloxham, J. (1987). Structural behaviour of reinforced concrete beams strengthened by epoxy-bonded steel plates. *Structural Engineer. Part A, 65*, 59-68.

Teng, J., De Lorenzis, L., Wang, B., Li, R., Wong, T., & Lam, L. (2006). Debonding failures of RC beams strengthened with near surface mounted CFRP strips. *Journal of Composites for Construction, 10*(2), 92-105.

Toutanji, H., Zhao, L., & Zhang, Y. (2006). Flexural behavior of reinforced concrete beams externally strengthened with CFRP sheets bonded with an inorganic matrix. *Engineering Structures, 28*(4), 557-566.

Wahab, N., Soudki, K. A., & Topper, T. (2011). Mechanics of bond fatigue behavior of concrete beams strengthened with NSM CFRP rods. *Journal of Composites for Construction, 15*(6), 934-942.

Wahab, N., Soudki, K. A., & Topper, T. (2012). Experimental investigation of bond fatigue behavior of concrete beams strengthened with NSM prestressed CFRP rods. *Journal of Composites for Construction, 16*(6), 684-692.

Yan, X., Miller, B., Nanni, A., & Bakis, C. (1999). *Characterization of CFRP rods used as near surface mounted reinforcement.* Paper presented at the 8th International conference on structural faults and repair.